CATALYTIC CRACKING OF TOLUENE USING A BIOCHAR DERIVED CATALYST

by

ANKITA JUNEJA

(Under the Direction of Sudhagar Mani)

ABSTRACT

This research investigated char naturally produced inside the gasifier, as a low cost catalyst, to decompose toluene as a model tar compound from the temperature range of 600-900°C. The reaction kinetics found from 650 to 900°C gave an activation energy of 90 kJ/mol for toluene decomposition (compared to 80.24 kJ/mol for Ni/Mayenite and 196 kJ/mol for olivine). The catalytic activity of char for toluene decomposition was comparable to other commercially available catalysts. It is theorized that metals in the char catalyzed a free radical reaction in which benzene, CO_2 and CH_4 was formed as end products. Additionally, when char was loaded with iron (9.89%, 13% and 18.7% by weight), the activity increased and the temperatures required for almost complete conversion were lowered from 900 to 800°C. The activation energy found for the iron loaded char (18.7%) was 49 kJ/mol. The results from this research may be used to design a catalytic cracking process using biochar catalysts for tars downstream of a gasifier or inside the gasifier and potentially replace energy intensive and costly processes.

INDEX WORDS: Biochar, toluene decomposition, tar, catalyst, iron impregnation, synthesis Gas

CATALYTIC CRACKING OF TOLUENE USING A BIOCHAR DERIVED CATALYST

by

ANKITA JUNEJA

B.Tech, Punjab Agricultural University, India, 2006

A Thesis Submitted to the Graduate Faculty of The University of Georgia in Partial Fulfillment of the Requirements for the Degree

MASTER OF SCIENCE

ATHENS, GEORGIA

2010

CATALYTIC CRACKING OF TOLUENE USING A BIOCHAR DERIVED CATALYST

by

ANKITA JUNEJA

Major Professor: Sudhagar Mani

Committee: James Kastner
Keshav C. Das

Electronic Version Approved:

Maureen Grasso
Dean of the Graduate School
The University of Georgia
August 2010

DEDICATION

Dedicated to The Almighty, my parents, Shelly Juneja and A.N. Juneja and my husband, Deepak Kumar.

ACKNOWLEDGEMENTS

It gives me immense pleasure to express my earnest gratitude and indebtedness to my major professor. Dr. Sudhagar Mani, for his valuable and judicious guidance, sustained efforts, constructive criticism and ever willing help. I also want to take pleasure in thanking Dr. James Kastner who guided me through every obstacle I met during my research work and filled the gaps to make my research complete. He not only guided me through the project but also shaped my scientific thinking. I also want to thank Dr. KC Das for his valuable insights, suggestions and encouragement during the research work. Special acknowledgments are due to our graduate coordinator, Dr. William Kisaalita and our head of the department Dr. Dale Threadgill for their valuable advice.

I sincerely acknowledge the assistance provided by Mr. Roger Hilten for his valuable inputs and support during the research. Ms. Joby Miller deserves special thanks for her excellent advice on chromatographic techniques. I would also like to thank Mr. Eric Gobert for his constant support during the work. I also thank Dr. Pan for letting us use the SEM and Mr. Yen-Jun Chuang for helping me use the equipment.

I take this opportunity to acknowledge my fellow graduate students and friends especially Naomi Hinton, Thiruvenkadam and Gerry Lindo. A special thanks goes to my friend Madhumita Dash for always being there for help whenever I needed and making a comfortable balance in my research and personal life. I owe to my parents, my brother Rahul and my husband Deepak for being a big support and source of inspiration for me till date and always encouraged me to do the challenging works.

Finally I would like to thank the financial source for this project, Dr. Mani's startup funds and B3I Seed grant-UGARF for funding this project.

TABLE OF CONTENTS

Page

LIST OF TABLES

Page

LIST OF FIGURES

Page

CHAPTER 1

INTRODUCTION

A drastic increase in the energy demand and simultaneous depletion of non-renewable sources of energy has led to an increasing need for renewable sources of energy. A recent report published by EIA (Energy Information Administration) projected that total world consumption of marketed energy is expected to increase by 44% from 2006 to 2030[1]. Fossil fuels are the major contributors (80%) to the world's energy consumption (332 EJ) (World's Energy Assessment Report 2004). Renewable sources contribute about 12% out of which biomass is 9%[2]. Renewable energy helps to lessen the consumption of fossil fuels. It covers the energy from solar, wind, hydroelectric, geothermal, and biomass sources. Unlike fossil fuels, renewable sources are in abundance as most of these sources are derived directly or indirectly through sun. Renewable energy in US account for 7% out of the total energy requirement in 2008, which consist of biomass as major contributor, 53%, to the total renewable sources[3]. Biomass is a renewable feedstock that can be used to produce fuel, power and chemicals from a range of conversion technologies. It has an added advantage of being CO_2 neutral. Thermo-chemical conversion system is a robust system and has an advantage of accepting a wide variety of biomass. These systems are quicker and are accomplished faster as compared to biological conversions (Milne et al., 1998; Foust et al., 2009). The main thermo-

[1] http://www.eia.doe.gov/oiaf/ieo/pdf/0484%282009%29.pdf
[2] http://www.energyandenvironment.undp.org/undp/index.cfm?module=Library&page=Document&DocumentID=5027
[3] http://www.eia.doe.gov/cneaf/alternate/page/renew_energy_consump/rea_prereport.html

chemical conversion platforms are combustion, pyrolysis and gasification. Combustion is the most traditional method of converting biomass to heat, mechanical power and electricity but the efficiency ranges only from 20% to 40% (Caputo et al., 2005). Also, combustion generates pollutants such as, particulate matter and the acid rain gases, sulfur dioxide (SO_2) and Nitrogen oxides (NO_x) (Demirbas, 2001). Pyrolysis is a process to convert biomass to bio-oil by heating it in absence of air under high temperature (400-600°C). Pyrolysis faces the challenge of limited uses and difficulty in downstream processing of bio-oil (Faaij, 2006).

Gasification is one of the most promising routes to produce syngas to liquid fuels or combined heat and power generation due to high thermal efficiency (Knoef and Ahrenfeldt, 2005). Gasification is a process of converting carbonaceous material into syngas ($CO + H_2$) by partial oxidation of in presence of high temperature (Neeft et al., 1998). Gasifiers are mainly of three types: updraft, downdraft and fluidized bed gasifier. The product gas of gasification contains carbon monoxide, carbon dioxide, hydrogen, methane, traces of higher molecular weight hydrocarbons such as ethane and ethane, H_2O, N_2 (in case of air gasification) and various contaminants such as small char particles, ash, tars and oils (Neeft et al., 1998). The syngas ($CO + H_2$) has a number of applications including direct combustion (Raskin et al., 2001), power generation by gas engines (Sridhar et al., 2001; Lin, 2007) and gas turbines (Shilling and Jones, 2003; Walton et al., 2007), production of liquid fuels (Lapidus et al., 1994; Tijmensen et al., 2002) and H_2 production (Watanabe et al., 2002; Hanaoka et al., 2005). The industrial use of syngas is determined by the quality of syngas as there are tolerance limits for all

applications in terms of impurities present in the syngas which are summarized by Milne et.al. (1998).

The major problem in using syngas is the formation of tars during the gasification. Producer gas from gasification usually contains unacceptable levels of tars. Tars can be defined as the large aromatic hydrocarbons produced under thermal or partial-oxidation regimes of any organic material having molecular weight (78 g/mol) higher than benzene (Neeft et al., 1998; Milne et al., 1998). Tars are formed during gasification in a series of complex reactions. Gasification of cellulose forms substantial amount of primary tar fractions (low molecular weight carbonyls, furans and carboxylic acids) with high gasification reactivity, and hence the cellulose gasification mainly proceeds via the tar fraction. Gasification of lignin is less effective and forms primary tars (aromatics with guaiacyl-units) which then converts to secondary tars (catechols, o-cresols, phenols) due to further reaction severities (Hosoya et.al., 2008). The formation of tar is highly dependent on the reaction conditions. Due to increased reaction temperature, secondary reactions occur in the gas phase which convert oxygenated tar compounds to light hydrocarbons, aromatics, oxygenates and olefins subsequently forming higher hydrocarbons and larger PAH in tertiary processes (Milne et al., 1997). Elliot (1988) showed the transition of biomass pyrolysis products as a function of process temperature from primary products to phenolic compounds to aromatic hydrocarbons (Figure 1.1).

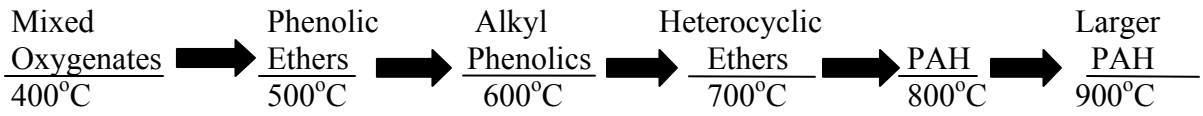

Figure 1.1: Tar maturation scheme (Elliott 1988)

The type and amount of tars depend upon the biomass type, operational parameters and type of gasifiers. Baker et.al. (Baker et al., 1988) reported the levels of tar for various reactors with updraft gasifiers having 12 wt% of wood and downdraft less than 1%.

Tar can cause operational problems associated with condensation in downstream processes and blocking gas coolers, filter elements and engine suction channels. Condensation also leads to formation of tar aerosols which are difficult to be separated from gas. Polymerization of condensed tars forms more complex structures, thus increasing the tendency for coking (Devi et al., 2003). Minimum allowable tar depends on the end use application of the syngas. Milne and Evans (Milne et al., 1998) have compiled the end use tolerance limits for tars reported by different researchers.

Considerable efforts have been made to clean fuel gas from tars. Tars can be removed by physical methods like wet/dry scrubbing, but this transforms the waste to a liquid or solid waste which has problems of disposal in an environmentally acceptable manner. Another method is the thermal cracking of tars, but high temperatures are required to crack all tars. Complete conversion of naphthalene like molecules requires temperature as high as 1400^{o}C (Jess, 1996). It also leads to formation of char (Li and Nelson, 1996) and soot (Wornat et al., 1987). Catalytic reforming of tars can be an attractive way to reform tars because of its efficiency to reform tars at much lower temperatures. Catalytic cracking accelerates the rate of reaction of tar decomposition so as to avoid using very high temperatures and compromising on quality of product gas. Syngas production increases due to decomposition of tar compounds. Many catalysts have been studied for tar removal and gas reforming, most studied of which are dolomite

(Yeboah et al., 1980; Donnot et al., 1985; Corella J., 1988; Aznar et al., 1992) and nickel (Ekstrom et al., 1985; Garg M., 1987; Coll et al., 2001; Zhang et al., 2004). Dolomite has limitations due to its lower melting point and its melting causes inactivation of the catalyst (Zhang, 2003). Nickel is an expensive catalyst (Kinoshita et al., 1995) and faces challenges in terms of coking and catalyst poisoning (Dayton, 2002). Other catalysts used are Fluid Catalytic Cracking catalysts (Radwan et al., 2000) and alkali metals (Radovic et. al., 1984; Suzuki et al., 1992). David (2001) summarized the characteristics of an effective catalyst as catalyst being inexpensive, easily regenerated and resistant to coking(Sutton et al., 2001). Complying with these properties, biochar seems suitable for use as a tar reforming catalyst. It is attractive due to low cost and its abundant production inside the gasifier. Char has been observed to have good catalytic properties for reforming of tar and its model compounds.(Ekstrom et al., 1984; Chembukulam et al., 1981; Brandt et al., 2000; Abu El-Rub et al., 2008). The catalytic properties of char for tar reforming can be related to its pore size, surface area and mineral content of the char. The surface area of char made from pine wood at 900^{o}C with heating rate of 10^{o}C/min was found to be 330 m^2/g (El-Rub and Kamel, 1990) which is comparable to the surface area of activated alumina (299 m^2/g) and zeolite (350 m^2/g) (Hatano and Suzuki, 2003) and much higher as compared to the other active catalysts like dolomite (5-20m^2/g) (Yeboah et al., 1980). Exposed to higher temperatures, char seems to refresh its surface area as steam gasification helps in maintaining the micro pores of char for catalytic activity. This study aims at investigating the catalytic properties of char for tar breakdown at different operating conditions.

CHAPTER 2

HYPOTHESIS AND OBJECTIVE

Hypothesis

1. Char contains Fe species (and other alkali metals, like Al, Ca, K and Mg) that are responsible for actually catalyzing the toluene decomposition reaction.
2. Reaction of toluene cracking is a surface phenomenon involving chemisorption of toluene molecule on char, reaction of Fe species and toluene and subsequent reduction of toluene resulting in complete or partial decomposition.
3. Char as a catalyst can steam reform toluene with high toluene conversion at high reaction rates and low temperatures.
4. Breakdown of toluene is through coking. Aromatics breakdown to coke over char.
5. Carbon in char also acts as a catalyzing material in decomposition of toluene.

Objectives

The specific objectives of this study can be summarized as

1. To investigate the catalytic properties of biomass char using toluene as a model tar compound in a fixed bed reactor.
    a. To evaluate the effect of reaction temperature on toluene breakdown.
    b. To analyze the effect of toluene inlet concentration on toluene decomposition and by-product formation.

2. To quantify the effect of Fe impregnation in char on toluene decomposition by using different loadings of iron for comparison of catalytic activity.
3. To determine the reaction kinetics and rate law for catalytic cracking of toluene using biomass char and iron loaded char.
4. To evaluate the longevity of biomass char and iron loaded char for tar cracking applications.
5. To correlate reaction kinetics, by-product formation, and activity with catalyst characterization.

CHAPTER 3

LITERATURE REVIEW

Tar formation is one of the major bottlenecks for use of syngas in many applications. This problem has been tried to be addressed in several ways, catalytic decomposition being one of the most attractive one. A review of tar removal methods and different catalysts used has been presented.

Tar Formation and Composition

Biomass gasification is a complex combination of pyrolysis and oxidation reactions in condensed and vapor phases. The products formed are dependent on the process variables and operating parameters such as temperature, pressure, oxygen level, biomass used, steam to biomass ratio and type of gasifier. The higher organic aromatic hydrocarbons formed are collectively termed as tars (Milne et al., 1998). A generic definition of tars may be "Tars are defined as all organic contaminants with the molecular weight larger than benzene (78 g/mol)". A typical composition of tars is shown in Fig. 2.1. These tars are formed due to the breakage of molecular bonds in the organic material/biomass due to heating (Neeft et al. 1998). The maturation and composition of tars from various processes is reviewed and shown schematically by (Elliott, 1988) (Fig. 1.3). The conversion of oxygenated tar compounds to PAH's occur due to increased reaction severity. This shows the transition of tars compounds to PAH's occur due to increased reaction severity (increased reaction temperatures and larger holding times).

This shows the transition of tars from primary products to large aromatic compounds as a function of temperature. Evans and Milne (Milne et al., 1997) identified four major classes of tars as a result of gas phase thermal cracking reactions using Molecular Beam Mass Spectroscopy (MBMS):

1. Primary products: characterized by cellulose-derived products such as levoglucosan, hydroxyl-acetaldehyde, and furfurals; analogous hemicellulose-derived products; and lignin-derived methoxyphenols
2. Secondary products: characterized by phenolics and olefins;
3. Alkyl tertiary products: include methyl derivatives of aromatics, such as methyl acenaphthylene, methylnaphthalene, toluene, and indene;
4. Condensed tertiary products: show the PAH series without substituents: benzene, naphthalene, acenaphthylene, anthracene/phenanthrene, pyrene.

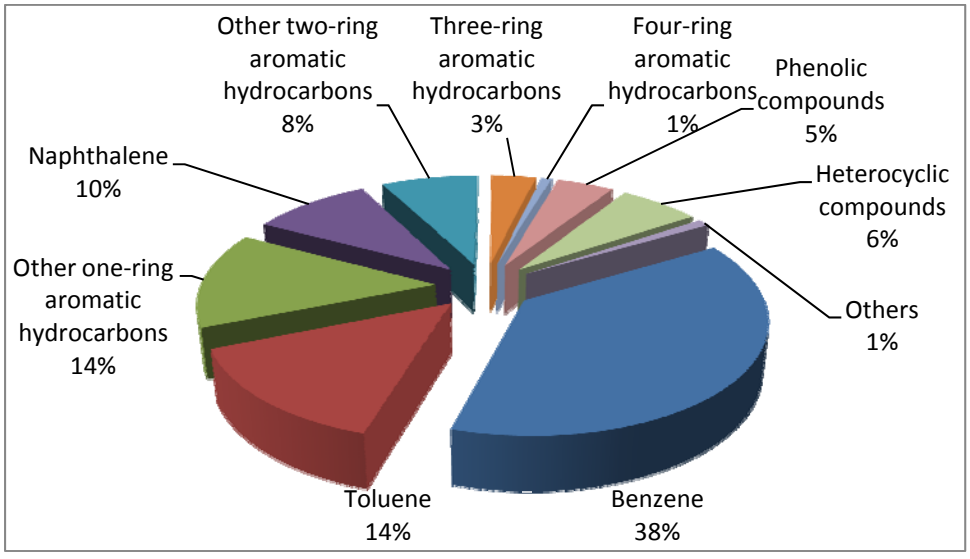

Figure 3. 1: Typical composition of biomass gasification tars (Coll, Salvado et al. 2001)

The primary tars are the fragments of the original biomass. They react and form secondary tars at the same temperature and tertiary tars at a higher temperature (Neeft et al., 1998). The primary tars are decomposed well before the tertiary ones are formed (Milne et al., 1998). The amount of tar produced is a function of gasifier type, operating conditions (temperature pressure and residence time) in the gasifier, and properties of biomass used (particle size, moisture content and chemical composition). The updraft gasifier is known to duce maximum tars followed by fluidized bed gasifier and downdraft gasifier produces the minimum (Milne et al., 1998).

Problems Related to Tars

Tars are problematic in end-use applications of syngas due to problems associated with condensation of tars, which cause blockage in process equipment, engines and turbines, used for the application of syngas. Tars also form tar aerosols (mist or fog with tiny droplets of tars may be less than 1μm in diameter), which are difficult to remove from the gas. These aerosols are a function of cooling rate. Rapid cooling rates yield very many and very small tar aerosols, but slow cooling rates yield few and large aerosols (Neeft et al., 1998). Polymerization of condensed tars forms more complex structures, thus increasing the tendency for coking (Devi et al., 2005b). The tars can also crack in the pores of filters and form coke. Moreover, tars are dangerous because of their carcinogenic nature. All end-use applications have a minimum allowable amount of tars which is well reviewed by Milne and Evans (Milne et al., 1998).

Considerable efforts have been undertaken to remove tar from biomass gasification syngas streams . Tars can be removed by primary methods (taking measures inside the gasifier) or secondary methods (using secondary reactor downstream of the

gasifier) (Devi et al., 2003). The major routes for gas clean up are the physical route, thermal cracking and catalytic cracking of tars.

Physical Methods

Physical methods are the mechanism methods which include scrubbers, filters, cyclones and electrostatic precipitators. These methods are demonstrated to be considerably efficient in removing tars and particulate materials. Cooling towers are one method of physical removal used to condense the tar components. Venture scrubbers are usually the next step (Milne et al., 1998). Tar levels were observed to decrease to 20-40 mg/m^3 and the particulate level was reduced to 10-20 mg/m^3 using a scrubber (Bridgwater, 1994). Dinkelbach (Dinkelbach et al., 2000) reported that using a cooler and scrubber was efficient in tar removal for short time, but was not suitable for long duration application of gas. They could remove about 60% tars by wet scrubbers. Nevertheless, these systems are fairly expensive. Also, these systems only remove tars from the product gas, whereas energy from the tar is lost because of the heat loss from tars (Han and Kim, 2008). Also, the liquid waste disposal and recycling is a major issue for this type of tar removal system.

A new tar removal system called OLGA (Dutch acronym for oil based gas washer) was developed by Boerrigter in ECN (Boerrigter et al., 2005). This system scrubs the product gas with oil, capable of dissolving desired tars, instead of water. The results of OLGA are quite satisfactory. It is efficient in removing the tars selectively from the product gas without affecting the main gaseous products. Almost 99% phenol and 97% heterocyclic tars were removed, but the operating costs became a more serious problem due to the addition of oil cost to scrub during the system.

Another option can be use of filters, in which fabric filters are a simple and very effective method of removing solid matter from gaseous stream by filtering it through a porous material. These are efficient in particle removal but not for tar filtration because of many problems associated with tars (Neeft et al., 1998). Electrostatic precipitator is one of the high efficiency particle collection device, used primarily in coal fired plant, metallurgical industry and cement industry. These precipitators can capture up to 99% of the particles with diameter as small as 0.05μm, but the efficiency for tar capture is to a maximum of 60% (Neeft et al., 1998). Certain problems associated with electrostatic precipitators are spark overs and tar deposition.

Thermal Cracking

Thermal cracking method involves heating the raw gases derived from the gasification/pyrolysis to a high temperature where tar molecules can be cracked to lighter gases by secondary reactions. In development of biomass gasification technology, thermal cracking has been considered an important option for tar removal. Therefore, it has been extensively studied. Studies have shown 90% conversion of tars between range 600-900^{o}C with residence time of 0.2-2s (Jenssen et al., 1996; Boroson et al., 1989; Stiles and Kandiyoti, 1989). Tar content in the gas decrease with the increase in temperature due to the tar cracking and steam reactions given below (Narvaez et al., 1996):

$$C_nH_x \longleftrightarrow nC + (x/2)H_2 \quad (3.1)$$

$$C_nH_x + mH_2O \longleftrightarrow nCO + (m + x/2)H_2 \quad (3.2)$$

The reaction of toluene (a major component of tars) decomposition in presence of steam is (Taralas et al., 2003):

$$2C_7H_{8(g)} + 21H_2O_{(g)} \longrightarrow 7CO_{2(g)} + 29H_{2(g)} + 7CO_{(g)} \quad (3.3)$$

The main components of tars are observed as naphthalene, phenol, cresols, benzene, toluene, xylenes, indene, methylnaphthalenes, biphenyl, acenaphthylene, fluorene, phenanthrene, anthracene, and pyrene (Vassilatos, 1992). The primary tars compounds are decomposed much before tertiary tars are even formed, so the primary tars are observed in a very small amount in overall tar composition. Kinoshita et al. studied tar under the effect of temperature and reported decrease in overall tars with increasing temperature. They reported the decrease of single ring and two ring aromatics (except naphthalene and benzene) to decrease and three ring and four ring compounds to increase with temperature (Kinoshita et al., 1994). Another study reported only naphthalene left as a major compound at 900^{o}C in post cracking of pyrolytic gasification tars from 700-900^{o}C. Phenol shows up to be quite stable till 700^{o}C but significantly decomposed at 900^{o}C. Indene and naphthalene are the two compounds that increase with temperature while the overall tars decrease (Vassilatos, 1992). This suggests that higher temperature favors the formation of aromatic compounds without substituent functional group as these aromatics, directly attached to benzoid rings are relatively more stable. Also, as shown by Elliot et.al. (1988), higher temperature favors formation of larger PAH's (Fig. 1.3). It is also supported by a report submitted by Evan and Milne (Milne et al., 1998), where they showed the formation of stable aromatics (without substituent functional groups) with increasing temperature. Some other studies have also shown that for the two most stable compounds, naphthalene and benzene, higher temperatures in range of 900-1250^{o}C are required for higher conversions (Bruinsma and Moulijn, 1988; Bruinsma et al., 1988; Jess, 1996; Tesner and Shurupov, 1997). Houben (2004) investigated the thermal cracking of tars in a separate tubular reactor in range of 900-

1150^{o}C and residence time of 1-12s. The tars were measured by SPA (solid phase adsorption) method. They reported a considerable decrease in overall tars with increasing temperature at a particular residence time. Brage et.al. (2000) observed that by increasing the temperature from 700 to 900^{o}C, there was a considerable destruction of phenol, a 50% decrease in toluene but a considerable increase in naphthalene (1.9 to 8.8 mg/l) and benzene (14.2 to 23.5 mg/l). These increased compounds at the same temperature with increased residence times are reported to be decreasing. Temperature and residence time are the two interlinked operating parameters that define the amount of tars after gasification. Deglise et.al. (1985) determined residence times for almost complete conversion of tars and found it to be 15s at 800^{o}C and 5s at 1000^{o}C which shows the dependence of two variables on each other for tar reduction. High temperature and low residence time give the same result as does the low temperature with higher residence time, which is true because the aim is to keep the feed material in contact with the desired temperature for desired time (Wornat et al., 1987).

Several others in the literature have also shown that higher temperatures favor reduction in the overall amounts of the tar. But there are certain problems associated with the thermal cracking of tars. The difficulties of attaining complete thermal cracking along with operational and economic considerations make thermal cracking less attractive in current large-scale gasifiers using cleaner biomass feedstocks. High temperatures create higher amounts of char. With the decrease in tar amounts, there is a simultaneous increase in char formation (Zanzi et al., 2002). It also decreases the efficiency of syngas in terms of heating value as CO oxidizes to CO_2. Thus the concentration of the CO in the syngas decreases, which leads to a decrease in the heating value of syngas. Another

problem is the soot formation. Primary tars, which are the small molecular weight fragments released during pyrolysis, are very reactive and when these primary volatiles are further exposed to high temperature, further thermal breakdown and cross linking reactions take place which leads to formation of char and some thermally stable secondary tars and soot and observable decrease in tar content (Li and Nelson, 1996). Wornat et.al (Wornat et al., 1987) studied the distribution of aromatic ring systems in tars from pyrolysis of coal at higher temperature and observed the decrease in polycyclic aromatic compounds (PAC's) with a simultaneous increase in soot as the temperature increased from 1100 to 1500K. They also reported a preferential destruction of substituted PAH, relative to unsubstituted PAH. This suggests that the PAC's are a precursor to soot when treated at high temperatures. According to report from EWA B (Neeft et al., 1998), when the evaporated tars around the tar aerosol combust (at high temperature), the inner part of the tar aerosol will be heated by radiation and start to pyrolyze as a result of lack of oxygen containing reactants which results in formation of PAH's and soot.

As thermal cracking involves high temperature, a special attention is required for the reactor design. Therefore, the reactor walls have to be constructed of high temperature resistant inorganic materials (Neeft et al., 1998).

Catalytic Cracking

Due to the problems faced in thermal cracking, like soot formation (Neeft et al. 1998; Wornat et al., 1987; Li and Nelson, 1996) and reduction in the heating value of syngas (Singh et.al., 1986), catalytic cracking is preferred for tar destruction. Catalysts are used to accelerate the rate of reaction of tar decomposition so as to avoid using very

high temperatures and compromising on quality of product gas. Catalysts have been intensively used in past for this purpose, either in-situ with the biomass or using a secondary bed. In-situ catalysts are added either by wet impregnation of the biomass or dry mixing with the biomass. In the other case, a secondary bed is placed downstream of the gasifier and the raw gas is passed over a catalyst through fixed or fluidized bed under temperature and pressure conditions simulating that of gasifier. The technical suitability of a catalyst for tar destruction depends on its activity (how fast the reactions proceed in presence of a catalyst), selectivity (fractional conversion obtained) and stability (lifetime of a catalyst in terms of its thermal, mechanical and chemical stability) (Hagen, 2006). The reforming of the hydrocarbons passing over the catalyst may be by steam (Eq.1) or carbon dioxide (Eq.2) to produce additional CO and H_2 (Yeboah et al., 1980)

$$C_nH_x + mH_2O \longleftrightarrow nCO + (m + x/2)H_2 \quad (3.4)$$

$$C_nH_x + nCO_2 \longleftrightarrow nC + (x/2)H_2 \quad (3.5)$$

Extensive study has been performed on different catalysts with varied pre-treatment methods for decomposition of tars.

Dolomite catalysts

Dolomite ($CaMg(CO_3)_2$) is the most popular and most studied catalyst (either in bed or in secondary reactor) for tar reforming as it is both effective and inexpensive. Dolomite is an effective catalyst for tar reforming (Ekstrom et al, 1985.; Yeboah et al., 1980; Donnot et al., 1985) but it lacks activity for methane conversion(Ekstrom et al.; Yeboah et al., 1980). The heating value of the reformed gas increases with tar reduction over dolomite (Donnot et al., 1985) which may be attributed towards formation of methane (Yeboah et.al., 1980). Use of secondary bed seems to be more efficient than in

bed additions. In bed catalyst showed about 83% tar conversion (Corella J., 1988) whereas secondary beds cracked about 95% of tars (Aznar et al., 1992) at 900^{o}C. The residual tar content after cracking is highly dependent on the temperature in the region, so 860^{o}C is reported as minimum temperature for sufficient reforming of tars (Alden et al., 1988). Dolomite has also been used to observe the tar breakdown taking one compound as a model compound (Taralas et al., 1991; Simell et al., 1997; Simell et al., 1999) and dolomite has worked effectively for reforming of the respective compounds. Devi et.al., (Devi et al., 2005b; Devi et al., 2005c) reported the conversion of naphthalene, used as model tar compound, as 40% with untreated olivine. The heating pretreatment of olivine catalyst at 900^{o}C in presence of air increased the conversion to as high as 80%. Also, it was expected that calcination could activate the olivine. The catalytic activity for tar elimination of the calcined rocks is attributed to several factors such as a large pore size and surface area of the corresponding calcinates and a relatively high alkaline (K, Na) content(Simell et al., 1992). Olivine, $FeMg(SiO_4)_2$, has a much higher resistance to attrition than dolomite, which prolongs its life in fluidized beds. Dolomite was ~1.40 times more effective than raw olivine ($(MgFe)_2SiO_4$); however, there were ~4-6 times more particulates generated in the gasification gas than olivine (Corella et al., 2004). Although dolomite is very effective in tar reduction, there are still certain problems associated with it. Dolomite is observed to deactivate rapidly (Aznar et al., 1989; Aznar et al., 1992). The attrition rate is too high for this soft catalyst under high turbulence conditions of gasifier (Delgado et al., 1996). The conversion rate of tar catalyzed by dolomite was difficult to reach or exceed 90–95%. Although dolomite could reduce the

tar in syngas and change the distribution of tar compositions, it was difficult to convert the heavy tars by dolomite. The dolomite would be inactive since the particle was easily broken during gasification. The melting point of dolomite was low and the catalyst would be inactived resulting from the melting of dolomite (Zhang, 2003).

Nickel catalysts

Nickel based catalysts are extensively used for reforming hydrocarbons such as naphtha and methane (Ekstrom et.al., 1985). Nickel has the ability to increase the ammonia conversion (Hepola et al., 1999) and reverse the ammonia reaction making NO_3 emissions to reduce during biomass gasification (Dayton, 2002). Nickel supported on silica was observed to be effective for tar removal even at a low temperature but the activity was for a shorter time due to the accumulation of large amounts of carbon on their surface (Zhang and Amiridis, 1998). An effort to solve this problem was use of a nickel based catalyst, NiMo, which along with giving 95% conversion at 550^{o}C, also showed anti-coking ability (Dou et al., 2003). Nickel has been observed to give almost complete conversions of tars and its model compounds in the temperature range 700-900°C (Ekstrom et al.1985; Garg M., 1987; Zhang et al., 2004), but its use for hot gas conditioning of biomass gasification product gases is limited by deactivation caused by several factors. Sulfur, chlorine, and alkali metals that may be present in gasification product gases act as catalyst poisons. Coke formation on the catalyst surface can be substantial when tar levels in product gases are high. Coke can be removed by regenerating the catalyst; however, repeated high temperature processing of nickel catalysts can lead to sintering, phase transformations, and volatilization of the nickel (Dayton, 2002). Also, nickel catalyst is costly, intolerant to oxygen breakthrough and

cumbersome to dispose of (Kinoshita et al., 1995). Nickel catalysts must be employed in a downstream reactor; because as an additive in a fluidized-bed gasifier, nickel experiences rapid deactivation (Caballero et al., 1997).

Alkali metals based catalysts

Alkali metals are the highly reactive and electropositive monovalent metals belonging to group 1A of periodic table, lithium, potassium, calcium, sodium, rubidium, cesium and francium (El-Rub et al., 2004). They are usually present in the ashes of the plants (Bridgwater, 1994). These ashes can be used in-situ (dry mixing or wet impregnation) or in secondary bed to reduce tar contents. Studies have shown that carbonate, oxides and hydroxides of alkali metals can efficiently help in tar reduction (Mckee, 1983). The alkali metals are termed advantageous in terms of catalyst because of their natural production inside the gasifier in form of ash production. Alkaline metals can act as promoters present in commercial steam-reforming catalysts by enhancing the gasification reaction of carbon intermediates deposited on the catalyst surface (El-Rub, 2004). Alkali metals are effective for CO_2 gasification of carbon (Suzuki et al., 1992). Radovic et.al. (Radovic et al., 1984) studied the comparison of catalytic effects of potassium and calcium on the gasification of biomass in air and steam. Potassium achieves relatively high catalytic activity by chemical interaction with the carbonaceous support and is independent of the method of preparation and addition. Potassium was observed as a very active and highly dispersed catalyst (Radovic et al., 1984; Lee and Kim, 1995).

Fluid Catalytic Cracking Catalysts

FCC catalyst is an acid solid and has crystalline zeolite as its major compound. The catalytic sites in the zeolite are strong acids and provide most of the catalytic activity. The acidic sites are provided by the alumina tetrahedra (Yang, 2003). The acidic properties of zeolites are dependent on the method of preparation, the form, the temperature of dehydration, and the Si/Al ratio. The key properties of zeolites are structure, Si/Al ratio, particle size, and nature of the (exchanged) cation. These primary structure/composition factors influence acidity, thermal stability, and overall catalytic activity (El-Rub et.al., 2004). FCC has been studied for bio-oil refinery and a significantly high gas yield has been observed at 973K by applying zeolite catalyst (Corma et al., 2007). In the case of gasification of wood, FCC has also been shown to significantly reduce tar formation with increased gas production and heating value (Gil et al., 1999). The catalytic activity of the zeolites can be attributed to large surface area, large pore diameter and high densities of acid sites (Seshadri and Shamsi, 1998). These catalysts have an advantage of low cost, but a major disadvantage is rapid deactivation due to formation of coke.

Char

Char is a non-metallic material which is produced by heating biomass/coal at 400-500^{o}C in the absence of air for a prolonged period of time. In the literature, char was already noticed to have a good catalytic activity for tar removal in downdraft gasifiers (Ekstrom et al., 1984; Chembukulam et al., 1981; Abu El-Rub et al., 2008). And a two-stage gasifier, developed by the Technical University of Denmark uses char for tar reduction (Brandt et al., 2000). In these systems high tar removal is realized by passing

the volatiles through a combustion or partial oxidation zone followed by a char bed. Another study (Chembukulam et al., 1981) reported nearly complete conversion at 950^{o}C over char of teakwood sawdust. The conversion of tar over char is highly affected by the temperature used. The properties of char that make it a suitable catalyst are its pore size, surface area and the ash or mineral content (El-Rub, 2004). Abu et.al. (2008) compared the effect of char with other catalysts for effective tar breakdown and examined the effect of char on two model compounds, phenol and naphthalene using a secondary bed reactor. Phenol conversion was 100% at 900^{o}C but more than 98% phenol is already thermally converted at 900^{o}C. But naphthalene, which is the predominant stable compound at 900^{o}C (Milne and Evans, 1998), was converted at an efficiency of 99.6% in presence of char at the same temperature. Char showed the highest activity after nickel for tar removal when compared with calcined dolomite, olivine, used fluid catalytic cracking (FCC) catalyst biomass ash and commercial nickel catalyst (Abu El-Rub et al., 2008).

Char is a very low cost catalyst and becomes much more attractive because of its natural production inside the gasifier and of the possibility to be integrated in the gasification process itself. The use of char for decomposing tar has some advantages over the traditional catalysts. Firstly, chars, if deactivated, can be gasified or burned. In other words, there is no need of regeneration. Secondly, char is a byproduct from gasification and therefore a cheap material. Thirdly, char may be free from poisoning by sulfur, chlorine and volatile alkali and alkaline earth metallic (AAEM) species. The major problems with char as a catalyst is the deactivation due to coke formation at lower temperature ranges, that blocks the pores of the char and reduces the surface area of catalyst, and loss of catalyst as char gets further gasified due to steam and dry reforming

reactions. As coal char (Griffiths et.al., 1967, Hayashi et.al., 2002) and biomass char (El-Rub et.al., 2005, Chembukalam et.al., 1981) have been observed to be very active for decomposition of tar from pyrolysis or aromatic compounds like naphthalene, this encouraged further investigation on characteristics and mechanism of tar decomposition over char.

Hosokai et.al. (2008) worked on finding a mechanism for the tar decomposition over char and concluded that the aromatics were decomposed mainly by the coking while the steam gasification played an important role in maintenance or enhancement of the coking activity of the charcoal by creating micropores. The catalytic effect of coke can be supported by the work done by Hosokai et.al. (2005) where the activity of the alumina was promoted as carbonaceous deposit from the tar, termed coke, accumulated within pores of the alumina, and became high enough to completely eliminate tar constituents except for benzene and naphthalene within a gas residence time of about 30 ms. Yet, there is no comprehensive study available on biomass char for tar removal. So the main objective of this study is to find out how active and useful biomass char is for tar removal.

Fe Species as Active Site

Many studies have theorized that Fe^{3+} is responsible for increasing the activity of catalyst for tar cracking (Simell et al., 1992; Orio et al., 1997; Rapagna et al., 2000; Courson et al., 2002). Devi et.al (Devi et al., 2005b) observed higher conversion of naphthalene with pretreated olivine as compared to the untreated one. The pretreated olivine was found to have Fe segregation on the surface when observed through X-ray photoelectron spectroscopy (Devi et al., 2005a). Surface Fe on the catalyst is found to be

active for tar cracking reactions. Metallic Fe is the site for high activity and is effective for C-C and C-H bond making and breaking (Kuhn et al., 2008). Furthermore, lattice oxygen in metal oxides can be utilized to reform hydrocarbons (Xu and Tomita, 1989). They tested 4 metal oxides (Al_2O_3, SiO_2, CaO and Fe_2O_3) and quartz beads for cracking of aromatic hydrocarbons and found Fe_2O_3 to be the most active metal oxide to decompose most of the hydrocarbons at 900^oC producing a small amount of CH_4. Impregnation of catalysts with iron has proved to be effective. Alumina impregnated with iron was observed to have a higher activity for tar reforming as compared to untreated alumina (Matsuoka et al., 2006). The hydrogen production is also improved with addition of iron oxide particles as catalyst because of the reaction pathway of cracking of coke on iron oxide particle which can be expressed as (Fukase and Suzuka, 1993).

$$\text{Coke}/Fe_3O_4 + O_2 \longrightarrow 3FeO + CO + CO_2 \qquad (3.6)$$

$$3FeO + H_2O \longrightarrow Fe_3O_4 + H_2 \qquad (3.7)$$

The hydrocarbon reforming and hydrogen production due to iron oxide can be shown by the following reaction mechanism (Fukase and Suzuka, 1993):

$$(2n+m)\ Fe_xO_y + C_nH_{2m} \longrightarrow (2n+m)\ Fe_xO_{y-1} + nCO_2 + mH_2O \qquad (3.8)$$

$$Fe_xO_{y-1} + H_2O \longrightarrow Fe_xO_y + H_2 \qquad (3.9)$$

Oreo et.al. (Orio et al., 1997) observed an increase in activity of dolomite with increase in percent iron oxide present in them, which indicates that iron oxides are responsible for catalytic activity of tar reforming. Another study declined the effect of iron oxides as catalyst for tar decomposition (Nordgreen et.al., 2006). This is regarded to oxygen potential in the product gas that varies quite sharply between metallic iron and its oxides. Metallic iron was observed to be a capable catalyst for carbon breakdown and if metallic

iron is used as a tar breakdown catalyst in a catalytic bed during biomass gasification, the product gas does not have sufficient oxidizing power to completely transform the metallic iron state to its first oxide. The tar content from pyrolysis gas reduced from ~17 to 2 mg/g of biomass in presence of metallic iron. Świerczyński *et.al.* (2008) attributed toluene conversion uniquely to the presence of reduced iron species using olivine as catalyst.

Decomposition of Model Biomass Tar

Many researchers have studied the activity of catalysts for tar decomposition using a model tar compound. Simell et.al. (1997) studied benzene as a model compound over dolomite as a catalyst. They reported maximum benzene conversion of ~10% with 1.5 *10^{-4} kg and ~14% with 2.3*10-4 kg of dolomite catalyst (*T* 1073 K; feed CO_2 10 vol %, benzene 50 ppmv, space time ~1000 kg-cat-h/kmol). In another study, five catalysts, CaO, SiO_2, Al_2O_3, CuMn and NiMo, were tested for their catalytic activity over methylnaphthalene as a model tar compound in a fixed bed reactor (Dou et al., 2008). They observed NiMo to be the most effective catalyst that gave around 80% conversion at 550^{o}C. This catalyst was found to have maximum surface area out of all five catalysts. NiMo catalyst is used in another study in comparison to limestone and dolomite for n-heptane conversion and has been found to give 97.8% conversion in comparison to 90% and 84% given by limestone and dolomite at 973K (Taralas, 1996). It was also observed that addition of CO_2 and H_2 decreased the conversion of n-heptane. Depner and Jess (1999) studied the reforming of tar model compounds, naphthalene and benzene, in a tubular flow reactor at elevated temperature and pressure (1150^{o}C, 160kPa). The gases (simulating the syngas) and the model compounds were passed over fixed bed of Ni catalyst. A complete conversion for naphthalene was obtained at 750^{o}C, but benzene

showed a maximum conversion of 30% (Depner and Jess, 1999). In the same experiment, when thermal effect was observed without adding any catalyst, the complete conversion of toluene could be seen at 1050^{o}C but that of naphthalene and benzene was observed at 1400^{o}C (Jess, 1996). They also observed that soot formed react with H_2O in the later reaction steps, but more than 1400^{o}C is required for complete soot destruction.

Nickel has also been used on a candle filter and has been observed for naphthalene conversion (Zhao et al., 2000). The pores of the candle filter were activated with a nickel based catalyst. Syngas mixture along with naphthalene was passed through the filter and exit was collected in an ice bath. The reaction temperature was maintained at 750-900^{o}C and a complete conversion was obtained at 800^{o}C. Nacken et.al. (2009) studied the performance of a catalytically activated ceramic hot gas filter for catalytic tar removal from biomass gasification gas. They used a filter element support coated with CeO_2, $CaO–Al_2O_3$ and MgO. They also observed 100% naphthalene conversion with 60 wt% NiO loading on a MgO coated filter element. This design is suitable for removal of tars and particulate materials. A disadvantage of this design is the manufacturing of several parts and its assembling in this special filter element design (Nacken et al., 2009).

Toluene is another model compound widely studied for the catalytic activity of different catalysts. It is used as model compound because it contains both aromatic moiety (phenyl) and aliphatic moiety (methyl) (Cheng et al., 2009). It constitutes about 24% of the total tars present in the syngas. Toluene is one of the least reactive among all tar components and it represents a stable aromatic structure in tar formed at high temperature processes (Amacz et al., 2009). Toluene is used in this study as a model tar compound because of this reason.

Using a nickel/olivine catalyst, toluene conversion was 100% at 650^{o}C, compared to using only olivine which gave <5% at 750^{o}C. A 40% conversion was obtained for Ni/olivine at 560^{o}C and for olivine at 850^{o}C (Swierczynski et al., 2008). Nickel on alumina has been used for toluene reforming but the conversions were no promising (20-60%) even when the high reaction temperatures were used (Coll et al., 2001). It was also observed that tendency of coke formation gets stronger with number of aromatic rings in the molecule.

The overview of the literature on decomposition of model compound of biomass tars is given in tabular form in Appendix A.

Kinetic models have been developed for reforming of tar and/or model compounds. The temperature dependence of the rate constant is determined by Arrhenius equation, from which activation energy and pre-exponential factor can be calculated. The activation energy of steam reforming of model tar compounds from other works can be summarized as in table 3.1.

Table 3.1: Summary of the activation energies calculated for tar/model compounds

Tar/Model compound	Catalyst	Activation energy (kJ/mol)	Reference
Toluene	No catalyst (Thermal cracking) + O_2	365 ± 5	(Taralas et al., 2003)
Toluene	No catalyst (Thermal cracking) + H_2	250 ± 10	(Taralas et al., 2003)
Toluene	Ni/Mayenite	80.24	(Li et al., 2009)
Toluene	Ni/Olivine	196	(Swierczynski et al., 2008)
Naphthalene	Char	61	Abu El-Rub et al., 2008
Naphthalene	Olivine	141	Devi *et. al.*, 2005
Tar	Ni based	72±12	Narvaez et.al.,1996
	Calcined dolomite	84±6	Narvaez et.al.,1996
Tar	Dolomite	42	Delgado et. al., 1997
	Calcite	42	Delgado et. al., 1997
	Magnetite	42	Delgado et. al., 1997
Tar	Norte Dolomite	100 ± 20	Orio et.al., 1997
	Chilches Dolomite	100 ± 21	Orio et.al., 1997
	Malagan Dolomite	100 ± 22	Orio et.al., 1997
	Sevilla Dolomite	100 ± 23	Orio et.al., 1997

CHAPTER 4

MATERIALS AND METHODS

Experimental Setup for Continuous Flow Study for Catalytic Conversion of Toluene

The catalytic conversion of toluene was studied in a continuous flow packed bed reactor system (fig. 4.1) at different temperatures (550-900^{o}C) and atmospheric pressure. Nitrogen, used as carrier gas was passed through the reactor and then streams of toluene and water were mixed in the main flow metered by 2 syringe pumps (Cole-Parmer-74900 series). Toluene (1000-4000 ppmv) was injected using a Cole Parmer stainless steel syringe (vol., 60 ml i.d 1 in) via a tee (stainless steel, swage lock) and water (3 times concentration of toluene) was added using Becton Dickinson syringe (Plastipak 60 ml, Luer lok tip) via a tee (stainless steel, swage lock) into the main N_2 flow. The nitrogen, toluene and water mixture was then passed through a static mixer (stainless steel, length21", o.d. ¼") and then transported down the reactor (stainless steel, length 60 cm, i.d. 1"), covered by a furnace (Lindberg Blue M), containing of 45 cm of preheating zone followed by 3 cm of reactive column packed with catalyst. Nitrogen used was from medium grade tank of nitrogen. Mass flow controller (UNIT UFC-8100) was used to control the flow rate of nitrogen. Two thermocouples (K-type, ¼" dia) and two pressure gauges (Span (0-30psi)) were used at inlet and exit of the reactor respectively. Additionally, five thermocouples (1/16" dia, K-type) were installed throughout the length of the reactor to observe the temperature profile of the reactor. All thermocouples were

logged on DaqPro data logger (DaqPro 5300) attached with a Dell Laptop. The catalysts used in the process were packed over a defined height (3 cm) in the reactor supported by steel wire mesh (1" dia) and quartz wool (Leco fine quartz wool). Tees (stainless steel, Swage-Lok) with septum were installed at the inlet and outlet of the packed-bed reactor column for sampling. There was an assumption of no temperature gradient between the surface and center of reaction zone. All tubing used was 9.5 mm (i.d.) Teflon with fittings constructed of stainless steel (Swage-Lock). All lines were traced at 200^{o}C to avoid any condensation in the lines. The exit gas was cooled using ice bath and exhausted.

The catalytic conversion of toluene using all catalysts was carried out with same mass of catalyst (3.8 g) for ease of comparison. The residence time of the gas mixture in the catalyst bed was calculated using the following equation

$$\tau = Residence\ time = \left(\frac{Packing\ volume}{Q}\right) = \left(\frac{HA}{Q}\right) \qquad (4.1)$$

where, Q is the flow rate (700 ml/min), H is the height of the packing (3 cm) and A is the cross sectional area of the reactor (13.14 cm^3).

Sampling Method

The adsorption and desorption of toluene was tested for 2 runs to determine the breakthrough time, which was found to be 130 minutes and that time was given to reactor to run idle for all remaining runs. During the run, a syringe (Hamilton Co. Reno, 1 ml syringe with stop valve) was used to withdraw 200 µl (split less) gas samples from inlet and exit directly from the septum. Four samples from the exit were run for 10 minutes to observe all possible peaks. The last peak observed in the exit was for toluene at 2.93 minutes, so the run time set for all other analysis was set to be 3.5 minutes. To make sure the exit is taken for the same inlet measured, it was taken 30 seconds later then the inlet

so that the same volume of inlet passes through the reactor and is measured in exit. The septum on inlet and exit was changed every two runs. The sample was injected in a GC-FID (Hewlett Packard, 5890 series II, HP 5 MS capillary column, 30m X 0.25µm, diameter 0.25 mm). The oven temperature of GC-FID was set at 50°C, detector at 220°C and injector at 200°C. The syringe was purged with nitrogen every two consecutive readings of inlet and exit. A blank was inserted in GC-FID every 16 readings.

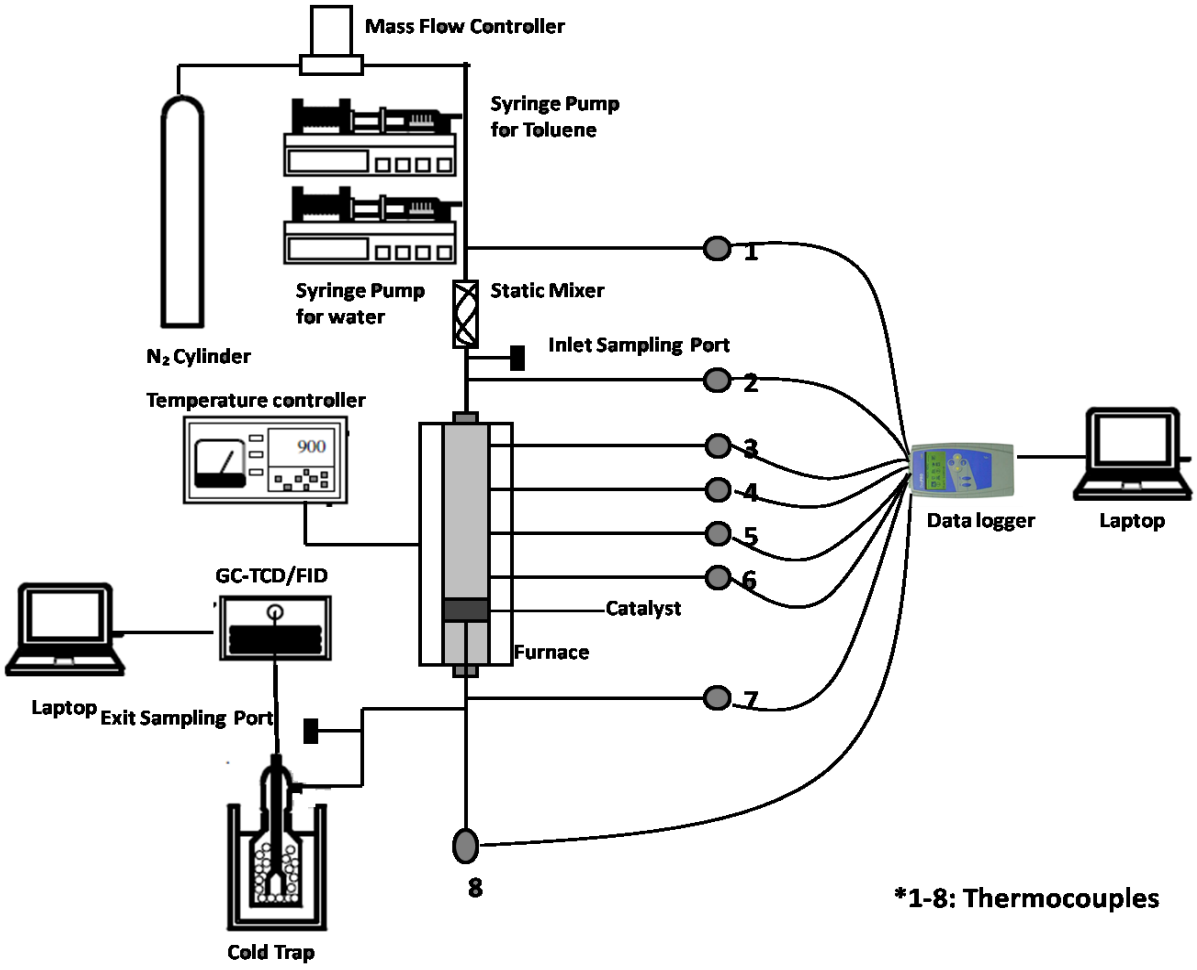

Figure 4.1: Experimental Setup for toluene decomposition

Catalyst Preparation

Four catalysts were compared for catalytic activity to decompose toluene. Char was the focus catalyst. Char was prepared by pyrolyzing the pine bark (Southern Pine bark, Waycross, GA) at 950^{o}C for 2 hours. The char was then crushed in a knife mill and then sieved to get particle size 212-420μm. Another catalyst used was char pretreated with ferrous nitrate in three combinations. Two of the combinations were made by dissolving 16 grams of ferric nitrate ($Fe(NO_3)_3.9H_2O$) (Sigma Aldrich 98+%) in 20 ml of acetone (Sigma-Aldrich) and adding 20 and 15 grams of char respectively. The third combination was made by dissolving 24 grams of ferric nitrate in 30 ml of acetone and adding 12 grams of char in it. These mixtures were soaked in the solution for 30 minutes. There was no excess liquid to be decanted left. The sample was dried at 105^{o}C in an air convection oven for 8 hours. The dried sample was calcined at 300^{o}C for one hour in a furnace with an air flow of 10 l/min.

Wood fly ash from a pulp mill was used as a catalyst. The physical and chemical characteristics of the fly ash, including pH, surface area, bulk density, and the elemental composition were previously determined (Kastner and Das, 2002).

Standard Curve

Standard curves for toluene were made from neat liquid toluene (Sigma-Aldrich, purity 99%) over a range of 50-5000 ppmv. A known volume of toluene was mixed with a known volume of Nitrogen in a tedlar sample bag (SKC, Houston, TX) and analyzed using the GC/FID. The corresponding peak area of the toluene was measured. The same procedure was repeated for different concentrations of toluene in the range of 50-5000 ppmv. Finally the standard curve was obtained by plotting the concentration of toluene

against the corresponding peak area. The standard curve obtained was used for the further analysis of the inlet and outlet concentrations of toluene. The standard curve is shown in Appendix A. Similarly standard curves were made for CO, H_2, CO_2 and CH_4 in GC/TCD. Pure sample of these gases mixed with known amount of nitrogen was injected in TCD to find the corresponding areas in GC/TCD. Combining all points, standard curves were made. Similar method was used for benzene calibration too. The calibration of CO_2 and CH_4 was done by adding known percentage of CO_2 and CH_4 in rest of nitrogen. The final concentration was injected in GC-TCD and area was calculated. The calibration curves for toluene, benzene, CO_2 and CH_4 are given in the Appendix B.

Thermal Cracking of Toluene

The continuous flow system was also used to measure the thermal cracking of toluene with (a) a bed of quartz beads as inert material and (b) empty bed reactor. In this case, the residence time was kept equal to the residence time used with catalysts (1.15 sec on empty bed reactor basis) for ease of comparison. The thermal cracking of toluene was then compared to the cracking obtained with all the catalysts.

Evidence of Catalytic Activity of Biochar

A series of experiments was conducted to confirm the catalytic activity of biochar using toluene as a tar model compound. Catalytic cracking of toluene was carried out at the same temperatures as thermal cracking experiments (600, 700, 800 and 900°C) with same inlet toluene concentration (2500 ppmv). An experiment was performed using quartz wool only at room temperature with ~2500 ppmv toluene passing through with 0.7 l/min N_2 gas to see if it contributes to toluene decomposition. Finally, char supported on quartz wool was used in the decomposition of toluene (~2500 ppmv) with a residence

time of 1.15 s over the temperature range of 600-900°C. Over the 730 min period for which the experiment was conducted, readings of each temperature were taken for 80 min and the rest of the time was for equilibration of the inlet, exit and conversions. After the fractional conversion of toluene was obtained for 550°C, the temperature was ramped to 600°C and readings were taken after the conversions stabilize (till the temperatures ramp). Similarly, readings were taken for 650, 700, 800 and 900°C.

Potential Reactions and End Products

One mechanism proposed by Morita (Simell et.al., 1994) is

$$C_7H_8 \longrightarrow 7C(s) + 4H_2 \quad (4.2)$$

$$C(s) + H_2O \longrightarrow CO + H_2 \quad (4.3)$$

$$CO + H_2O \longrightarrow CO_2 + H_2 \quad (4.4)$$

$$C(s) + 2H_2O \longrightarrow CO + 2H_2 \quad (4.5)$$

During steam reforming, there are many parallel reactions going on. Main gaseous products of toluene steam reforming are H_2, CO, CO_2 and benzene (Taralas, 2000). The dealkylation reaction of toluene by water is

$$C_7H8 + 2\ H_2O \longrightarrow C_6H_6 + CO_2 + 3H_2O \quad (4.6)$$

$$\Delta H_{r\ (1173K)} = -90KJ\ mol^{-1}$$

$$C_7H_8 + 3H_2O \longrightarrow C_6H_6 + CO + 2H_2 \quad (4.7)$$

$$\Delta H_{r\ (1173K)} = -123KJ\ mol^{-1}$$

The net reaction is

$$2C_7H_8 + 3H_2O \longrightarrow 2C_6H_6 + CO_2 + 5H_2 + CO \quad (4.8)$$

$$\Delta H_{r\ (1173K)} = -213KJ\ mol^{-1}$$

Steam reforming:

$$C_7H_8 + 7H_2O \longrightarrow 7CO + 11H_2 \quad (4.9)$$

$$\Delta H_{(800^oC)} = 927.2kJ\ mol^{-1}$$

$$C_7H_8 + 14H_2O \longrightarrow 7CO_2 + 18H_2 \quad (4.10)$$

$$\Delta H_{(800^oC)} = 688.5kJ\ mol^{-1}$$

Water–gas shift

$$CO + H_2O = CO_2 + H_2 \quad (4.11)$$

$$\Delta H_{(800^oC)} = -34{:}1kJ\ \_mol^{-1}$$

Dry reforming

$$C_7H_8 + 7CO_2 \longrightarrow 14CO + 4H_2 \quad (4.12)$$

$$\Delta H_{(800^oC)} = 1166.0kJ\ mol^{-1}$$

Hydrodealkylation

$$C_7H_8 + H_2 \longrightarrow C_6H_6 + CH_4 \quad (4.13)$$

$$\Delta H_{(800^oC)} = -50.9kJ\ mol^{-1}$$

Methane steam reforming

$$CH_4 + H_2O = CO + 3H_2 \quad (4.14)$$

$$\Delta H_{(800^oC)} = 225.7kJ\ mol^{-1}$$

Other reactions such as carbon formation reaction by toluene decomposition and cracking also are included in the process.

Catalytic Cracking of Toluene with Biochar

Reaction Temperature Effect

In the continuous flow experiments, char (3.8 g) was used in the above described packed bed reactor with toluene concentration of ~2500 ppmv passing through the reactor with 0.7 l/min of nitrogen as carrier gas. The temperatures 600, 700, 800 and 900°C were

used to measure the fractional conversion of toluene and the formation of by-products. After reaching 600°C temperature, toluene was made to flow at a particular flow rate (~2500 ppmv). Once the toluene is injected, it took around 75 minutes to equilibrate the exit and the corresponding conversion due to adsorption and desorption on the char surface. The setup was run for 130 minutes in total before any conversion values for a temperature were taken. 80 minutes was the run time for each temperature and 35-45 minutes were given for temperature ramping in between the two temperatures. This procedure was followed for all the runs made. The GC/FID unit was used to measure the inlet and outlet concentrations of toluene and other hydrocarbons produced as by-products. GC/TCD unit was used to find the concentrations of CO_2 and CH_4. Thirty µl of gas sample was injected in the TCD with a syringe (Hamilton 0.1ml syringe). An online GC/TCD unit was used to measure the H_2 and CO concentrations. Gas samples were directly drawn from septum in tees at the inlet and outlet of the reactor column. The gas samples were analyzed under isothermal conditions (30^oC).

The toluene conversion was measured using the formula in eq. 4.15. The data points that represent the model tar compound conversion were average points. For every point, 8 pseudo-replicates and 3 run replicates, on average, were taken.

$$X\ (\%) = \frac{C_{in} - C_{out}}{C_{in}} \qquad (4.15)$$

where,

X = tar conversion

C_{in} = inlet tar concentration

C_{out} = outlet tar concentration

Hydrogen yield, Y_{H_2} is expressed as the percentage of the stoichiometric potential corresponding to the total conversion of toluene according to the steam reforming reaction 4.16

$$Y_{H_2}(\%) = \frac{[C_{H_2}]_{out}}{18[C_{T,in} - C_{T,out}]} * 100 \qquad (4.16)$$

The carbon containing products (CO, CO_2, CH_4) are calculated by the selectivity S_i (Eq.4.17), which are defined as the ratio of the amount of carbon in the product *i* to the amount of carbon in the reacted toluene.

$$S_i(\%) = \frac{[C_i]_{out}}{7[C_{T,in} - C_{T,out}]} * 100 \qquad (4.17)$$

$[C_i]$: molar flow rate *i*=CO, CO_2, CH_4

The selectivity of benzene S_B is calculated by Eq. (4.18)

$$S_B(\%) = \frac{[C_B]_{out}}{[C_{T,in} - C_{T,out}]} * 100 \qquad (4.18)$$

$[C_B]$: molar flow rate of benzene in the products.

Inlet Concentration Effect

Four concentrations were used for observing the effect on fractional conversion of toluene and the reaction rate. The procedure of sampling and analysis was same as previous. These concentrations with their respective fractional conversions of toluene were further used to calculate reaction rates for the decomposition of toluene. Therefore, the temperatures of reaction were chosen on the criteria of the fractional conversion being less that 25% as a requirement for differential reactor. So, the temperatures chosen were 500, 550, 600 and 650°C.

Catalytic Cracking with Iron Loaded Biochar

Reaction temperature effect

The procedure for determining the effect of temperature on toluene decomposition with char was followed for iron loaded char also. All three loadings were subjected to the same operating parameters (3.8 g of catalyst, 600-900°C temperature range, 2500 ppmv inlet concentration of toluene and 0.7 l/min flow rate of nitrogen). Same parameters were chosen for valid comparison between char and the different loadings of iron.

Inlet concentration effect

Procedure followed for iron loaded char was the same as for char, but the temperatures were chosen so as to give <25% conversion. So the temperatures chosen were 400, 450, 500 and 550°C. The effect of concentration and kinetic study was done only on 1 loading of char (18.7%).

Kinetics Calculations

The kinetics of catalytic oxidation was studied based on the following premises:

(i) In order that the experimental data could be used in the kinetic analysis, potential external and internal mass transfer resistance had to be ruled out.

(ii) Due to the inability to obtain to VOC concentrations along the length of the reactor column, a differential reactor with a small amount of catalyst was used and hence a low conversion of reactant was obtained.

(iii) To reduce the relative error caused by using an approximate rate equation for calculating the reaction rate, average concentrations of inlet and outlet reactants should be adopted.

(iv) To reduce relative error caused by using an approximate rate equation for calculating reaction rate of a differential reactor, average concentrations of inlet and outlet reactants should be adopted.

(v) The heat of reaction in the packed-bed reactor did not increase the temperature and thus the temperature across the reactor radially was assumed to be constant (isothermal) i.e., it was assumed that there was no radial temperature difference.

To verify plug flow conditions in the fixed bed, we need to calculate the dimensionless Peclet number (Pe).

$$Pe = v.\frac{L}{D} \qquad (4.19)$$

Pe ⟶ 0, large dispersion, hence mixed flow
Pe ⟶ ∞, negligible dispersion, hence plug flow

Where,
L = length of the catalyst bed, m
v = velocity, m/s
D = dispersion coefficient, m^2 /s

The Peclet number for the present experiments was found to be very high, hence plug flow conditions can be assumed. The volumetric flow rate through the catalyst bed is monitored, as are the entering and exiting concentrations. Therefore, if the mass of catalyst, ΔW, is known, the rate of reaction per unit mass of catalyst, $-r_A'$, can be calculated. Since the differential reactor is assumed to be gradientless, the design equation will be similar to the CSTR design equation. A steady-state mole balance on reactant A gives

[Flow rate in] – [Flow rate out] +[Rate of generation] = [Rate of accumulation]

$$[F_{T0}] - [F_{Te}] + \left[\left(\frac{Rate\ of\ reaction}{Mass\ of\ catalyst}\right)(Mass\ of\ catalyst)\right] = 0 \qquad (4.20)$$

$$[F_{T0}] - [F_{Te}] + (r'_A)(\Delta W) = 0 \qquad (4.21)$$

The subscript e refers to the exit of the reactor. Solving for - r_A , we have,

$$-r'_A = \frac{F_{Ao} - F_{Ae}}{\Delta W} \qquad (4.22)$$

The mole balance equation can also be written in terms of concentration (Differential reactor equation)

$$-r'_A = \frac{v_0 C_{A0} - v C_{Ae}}{\Delta W} \qquad (4.23)$$

Concentration of A at inlet is termed C_{Ao} and at exit is C_{Ae}

or in terms of the conversion or product flow rate F_p,

$$-r'_A = \frac{F_{Ao} X}{\Delta W} = \frac{F_p}{\Delta W} \qquad (4.24)$$

X refers to fractional conversion of A

The term $F_{A0}X$ gives the rate of formation of the product, F_p, when the stoichiometric coefficients of A and of P are identical. For constant volumetric flow, Equation (4.9) reduces to

$$-r'_A = \frac{v_0 (C_{A0} - C_{Ae})}{\Delta W} = \frac{v_0 C_p}{\Delta W} \qquad (4.25)$$

Plotting different r'_A 's with concentrations, give a straight line that provide with the rate constant assuming a first order rate law. Temperature dependence of rate constant is calculated by plotting Arrhenius equation (equation 4.12). The activation energy of toluene decomposition in presence of char can be calculated using the slope of the line.

$$k = Ae^{-E_a/RT} \qquad (4.26)$$

where,

k = Reaction rate constant (s^{-1})

A = Pre-exponential factor

R = Universal Gas constant ($JK^{-1}mol^{-1}$)

E_a = Activation energy (kJ/mol)

T = Reaction temperature (K)

In case R^2 values for plot of natural log of rate constant versus inverse of Temperature are low (as in our case), then the first order rate constants can be calculated according to the equation (9) derived from an integral plug flow reactor model (Levenspiel, 1975).

As in differential reactor, a steady-state mole balance on reactant T (Toluene) gives (continuing from eq. 4.8)

$$-r'_A = \frac{F_{To} - F_{Te}}{\Delta W} \qquad (4.27)$$

which can be written as

$$-\frac{dF_t}{dW} = -r_A \qquad (4.28)$$

As $-r_A = kC_T$ and $F_T = Q\,C_T$ (Q is the total flow rate in the reactor and C_T is the toluene concentration passing through the reactor)

$$-Q\frac{dC_T}{dW} = kC_T \qquad (4.29)$$

Integrating,

$$-\int_{C_{T_o}}^{C_T} \frac{dC_T}{C_T} = \frac{k}{Q}\int_0^W dW \qquad (4.30)$$

$$-\ln\frac{C_T}{C_{T_o}} = k\left(\frac{W}{Q}\right) \qquad (4.31)$$

W/Q is regarded as space time with units, kg-hr m^{-3}

$$\ln\frac{C_{T_o}}{C_T} = k\left(\frac{W}{Q}\right) \qquad (4.32)$$

The conversion (X) can be written as

$$X = \frac{C_{T_o} - C_T}{C_{T_o}} \qquad (4.33)$$

$$\Rightarrow\ C_T = C_{T_o}(1 - X) \qquad (4.34)$$

$$\ln\left(\frac{1}{1-X}\right) = k\left(\frac{W}{Q}\right) \qquad (4.35)$$

$$-\ln(1-X) = k\frac{W}{Q} \qquad (4.36)$$

$$k = \frac{-\ln(1-X)}{W_{cat}/Q} \qquad (4.37)$$

Using this k value for all temperatures, where calculated toluene conversion is higher than 25%, the Arrhenius equation can be plotted to calculate the activation energy (eq. 4.12).

Catalyst Longevity

A measure amount (3.8 g) of both char and the 13% iron loaded char were subjected to continuous flow reactor at 800°C with an inlet flow rate of 0.7 l/min of nitrogen with 2500 ppm of toluene flow and 6250 ppm of water flow for a long time till the conversion becomes zero. This would give us the life of catalyst; i.e. for what time and how many reactor volumes of tar can it pass through keeping the conversion constant.

Catalyst Characterization

Characterization of the catalysts had been done to investigate the cause for catalytic properties responsible for decomposition of toluene. The study included X-Ray

Diffraction (XRD) and scanning electron microscopy-Energy Dispersive Spectroscopy (SEM-EDS) analysis.

Proximate analyses and CHNS composition was performed on the char. The CHNS composition was determined in a LECO CHNS932 that was calibrated using sulfa methazine as a standard. The CHNS composition was determined in accordance to ASTM D5291. The proximate analysis was performed on a LECO TGA731 according to ASTM D3176.

The SEM gives the surface images of the catalyst which indicated the metals present and their dispersion on the surface. It characterizes sample's surface topography, composition and electrical conductivity. *FEI Inspect F* field emission gun scanning electron microscope (*FEG-SEM*) equipped with an *EDAX* energy dispersive x-ray spectrometer was used to observe the sample surface and analyze the elements present on the surface.

Table 4.1: Compositional analysis of catalysts (Elements in % of total composition)

	Pine (Pinus Insularis) Bark	Char@950^{o}C
Carbon	52.10	88.18
Hydrogen	6.241	0.483
Nitrogen	0.393	1.049
Sulfur	0.032	0.024
Fixed carbon	23.42	93.54
Volatiles dry	75.77	3.78
Ash dry	0.81	2.68
Oxygen (By difference)	40.46	7.61

CHAPTER 5

RESULTS AND DISCUSSION

Thermal Cracking of Toluene

Thermal cracking of toluene was conducted with (a) quartz beads in place of catalyst and (b) empty reactor without any packing. A constant concentration of toluene (2500 ppmv diluted with N_2 gas) and steam (7500 ppmv) was used to determine the fractional conversion of toluene at four different temperatures (600, 700, 800 and 900°C). Figure 4.1 showed the fractional thermal cracking of toluene with (a) quartz beads and (b) empty reactor . In case of the thermal cracking of toluene with quartz beads, the fractional conversion started to increase from 3.36% at 600°C to 63.77% at 900°C.The thermal cracking of toluene with an empty reactor also showed the similar trend with reaction temperature, but the fractional conversion was statistically lower than that with the quartz beads. This may be because when toluene passes through quartz beads, there is an increased heat transfer to toluene due to conductance which raises the temperature of toluene quicker than that in empty bed, resulting in higher thermal conversion of toluene at same reaction temperature. Thermally, toluene seemed to be quite stable until 700°C reaction temperature. The results were in agreement with other works on thermal cracking on toluene (Taralas et.al.,2003; Zhang et.al., 2009). Complete thermal cracking of toluene can be possible at reaction temperature higher than 900°C, but may require additional energy input.

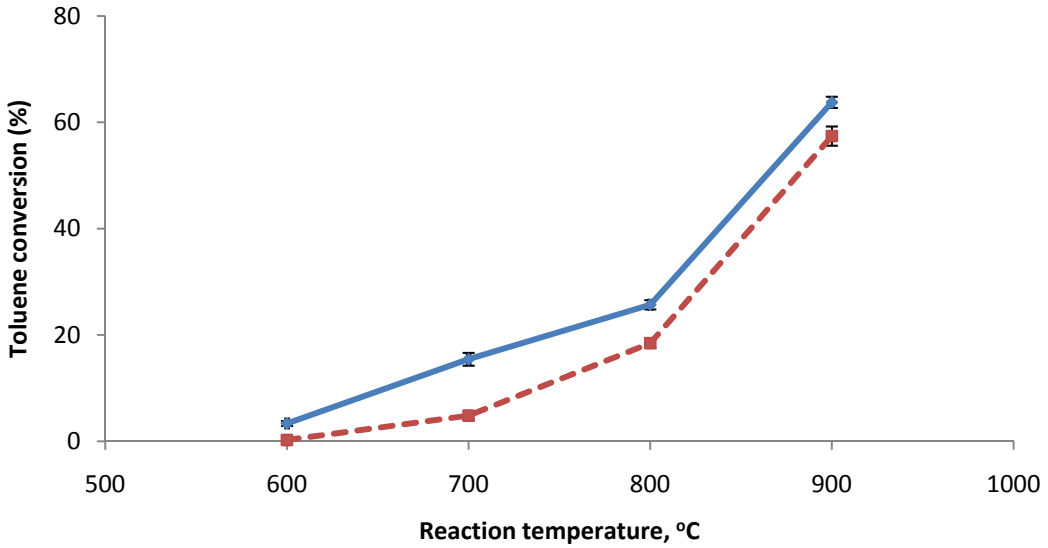

Figure 5.1: Percent conversion of toluene without catalyst as a function of reaction temperature (Nitrogen gas flow 0.7 l/min, inlet toluene concentration ~2500 ppmv, space time = 0.09 kg_{cat} h m^{-3}), with quartz beads, empty reactor.

Evidence of Catalytic Activity of Biochar

Figure 5.2 shows the fractional conversion of toluene with quartz wool only at room temperature to check effect of support material on the toluene conversion. Based on the inlet and outlet concentrations of toluene over the time period of the experiment, there was no statistical evidence to prove that quartz wool had played a role in the breakdown of toluene and hence the effect of quartz wool in the catalytic decomposition of toluene when used as the support material for char can be neglected.

Char supported on quartz wool used in the decomposition of toluene (~2500 ppmv) with a residence time of 1.15 s over the temperature range of 600-900^{o}C gave conversions higher than thermal cracking. Preliminary study on catalytic breakdown of toluene was investigated with gas samples analyzed using GC-FID. Gas chromatography

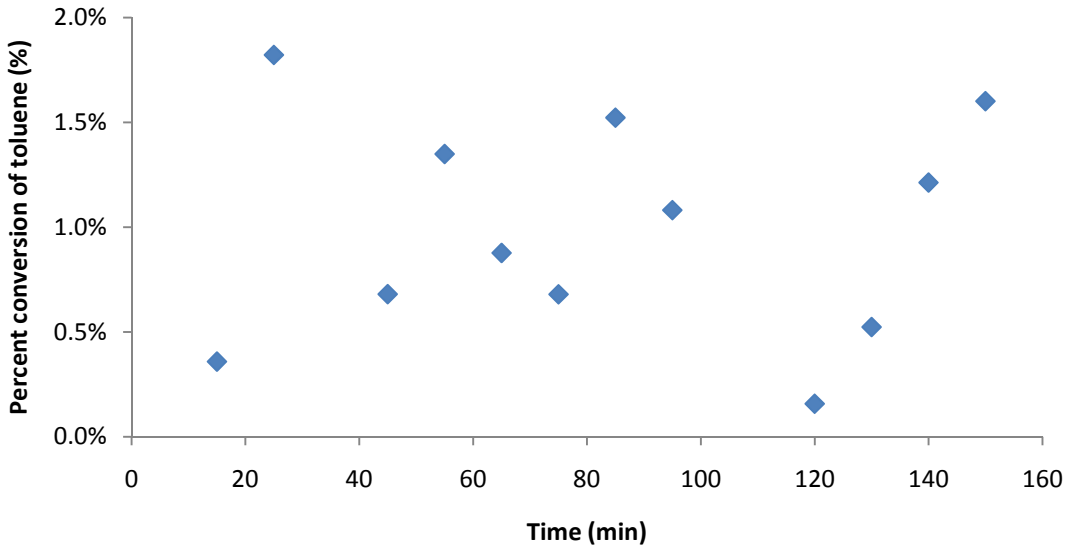

Figure 5.2: Percent conversions of toluene with quartz wool over a time period of 150 min at room temperature (~2500 ppmv toluene inlet concentration).

data presented in Fig 5.3 showed two unknown peaks on the exit of the gas samples indicating breakdown of toluene compound during catalytic reaction. The result clearly indicated that biochar was acted as a catalyst to partially or completely breakdown toluene at 900°C. The varying response in the percentage conversions could be because of the fluctuations in toluene flow and any experimental errors.

Figure 5.4 showed the typical fractional conversion data collected at all reaction temperatures In this run, after 75 minutes, when the equilibrium was reached, the char gave 11.6% conversion at 550°C. It increased to 12.5% at 600°C, which was a very slight increase. There was a steady increase thereafter till 700°C with conversions 19.5 and 26.5% at 650 and 700°C, but a sharp increase was observed at 800 and 900°C where the conversions were 45% and 94% respectively on an average.

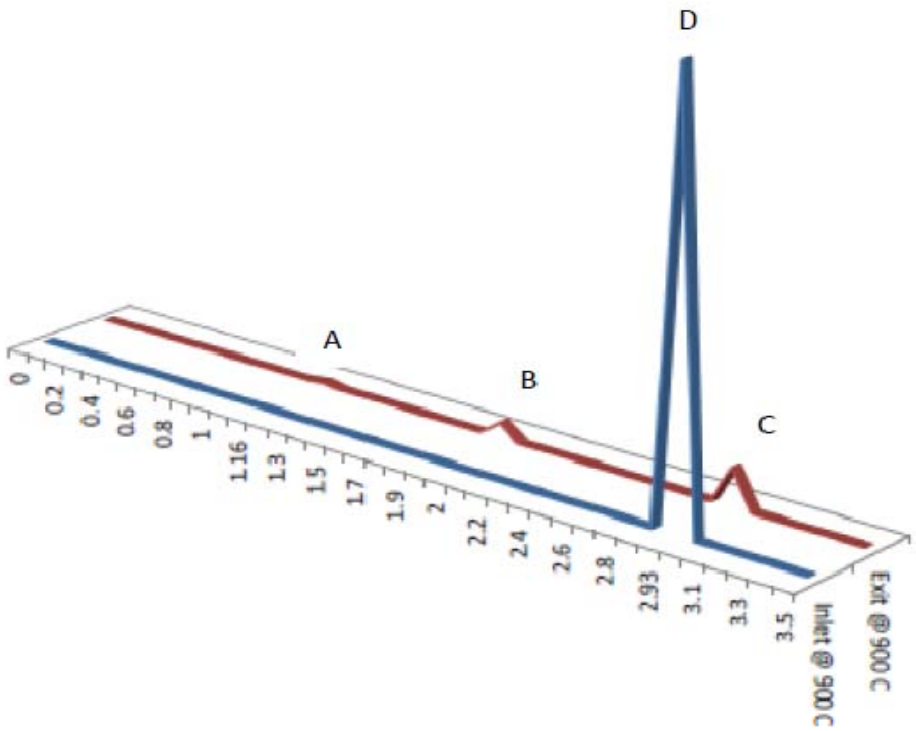

Figure 5.3: GC/FID chromatograms (peak signal versus time) for inlet and off gases in exit (passed through char bed)-3.8g of char, ~2500ppmv inlet concentration, 900°C reaction temperature. The spikes C & D are toluene peaks (retention time or RT of 2.93 minutes). The passing of toluene through char surely showed reduction in toluene peak. A & B are the unknown peaks formed by catalytic reaction (A: RT of 1.13 minutes and B: RT of 1.93 minutes).

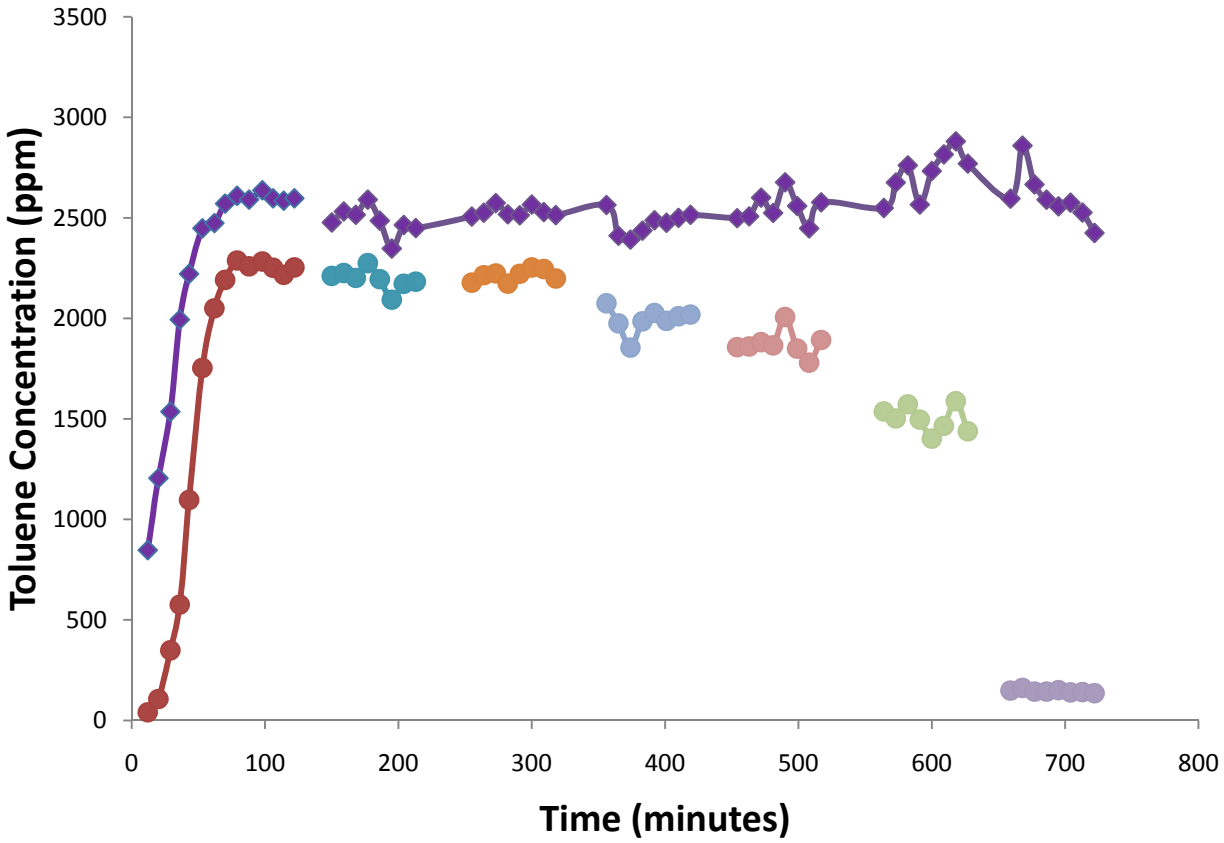

Figure 5.4: Complete run of toluene decomposition with biochar as catalyst with respect to time, inlet toluene concentration ~2500 ppmv, mass of catalyst = 3.8 g, space time =0.09 kg-hr m^{-3}. Inlet, Equilibrium Exit, Exit@550°C, Exit@600°C, Exit@650°C, Exit@700°C, Exit@800°C, Exit@900°C.

Temperature Profile of Reactor

Five thermocouples were installed throughout the length of the reactor excluding the thermocouples at the inlet and exit of the reactor. The temperature for which conversions are reported is the reaction temperature which is the temperature of the catalyst. The temperatures recorded on all the thermocouples show the temperature profile of the reactor (Figure 5.5). The temperatures recorded at the inlet and exit of reactor approached room temperature because of the distance of the points from the

furnace. This distance was deliberately maintained so as to take the sample at NTP conditions.

Operating Parameters

The operating parameters at which the decomposition of toluene was carried out are tabulated in Table 5.1.

Table 5.1: Operational parameters for toluene catalytic cracking/reforming reactions.

Temperature	^{o}C	600-900
Initial tar concentration	ppmv	1100-4600
Pressure	Atm	1
Gas residence time	S	1.15
Catalyst bed volume	cm^3	13.14
Catalyst bed height	Cm	3
Space time	$kg\text{-}hr/m^3$	0.09
H_2O concentration	Ppmv	2.5*toluene concentration

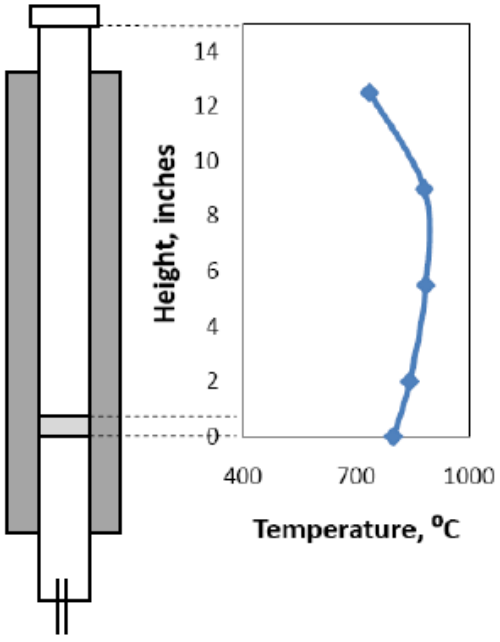

Figure 5.5: Temperature profile of reactor for reaction temperature of 800°C.

Fractional Conversion of Toluene using Biochar as a Catalyst

Effect of Reaction Temperature on Toluene Decomposition

Figure 5.6 shows the fraction conversion of toluene at various reaction temperatures with and without biochar as a catalyst. Toluene conversion with biochar was significantly higher than that of thermal cracking experiment at all studied temperatures. No catalyst deactivation was observed after 8 hours of run on stream. From the results, there was a significant difference in toluene conversion with and without catalyst. It was found that at each temperature the toluene fractional conversion was significantly different to each other. It suggests that temperature has a significant effect on toluene fractional conversion (Figure 5.6). Reaction temperature has been shown to increase toluene conversions with Nickel based catalysts too (Srinakruang et.al., 2005, Li et.al., 2009).

In order to study the toluene breakdown products, the exit gas samples were analyzed with both GC-FID and GC-MS. There was also a significant difference in benzene selectivity with temperature. Benzene was observed as an intermediate product during toluene breakdown reaction as identified by GC/MS. There was no observed benzene formation at 600°C. It steadily increased from 600 to 800°C, but the rate of increase decreased from 800 to 900°C (Figure 5.7). This may be due to the further decomposition of benzene at higher temperatures. The observed percentage of benzene formation was 9.46%, 21.85% and 27.47% at 700, 800 and 900°C. The benzene selectivity observed with char is comparable to other works. Li et. al. (2009) observed significant benzene selectivity of 22.1% at 850°C and 25.8% at 950°C with mayenite ($Ca_{12}Al_{14}O_{33}$ or $12CaO.7Al_2O_3$) as catalyst for toluene decomposition. Świerczyński

et.al. (2008) used Ni-olivine for toluene steam reforming and found selectivity towards benzene to be 6% and 14% for polyaromatic compounds at 850°C. Along with the selectivity of benzene based on the toluene conversion, the concentration of benzene in the exit in the reactor also increased with temperature. The concentration of benzene produced was 87, 429 and 770 ppmv at 700, 800 and 900°C for a toluene inlet of 2500 ppmv. According to ECN (Energy Research Center of the Netherlands), the benzene is not considered to be a component of tar, but this exit concentration of benzene is much less than the maximum allowable concentration for benzene in tar for end-use applications. Also, benzene is a non-condensable component of tar, so it does not create problems of clogging. Benzene formation with char is not favorable at low temperatures (<700°C).

Other breakdown products, CO_2 and CH_4, showed a different trend with an increase in temperature. There was no general trend in change of CO_2 selectivity with temperature, but overall it decreased with temperature. A decrease in CO_2 formation after 800°C was observed due to the reverse equilibrium of water gas shift reaction, which is thermodynamically favorable at higher temperatures. CH_4 was below detectable limits below 800°C. After CH_4 was detected at 800°C, it decreased from 800 to 900°C (Figure 5.8). This indicates the ability of char to reform methane. H_2 selectivity increased with increasing reaction temperature (Figure 5.9). High temperature favors high yield H_2 because of the endothermic nature of the reforming reactions (Li et.al., 2009). A higher treatment temperature favored cracking of the hydrocarbons in the gaseous products and thus increased the yield of hydrogen. As explained in the mechanism previously, the aromatics break down to coke and hydrogen, increasing the hydrogen percentage with

increase in decomposition of toluene. Almost the same percentage of hydrogen formation at these temperatures was reported by Matsuhara et.al. (2010).

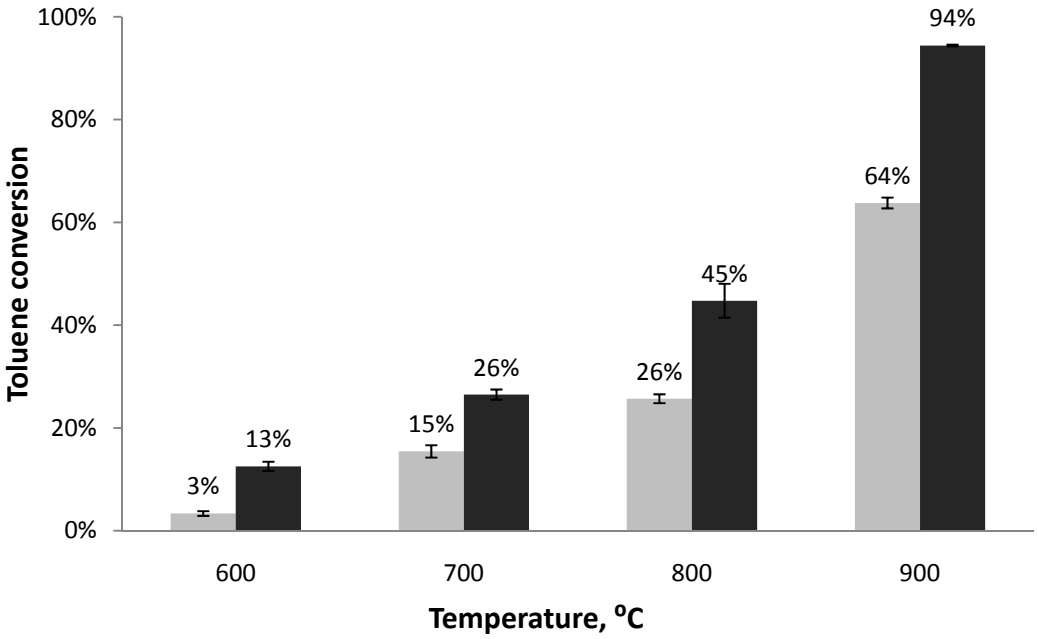

Figure 5.6: Effect of temperature on toluene conversion (Nitrogen flow 0.7 l/min, toluene inlet ~ 2500 ppmv, space time = 0.09 kg_{cat} h m^{-3}) Thermal cracking with quartz beads, Catalytic cracking with char

Effect of inlet concentration

Inlet concentration of toluene was changed by varying the toluene feed rate in same flow of nitrogen gas. The operating parameters were kept same as char except the different range of temperatures (550-700^{o}C). One way ANOVA was conducted to statistically analyze the effect of inlet toluene concentration on fractional conversion of toluene. The ANOVA outputs for all temperatures are shown in appendix C. Inlet toluene concentration had significant effect on the fractional conversion of toluene at all

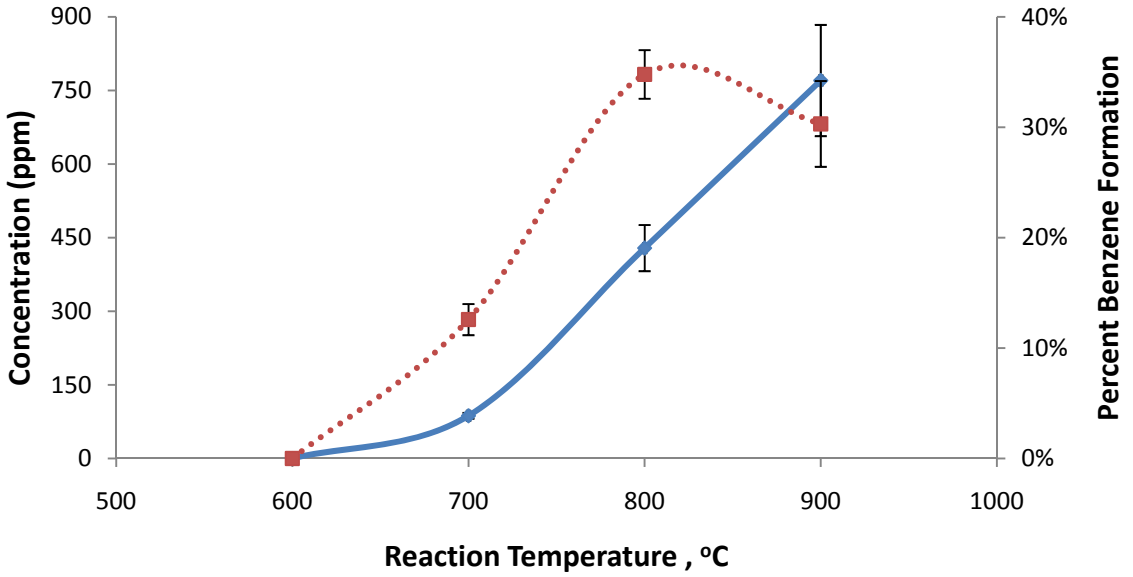

Figure 5.7: Effect of temperature on benzene formation (Nitrogen flow 0.7 l/min, toluene inlet ~ 2500 ppmv, char as catalyst 3.8 g, space time = 0.09 kg_{cat} h m^{-3}) Benzene concentration (ppmv), Percent benzene formed.

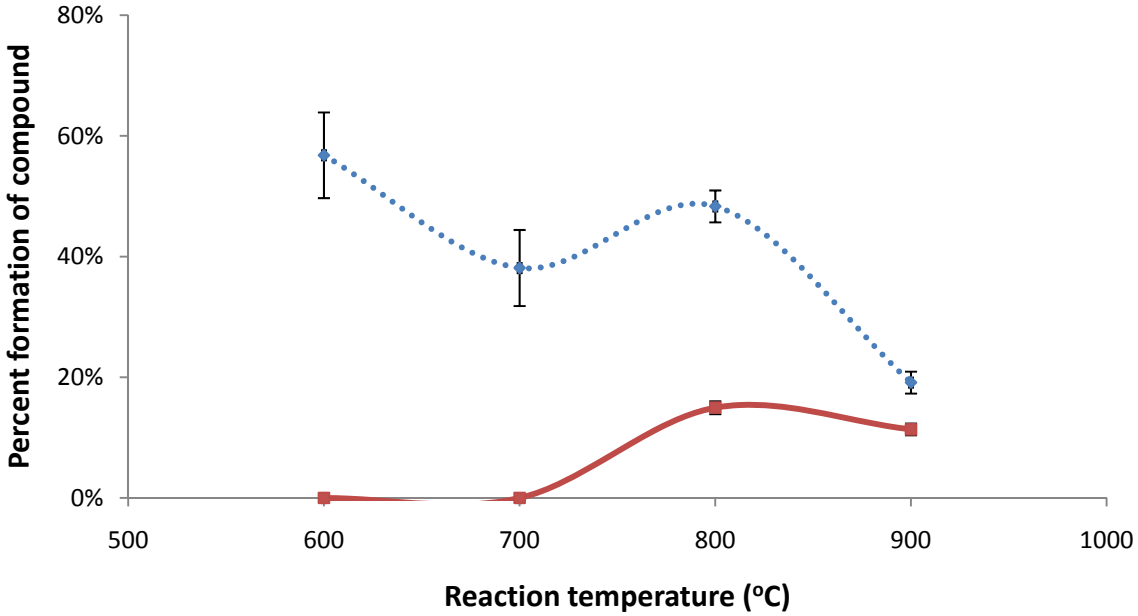

Figure 5.8: Effect of temperature on CO_2 and CH_4 formation (Nitrogen flow 0.7 l/min, toluene inlet ~ 2500 ppmv, char as catalyst 3.8 g, space time = 0.09 kg_{cat} h m^{-3}) CO_2, CH_4

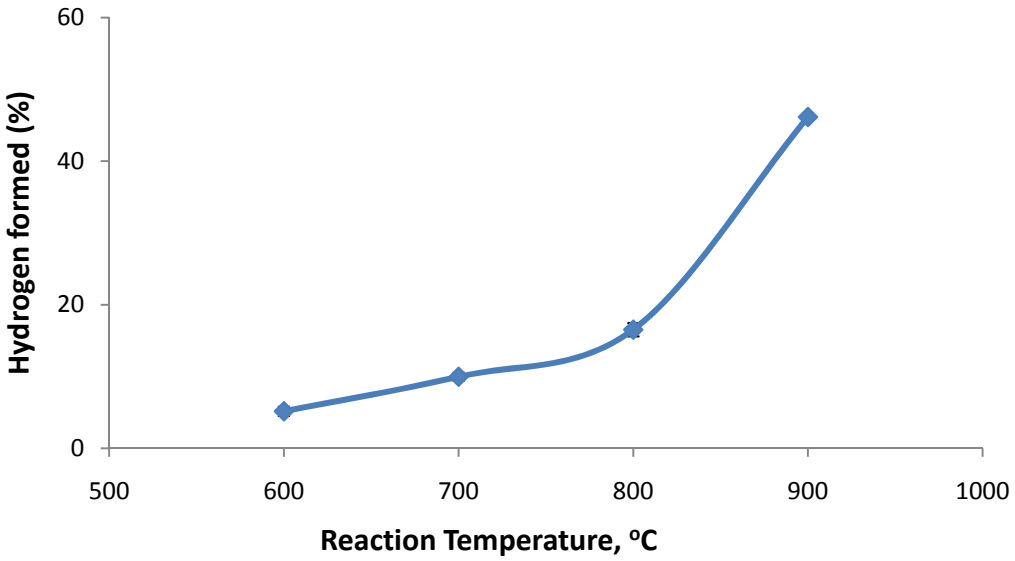

Figure 5.9: Effect of temperature on H_2 formation (Nitrogen flow 0.7 l/min, toluene inlet concentration ~ 2500 ppmv, char as catalyst 3.8 g, space time = 0.09 kg_{cat} h m^{-3})

temperatures. The increase in fractional conversion of toluene with increase in inlet toluene concentration may be due to increased surface reactions of toluene decomposition with increased toluene molecules. This may continue till the saturation inlet concentration. Increase in fractional conversion with the toluene inlet concentration for temperatures 550 to 700°C is shown in Figure 5.10. As shown later, the rate of reaction increased with inlet toluene concentration. Char has already shown the trend of increasing tar conversion with increased inlet loadings with naphthalene as a model compound (Abu El-Rub et al., 2008).

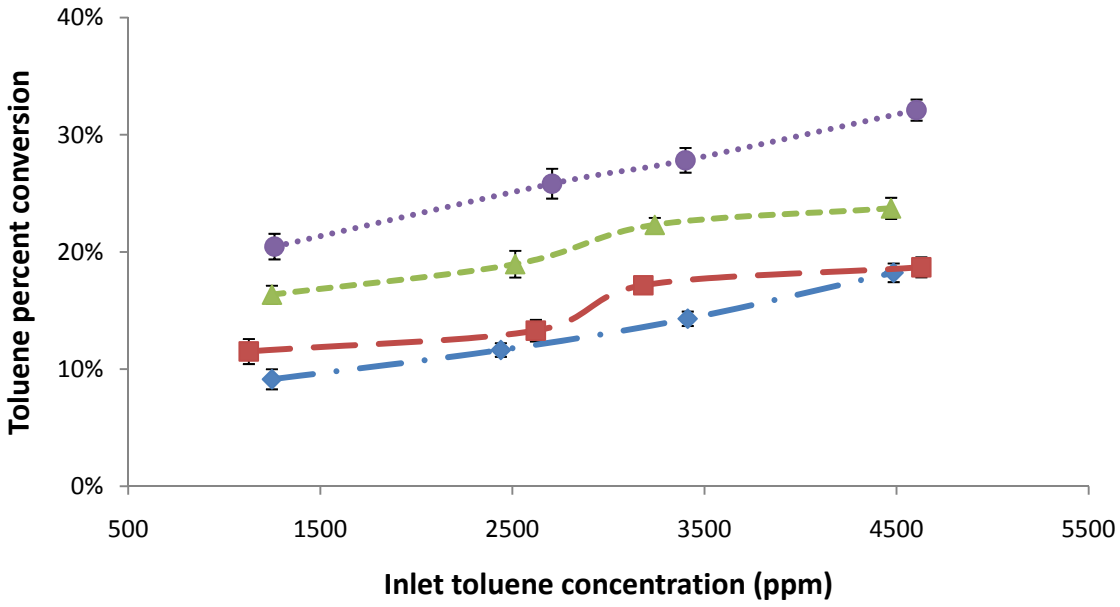

Figure 5.10: Effect of inlet toluene concentration on fractional conversion of toluene. (Nitrogen flow 0.7 l/min, toluene inlet concentration 1000-4600 ppm, temperature range 550-700°C, space time = 0.09 kg_{cat} h m^{-3}) 550°C, 600°C, 650°C, 700°C.

Fractional Conversion of Toluene using Iron Loaded Biohar as Catalyst

To test the hypothesis that iron (Fe^{3+}) is responsible for toluene decomposition, three loadings of iron on char were tested. The results of the iron content for all loadings on char are reported in Table 5.2.

Table 5.2: Percentage of iron loading on 3 wet impregnated chars

Loading	Iron content (%)
Loading 1	9.89%
Loading 2	13.00%
Loading 3	18.70%

The natural iron loading on char was 263 ppm (found by mineral analysis presented in Appendix E). Three different iron percentages were loaded on char. All three loadings were tested for fractional conversion of toluene, benzene formation, and CO_2

and CH_4 selectivity in the decomposition of toluene under temperature conditions of 600-900°C. The comparison of all three loadings with no loading in terms of toluene fractional conversion is shown in Figure 5.11. The fractional conversion of toluene with 9.89% iron loaded char was found to be 23.26%, 30.77%, 96.08% and 95.70% for temperatures 600, 700, 800 and 900°C respectively. As compared to no loading on char, the fractional conversion reached to almost complete conversion at 800°C rather than 900°C (as in unloaded char). This indicates the effect of iron as a catalyst for toluene decomposition. The iron loaded on the char acted as the active site for the complete conversion of toluene at temperature lower (800°C) than that required by unloaded char (900°C). The conversions at lower temperatures (600 and 700°C) increased almost 2 fold with an increase of iron loading of about 3%. The conversions with 13% iron loaded char are 40.50%, 46.22%, 95.28% and 96.23% at temperatures 600, 700, 800 and 900°C respectively. Iron based catalysts are active in high temperature water gas shift reaction (Md. Azhar et.al., 2008). Further increase of iron did not increase much of the conversions. This can be regarded to the saturation of char with iron species at a loading less than 18.7% loading due to which the active sites on char did not increase with further increase in iron loading. 18.7% iron loading gave fractional conversions of toluene to be 46.58%, 56.58%, 94.29% and 96.55% for temperatures 600, 700, 800 and 900°C respectively. Benzene formation (Figure 5.12) was observed at 600 and 700°C unlike with char. At 800°C, the benzene formation was negligible (2.25%) with 8.7% loaded char as compared to that with unloaded char (34.10%). The benzene formation was observed to be decreasing with temperature, except at 900°C, where it increased by 5% from 800°C. A similar trend was observed for all other loadings giving almost complete

conversion at 800°C. Benzene formation was the smallest at 700°C for 18.7% iron loaded char.

CO_2 selectivity did not follow any trend with respect to temperature (Figure 5.13) but both 9.89% and 18.7% loadings showed CO_2 to be increasing from 600 to 700°C but then decreasing till 900°C. In case of 13% loading, CO_2 selectivity continuously decreased from 600 to 900°C reporting 68.43%, 61.59%, 5.59% and 3.39% at temperatures 600-900°C. The decrease in CO_2 with temperature can be accredited to reverse water gas shift reaction at higher temperatures. Same trend was observed by Li et.al., (2009) by using Ni/Mayenite for toluene reforming. CO_2 formation was minimal in case of 18.7% iron loaded char for all the temperatures. The CH_4 was not in detectable limits below 800°C (Figure 5.14). The selectivity for CH_4 increased from 800 to 900°C for all three loadings. ANOVA with Duncan analysis was done to find out if there was any difference in the loadings for toluene conversion, benzene formation, CO_2 and CH_4 selectivity (Refer Appendix C).

For all the parameters, there was a significant difference between the four temperatures except for CO_2 where the temperatures 800 and 900°C did not have significant difference within each other as CO_2 selectivity was negligible at both these temperatures. The toluene conversion is significantly different for all loadings at 600 and 700°C, but not for 800 and 900°C because there was almost complete conversion at 800°C and stayed almost the same at 900°C. In case of benzene formation, at 600°C, there was no significant difference in 9.89% and 18.7% iron loaded char. At 700°C, 9.89% and 13% iron loaded char were not statistically different from each other. For CH_4, increasing the iron content over 13% decreased the CH_4 selectivity, which is a

favorable characteristic for a catalyst used for tar reforming. Out of the 3 iron loadings tested for decomposition of toluene, it was found that increase in iron content increased the toluene conversion and also reduced the benzene, CO_2 and CH_4. So, iron proved to be an important element in char for toluene decomposition.

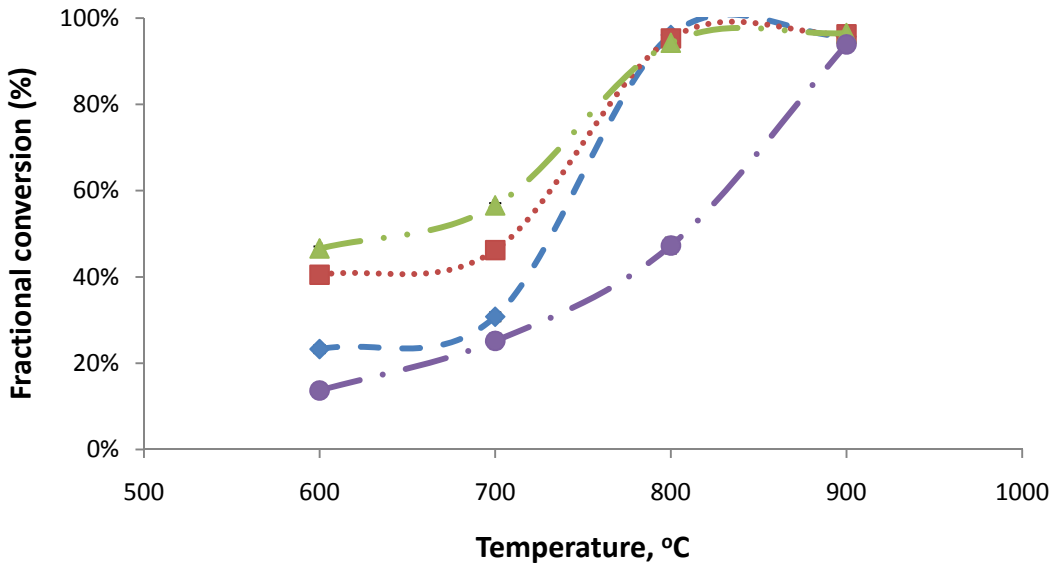

Figure 5.11: Comparison of different iron loadings for percent conversion of toluene. (Temperatures 600-900°C, Nitrogen fow rate 0.7 l/min, inlet toluene concentration ~ 2500 ppmv, space time = 0.09 kg_{cat} h $m^{-3)}$ 9.89% loading, 13% loading, 18.7% loading, no loading. Note: The error bars not visible are smaller than the symbols.

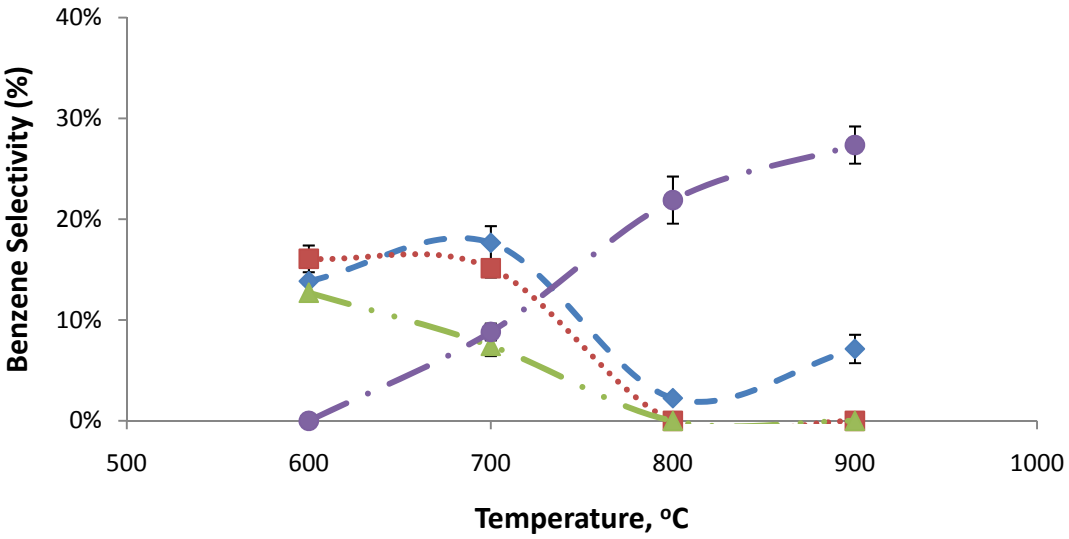

Figure 5.12: Comparison of different iron loadings for benzene formation in the decomposition reaction of toluene. (Temperatures 600-900°C, Nitrogen fow rate 0.7 l/min, inlet toluene concentration ~ 2500 ppmv, space time = 0.09 kg_{cat} h m^{-3}) 9.89% loading, 13% loading, 18.7% loading, no loading. Note: The error bars not visible are smaller than the symbols.

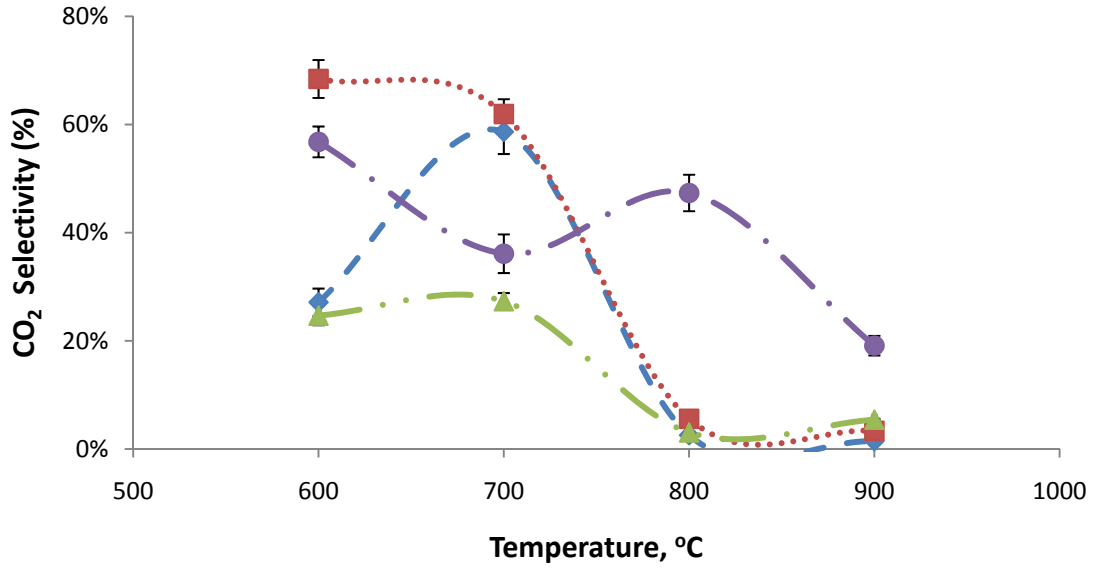

Figure 5.13: Comparison of different iron loadings for CO_2 selectivity in the decomposition reaction of toluene at temperatures 600-900°C, Nitrogen fow rate 0.7 l/min, inlet toluene concentration ~ 2500 ppmv, space time = 0.09 kg_{cat} h m^{-3}, 9.89% loading, 13% loading, 18.7% loading, no loading. The error bars not visible are smaller than the symbols.

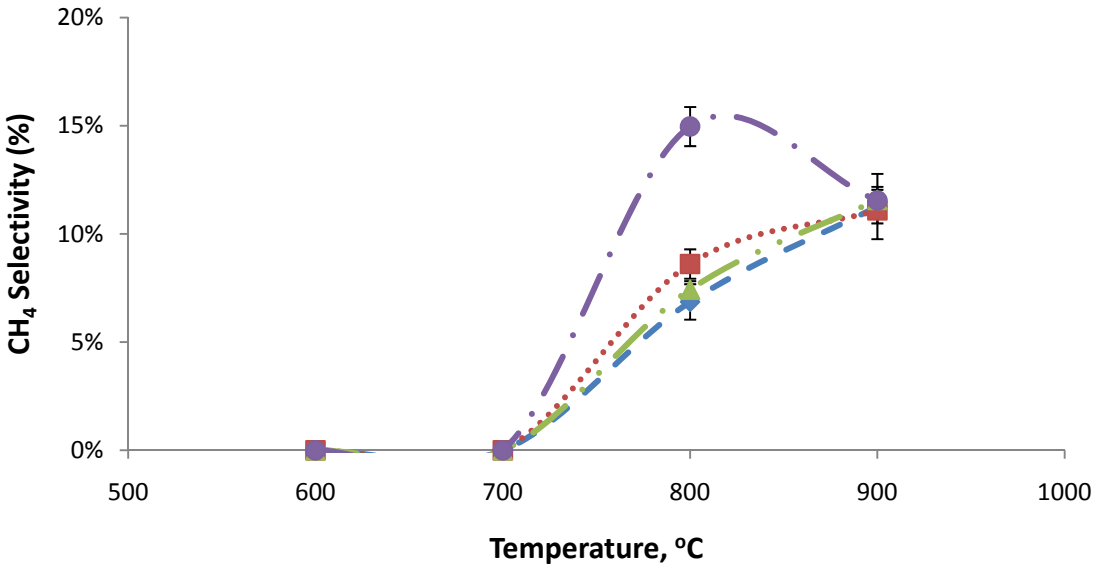

Figure 5.14: Comparison of different iron loadings for CH_4 selectivity in the decomposition reaction of toluene. Temperatures 600-900°C, Nitrogen fow rate 0.7 l/min, inlet toluene concentration ~ 2500 ppmv, space time = 0.09 kg_{cat} h m^{-3}, 9.89% loading, 13% loading, 18.7% loading, no loading. Note: The error bars not visible are smaller than the symbols.

Effect of toluene inlet concentration

The effect of toluene inlet concentration was tested on 18.7% iron loaded char. The variation in the fractional conversion of toluene with inlet toluene concentration at different reaction temperatures is shown in figure 5.15. The conversion over all four temperatures increased with increasing toluene inlet concentration until approximately 1800 ppmv but decreased with a further increase in concentration. This may be due to the reason that the active sites on the catalyst saturates with 1800 ppmv and thereafter, some of the toluene passes unreacted resulting in a reduction in toluene fractional conversion. Also, these reactions were performed at temperatures lower than that for char. So, a little of adsorption effect might have caused to decrease the saturation capacity of the catalyst.

It was also observed that rate of reaction increases with increase in toluene inlet concentration.

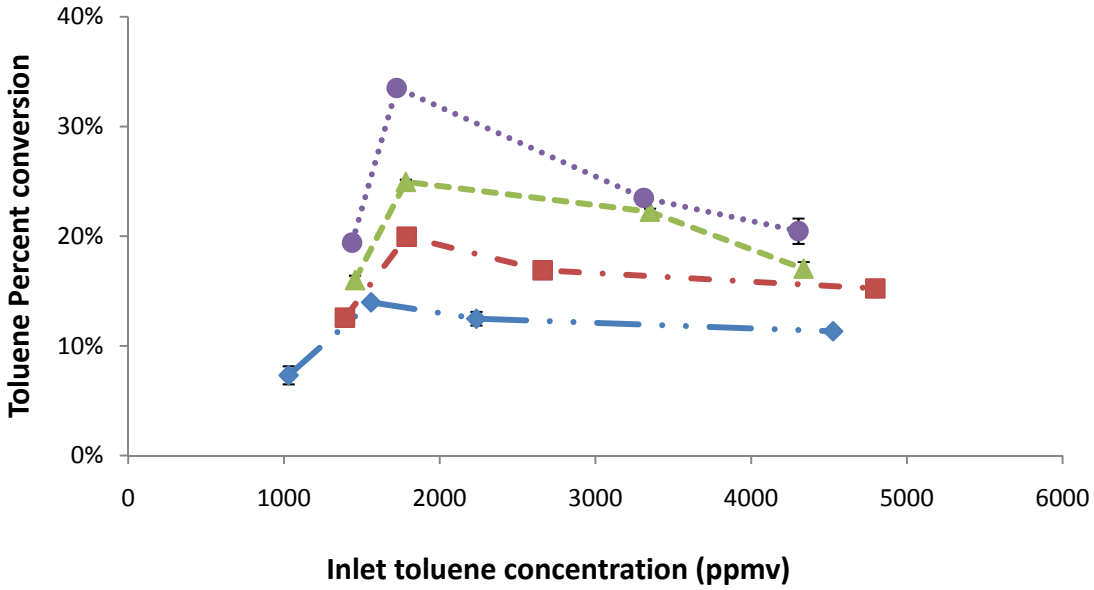

Figure 5.15: Effect of inlet toluene concentration on the fractional conversion of toluene with 18.7% iron loaded char (Temperatures 400-550°C, space time =0.09 kg_{cat} h m^{-3}) 400°C, 450°C, 500°C, 550°C. Note: The error bars not visible are smaller than the symbols.

Fractional Conversion of Toluene using Fly Ash as Catalyst

The toluene conversions with fly ash compared to char as catalyst are shown in figure 5.16. The fractional conversion is found to be statistically less than char but higher than thermal cracking, also the benzene formation was statistically higher in case of fly ash than char. This seems to be in contradiction of the theory that the ash/mineral particles are the catalytic site for tar decomposition. This may be due to the source of biomass both char and fly ash were made out from. Mineral content may vary in both the catalysts. As hypothesized, carbon also takes part in acting as active agent for catalysis (Griffiths and Mainhood, 1967); fly ash has less carbon content than char, due to which this compromise of catalytic activity may occur.

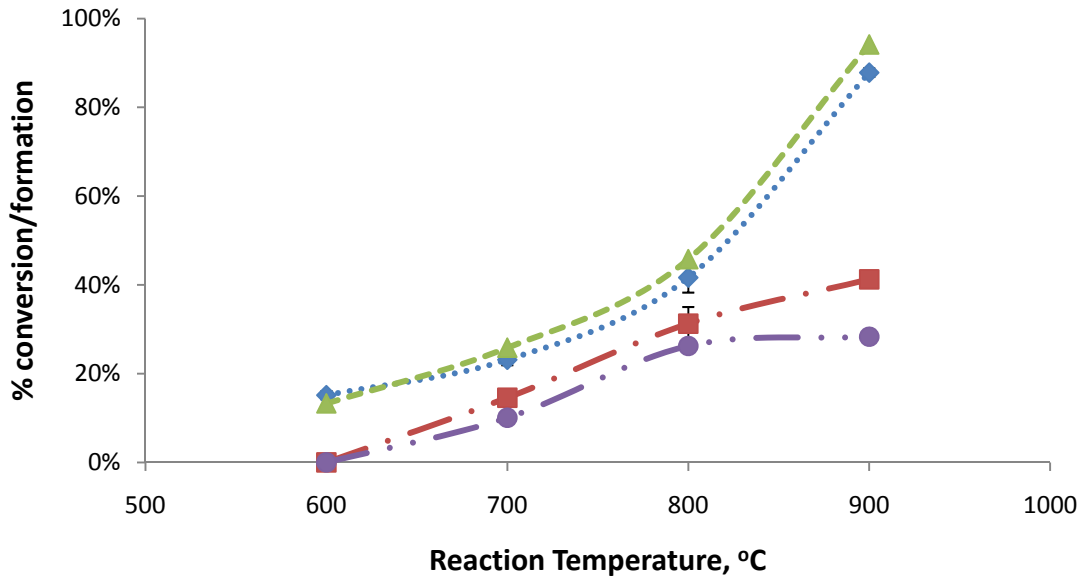

Figure 5.16: Effect of reaction temperature on fractional conversion of toluene and benzene formation using fly ash and biochar as catalyst ····· Toluene conversion with fly ash, - - - toluene conversion with char, —— Benzene formation with fly ash, —— Benzene formation with char.

Kinetic Analysis

The reactor used in the study is considered to be of the plug flow reactor type without gas expansion (i.e., a constant volumetric flow rate). An assumption of no mass and heat transfer resistances are also assumed. The rate law of the power law form that describes the rate of toluene transformation can be expressed as

$$-r_T = k' C_T^n C_{H_2O}^m \qquad (5.1)$$

where,

r_T= rate of reaction

k' = Rate constant

C_T = Concentration of toluene in the inlet

C_{H_2O}= Concentration of water in the inlet

The ratio of steam/toluene provided (2.5) was much higher than the stoichiometric requirement (1.7), therefore, it is assumed that it has no effect on the toluene reaction rate (Yamaguchi et al., 1986; Swierczynski et al., 2008). So, the binary reaction with H_2O can be expressed as a pseudo-order reaction with respect to only toluene concentration. That is, k = $k'C_{H_2O}^m$ giving eq. 5.2 and the order of reaction with respect to H_2O is zero and thus C_{H_2O} remains constant across the catalytic bed during testing. According to the experiments conducted in this study at different toluene concentrations and temperatures, the rate of decomposition of tar was found to be first order. Then the equation can be expressed as

$$-r_T = kC_T \qquad (5.2)$$

Four concentrations were plotted against their respective rate of reactions to calculate rate constant k (Figure 5.17 and 5.18). Each point is indicative of 24 replicates (3 replicates s with 8 replicates in each run) in case of char and 8 replicates in case of 18.7% iron loaded char. The calculation of the rate of reaction is shown in Appendix D. Rate constants were calculated for four temperatures so as to find the temperature dependence of rate constant. The temperatures chosen to find the rate constant were based on the measured fractional conversion being less than 25% at those temperatures, being the criteria for differential reactor. The R^2 values for all temperatures (550-700°C) with char as catalyst was very high (>99%), so it can be said that the rate of decomposition was first order reaction. Same was the case with 18.7% iron loaded char as catalyst, the fit was linear with R2 values lower than that for char (see Table 5.4). To calculate rate constant (k) for the catalysts, the rate law was fitted.

The rates of reaction calculated at 4 different temperatures are given in table 5.3 for char and 5.4 for iron loaded char.

It can be observed in Figure 5.17 and 5.18 that the rate of reaction was increasing with inlet toluene concentration. Addition of iron further increased the rate of reactions with respect to temperature (Figure 5.19). It shows the effect of iron in the catalytic activity of char and is supported by other works (Md. Azhar et.al.,2006; Nordgreen et.al., 2006).

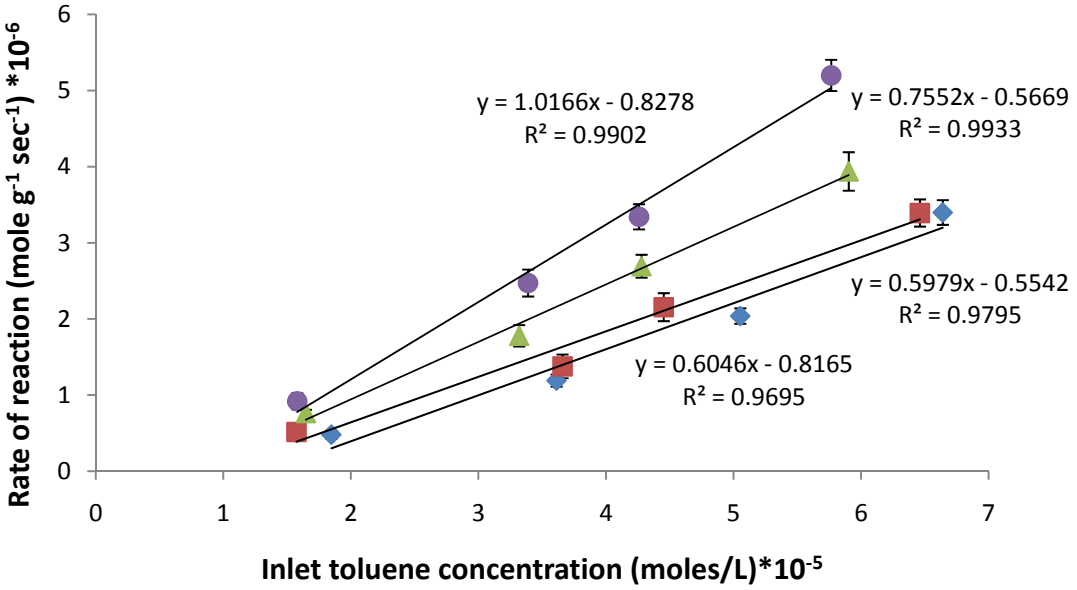

Figure 5.17: Rate constants calculated from plot of reaction rate versus inlet toluene concentration for biochar (equation 5.2) ◆ 550°C, ■ 600°C, ▲ 650°C, ● 700°C. Error bars not visible are smaller than the symbols.

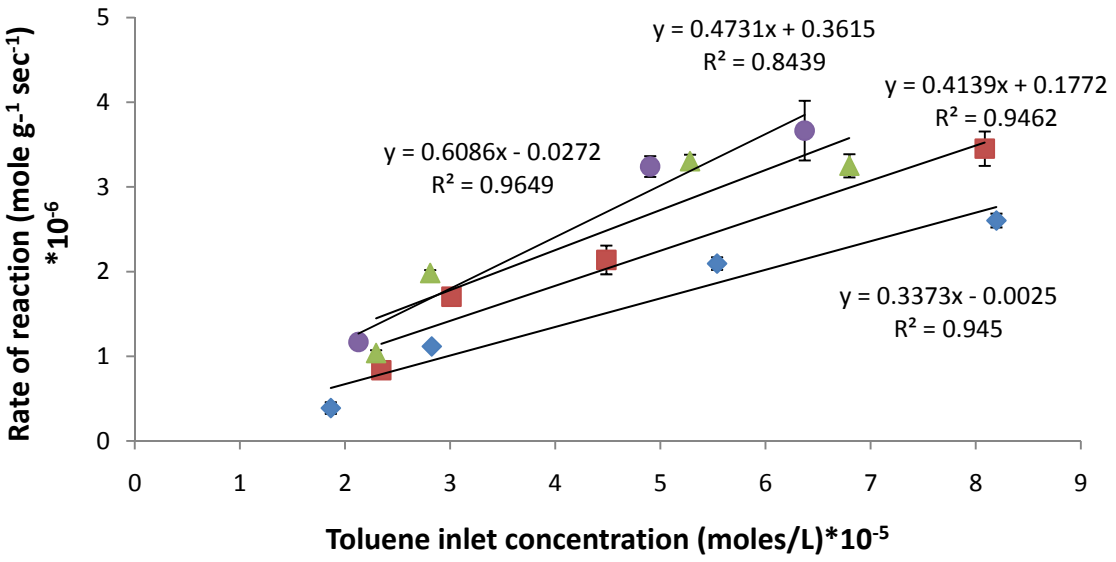

Figure 5.18: Rate constants calculated from plot of reaction rate versus inlet toluene concentration for 18.7% iron loaded biochar (equation 5.3) ◆ 400°C, ■ 450°C, ▲ 500°C, ● 550°C. Error bars not visible are smaller than the symbols.

Table 5.3: Rate constants for different temperatures for biochar as catalyst (600-900°C, inlet toluene concentration 2500 ppmv, space time 0.09 kg_{cat} h m^{-3} at 25 °C)

Temperature, °C	Reaction rate constant (s^{-1})	R^2 value
550	$(6.05 * 10^{-2}) \pm 0.001$	0.9695
600	$(5.98 * 10^{-2}) \pm 0.002$	0.9795
650	$(7.55 * 10^{-2}) \pm 0.002$	0.9933
700	$(1.02 * 10^{-1}) \pm 0.00$	0.9902

Table 5.4: Rate constants for different temperatures for 18.7% iron loaded biochar as catalyst (500-900°C, inlet toluene concentration 2500 ppmv, space time 0.09 kg_{cat} h m^{-3} at 25 °C)

Temperature, °C	Reaction rate constant (s^{-1})	R^2 value
400	$(3.37* 10^{-2})$	0.9450
450	$(4.14* 10^{-2})$	0.9462
500	$(4.73* 10^{-2})$	0.8439
550	$(6.09* 10^{-2})$	0.9649

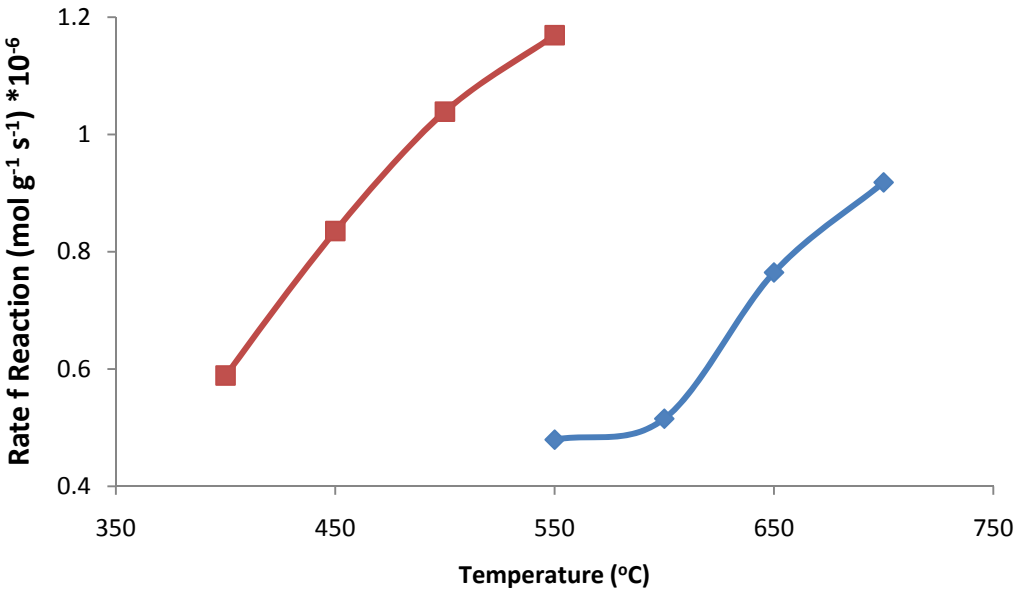

Figure 5.19: Change in reaction rate with temperature using Biochar and 18.7% Iron loaded Biochar (~1250 ppmv inlet toluene concentration).

The temperature dependence of the rate constant was determined by the Arrhenius equation, from which activation energy (E_a) and pre-exponential factor (A) can be calculated.

$$k = Ae^{-E_a/RT} \qquad (5.3)$$

k = Reaction Rate Constant

R = Universal Gas Constant

T = Reaction Temperature

As the Arrhenius plot from the rate constants calculated with differential reactor assumption (<25% conversion) did not give high R^2 values, the rate constants were calculated with other temperature conditions assuming an integral reactor (conversions >25%).

$$k = \frac{-(\ln(1-X))}{W/V_o} \qquad (5.4)$$

To plot the Arrhenius equation, these rate constants were plotted with temperature. The activation energy and pre-exponential factor were calculated from the plot in figure 5.20 for char and 18.7% iron loaded char and are shown in Table 5.5. The activation energies calculated for char and iron loaded chars are in comparison with other studies (Table 5.6). There was a statistically high difference observed between the activation energy calculated for char and 18.7% iron loaded char. The activation energy to decompose toluene calculated for char (90.33kJ/mol) and iron loaded char (49.18kJ/mol) was comparable to Ni/Mayenite (196kJ/mol) ((Swierczynski et al., 2008) and Ni/Olivine (80.44kJ/mol) (Li et al., 2009).

Table 5.5: Estimates of the kinetic parameters for toluene steam reforming on biochar and iron loaded biochar char (toluene 2500 ppm diluted by Nitrogen, S/C: 2.5, temperature from 550-700°C for char and 400-500°C for WI char, $w_{cat}/F_{toluene}$=0.09 kg_{cat} h m^{-3} at 25 °C).

Catalyst	**Parameters** A(m^3 kg_{cat}^{-1} h^{-1})	**Estimated Values** E_a(kJ mol^{-1})
Char	2.63 * 10^5	90.33
18.7% Iron Loaded Char	6.04 *10^3	49.18

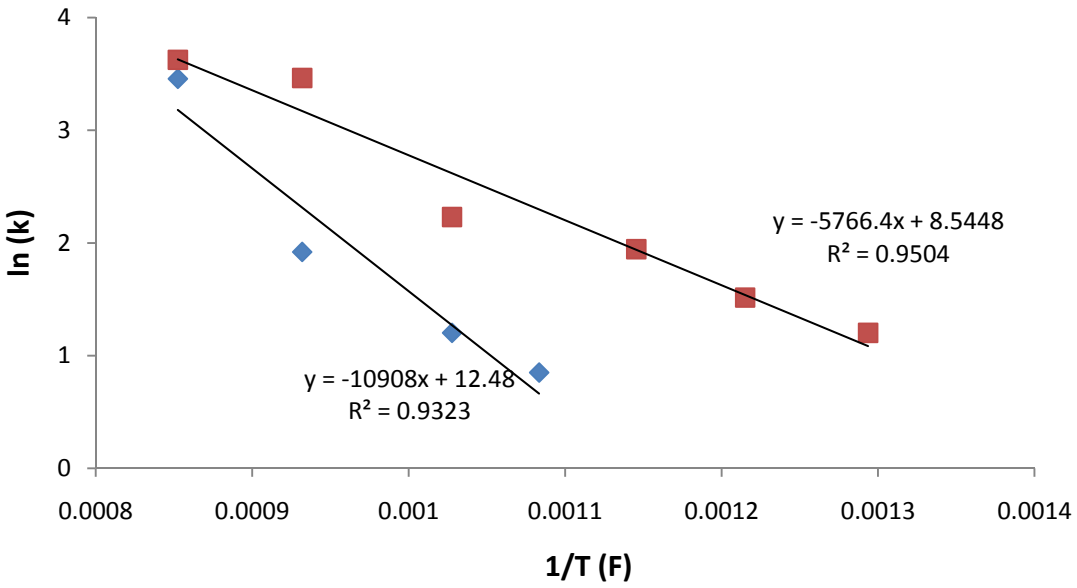

Figure 5.20: Arrhenius plot for calculation of apparent activation energy for ◆ biochar and ■ 18.7% iron loaded biochar (T: 500-900°C, inlet concentration 2500 ppmv; space time: 0.09 kg_{cat} h m^{-3}).

Catalyst Longevity

To confirm the practical applicability of the promising catalyst, long-term durability tests were conducted at the condition of 800°C, a space time of 0.09 kg_{cat} hr m^{-3} at 25°C, an inlet toluene concentration of 2500 ppmv, and a S/C (steam to carbon) ratio of 2.5 for 6 days. The results showed that char maintained the toluene fractional conversion at ~46% for 25 hours and then suddenly the fractional conversion increased to ~96% (Figure 5.22). This points towards the effect of coke on decomposition reactions as coke deposition on alumina catalyst has been observed to increase the tar decomposition (Hosokai et.al., 2005, Bayarsaikhan et.al., 2006). Eight hours later, the conversion started decreasing from 96% and came down to ~50% in next 4 days. The conversion did not go below the starting value for all 6 days. This shows that the catalyst has a capability to withstand high temperature (800°C) for a long duration (more than 6 days) and still give

a constant expected conversion (Figure 5.21). Char, being naturally produced inside the gasifier, will have this added advantage of having a long life with the same efficiency.

The 13% iron loaded char was chosen to be tested for its life to reform hydrocarbons at 800°C (this catalyst gave almost complete conversion at this temperature). Starting period of 9 hours gave conversion of ~95% (Figure 5.22). It then decreased for 8-10 hours but it went back up to ~ 100% for rest of the time until last 5 hours where it again started decreasing. No benzene was seen for most of the time, except for the times where the conversion went below 96%. Presence of metallic iron as a tar breakdown catalyst, neither carbon deposits not any decline in the activity is noticed (Nordgreen et.al., 2006).

In case of both the catalysts, during the intervals of complete conversions, benzene formation was not noticed. It indicated that the coke formation is helping the catalyst to perform better and therefore during this reaction, all tars were decomposed. But with further steam gasification of coke, the conversions decreased and started increasing with further formation of coke (Hosokai et.al., 2009).

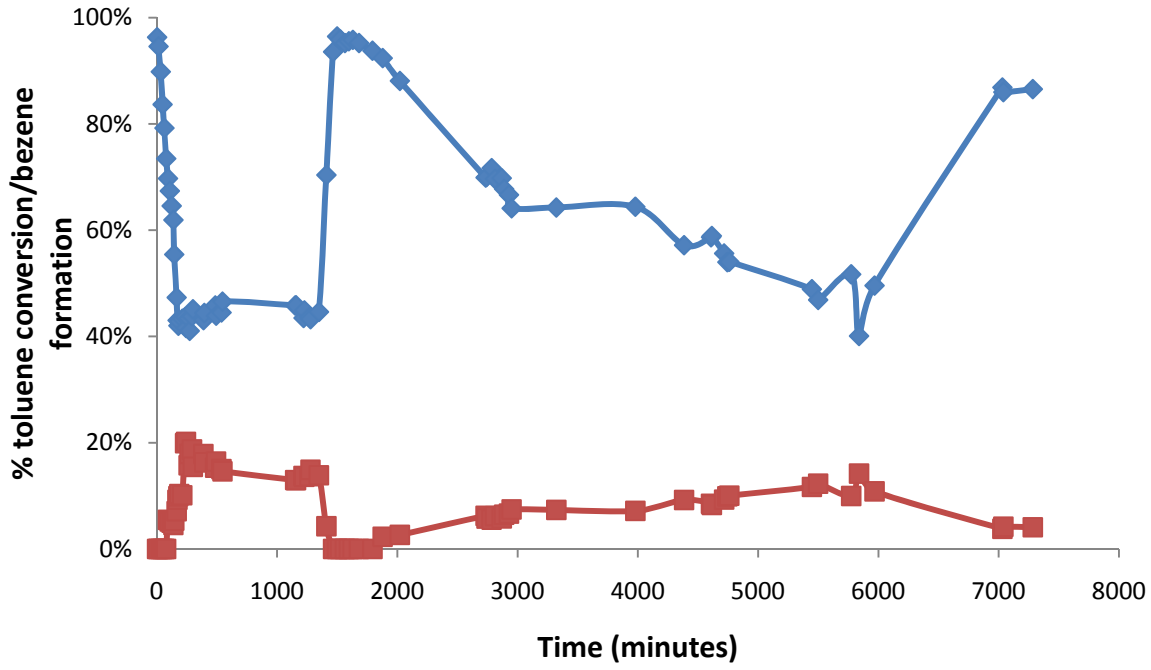

Figure 5.21: Longevity run for life of biochar as catalyst (800°C, inlet concentration 2500 ppmv, mass of catalyst 3.8 g, space time 0.09 kg_{cat} h m^{-3}) Toluene conversion Benzene formation

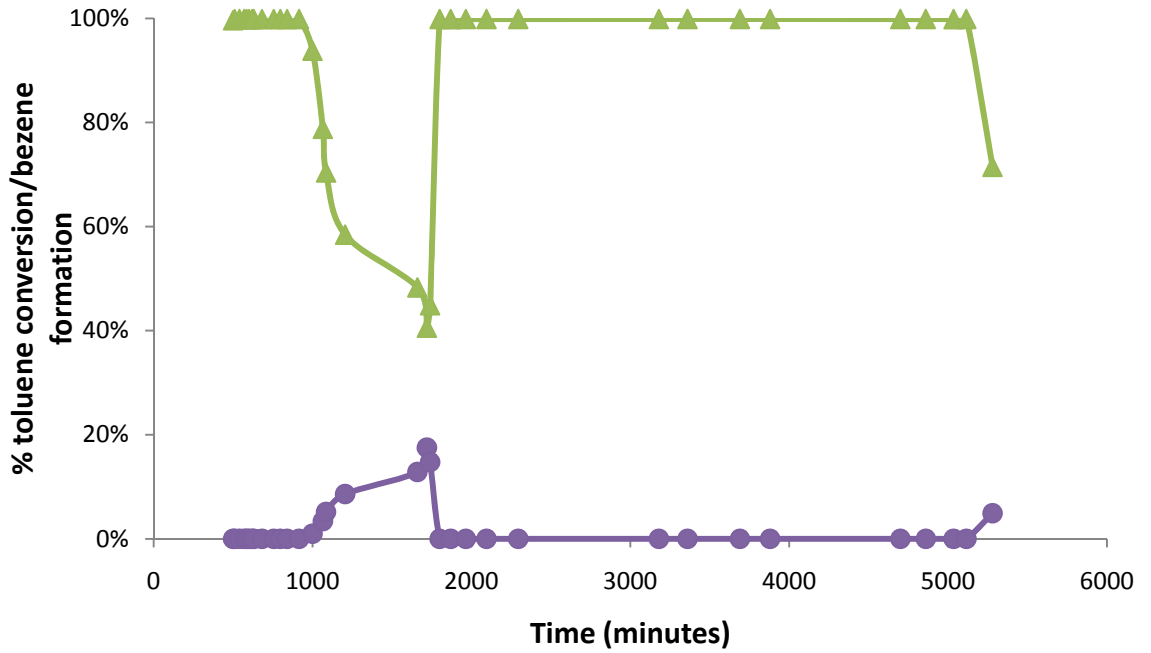

Figure 5.22: Longevity run for life of 13% iron loaded biochar as catalyst (800°C, inlet concentration 2500 ppmv, mass of catalyst 3.8 g, space time 0.09 kg_{cat} h m^{-3}) Toluene conversion, Benzene formation.

Carbon Balance

The carbon balance for the toluene decomposition with char as catalyst was verified. Sample calculation for carbon balance is shown in Appendix F. The carbon balance for all catalysts at all temperatures did not completely close. The carbon balance with 8.87% iron loaded char at 700°C, 13% iron loaded char at 600 and 700°C and char at 800°C closed within 20% of theory (see fig.5.22). The rest of the combinations (600, 700 and 900°C for char, 600, 800 and 900°C for 9.89% iron loaded char, 800 and 900°C for 13% iron loading and all four temperatures for 18.7% iron loaded char) did not close within a significant level which states that there was a considerable amount of carbon loss which could not be reported. Some part of this error could be contributed to the peak in the exit gas in GC-FID at higher temperatures that could not be identified. This unknown peak turned out significantly higher at 900^{o}C than at other temperature reactions. Most of carbon loss can be contributed to the coke formation by aromatics, which stay on the catalyst itself and is not present in the exit gas sample and thus, cannot be identified (as explained earlier in this report). Also, biomass char is not an inert material and it reacts with the steam in feed gas (El-Rub et.al., 2005).

Catalyst Characterization

Fresh char was observed under an SEM (Figure 5.23) which shows the porous structure of char that one of its important property to act as catalyst. Two fractions were obtained after the longevity study on char (6 days). One of the fractions had ~96% carbon, which we term as “coke” (figure 5.24) and the other had ~ 86% carbon, which was char (figure 5.25). These two fractions were obtained as coke layered over char. Both

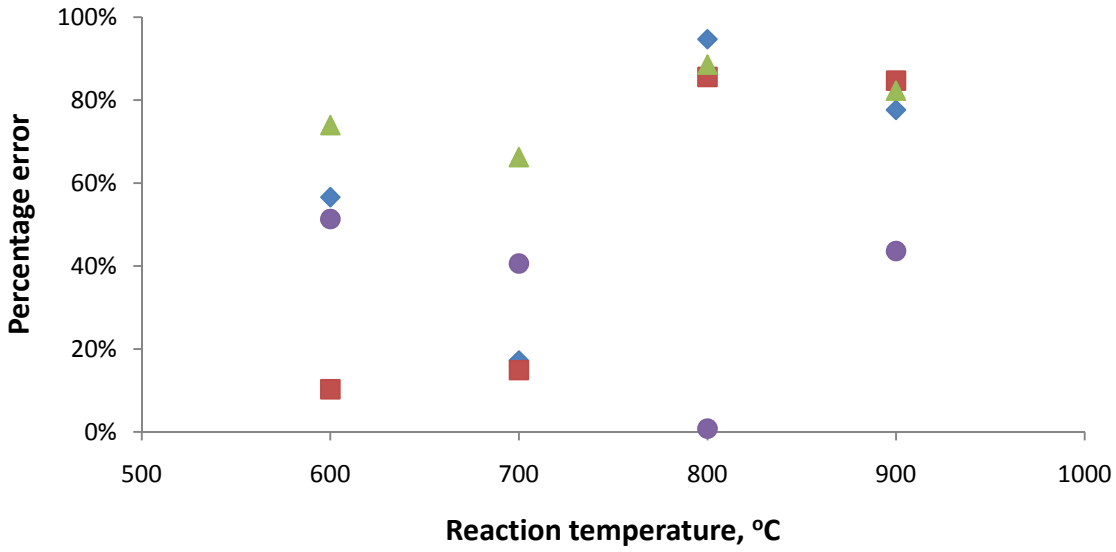

Figure 5.23: Closing error for carbon balance at all temperatures for catalysts ◆ 9.89% iron loading, ■ 13% iron loading, ▲ 18.7% iron loading, ● char.

the layers had totally different texture and were easily distinguishable. The char texture was same as that for the fresh char catalyst, but the texture of coke was a very fine black powder.

As seen in the Figure 5.25, the structure of char is not disrupted, but there appears to be a deposition of coke (deposition has same structure as coke shown in figure 5.24) in the porous structure. This might be the reason that the activity of char decreases i.e., coke deposits in the pores and on the surface of char catalyst.

The iron loaded catalysts were also compared before and after use by SEM analysis. The 9.89% iron loaded catalyst before use had iron spread over the entire surface (Figure 5.26). The elemental compositions of the places marked in the pictures are presented in Table 5.6. The EDS shows the dispersion of iron over the surface. The iron percentage is almost equal at all over the surface. In case of fresh 9.89% iron loaded

char, the three places shown have 48.46%, 41.48% and 63.56% Fe content. But if we observe the used catalyst (Figure 5.27), the iron is not dispersed all over the surface rather it is clustered in some places. One place has 50.63% Fe and other has 13.27% Fe. This agglomeration of iron over char surface was also seen by Yu et. al. (2007). Another noticeable difference in the fresh and used iron loaded char is the oxygen percentage. The oxygen percentage has reduced from around 19% to around 3%. This shows the reduction of Fe species during the run. The reduced Fe specie (Fe^{3+}) then acts as the active site for catalytic toluene decomposition.

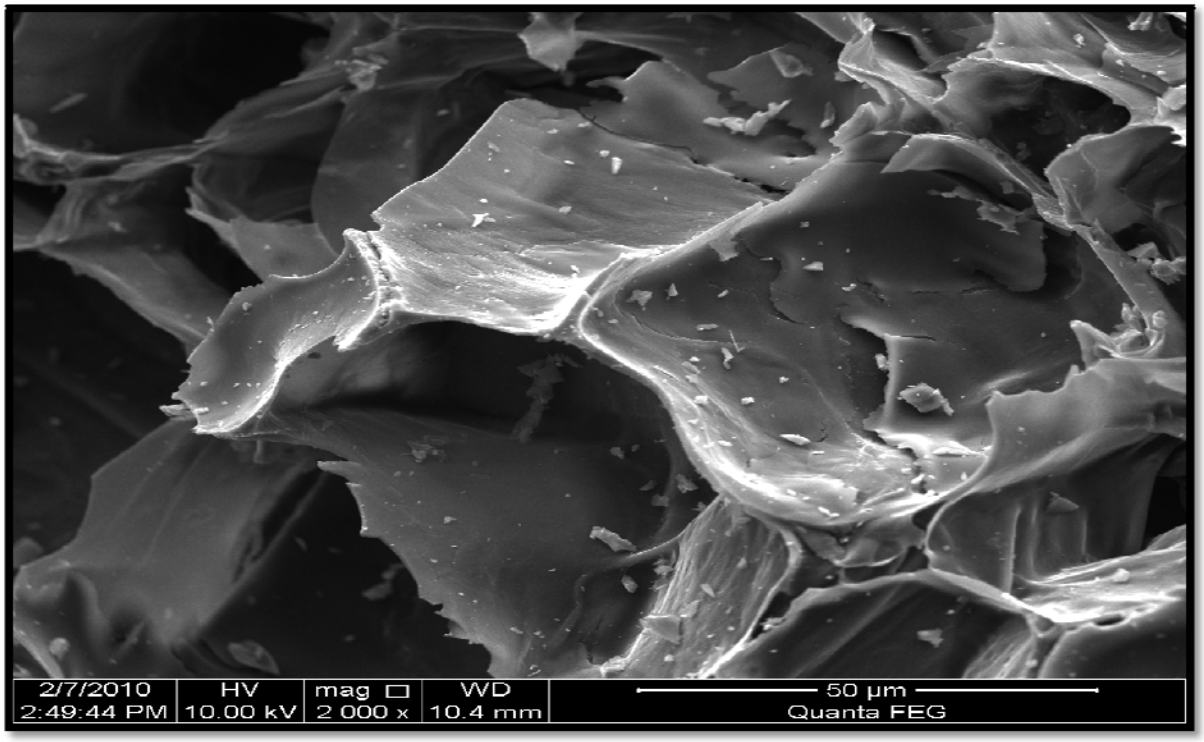

Figure 5.24: SEM Picture of fresh biochar (pyrolysis of pine bark at 950°C for 2 hours)

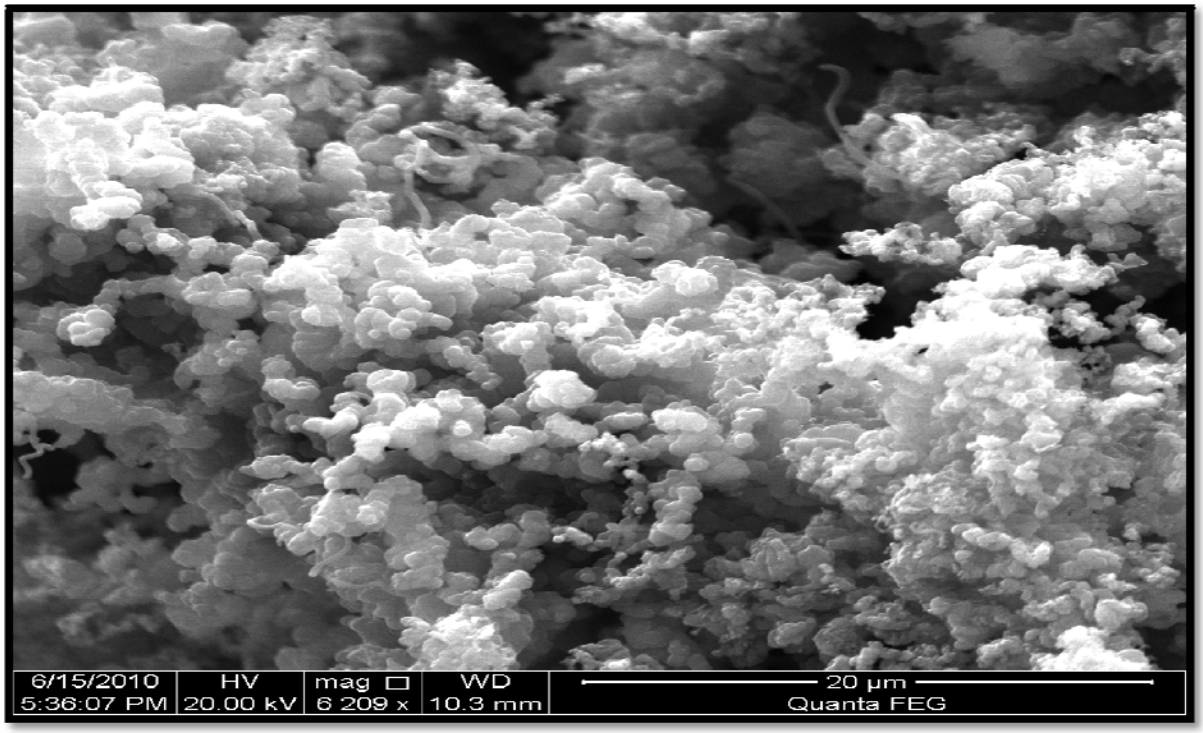

Figure 5.25: SEM Picture of coke fraction retrieved after longevity study with biochar (6 days run at 800°C, inlet toluene concentration ppmv, mass of catalyst 3.8 g, space time 0.09 kg_{cat} h m^{-3}).

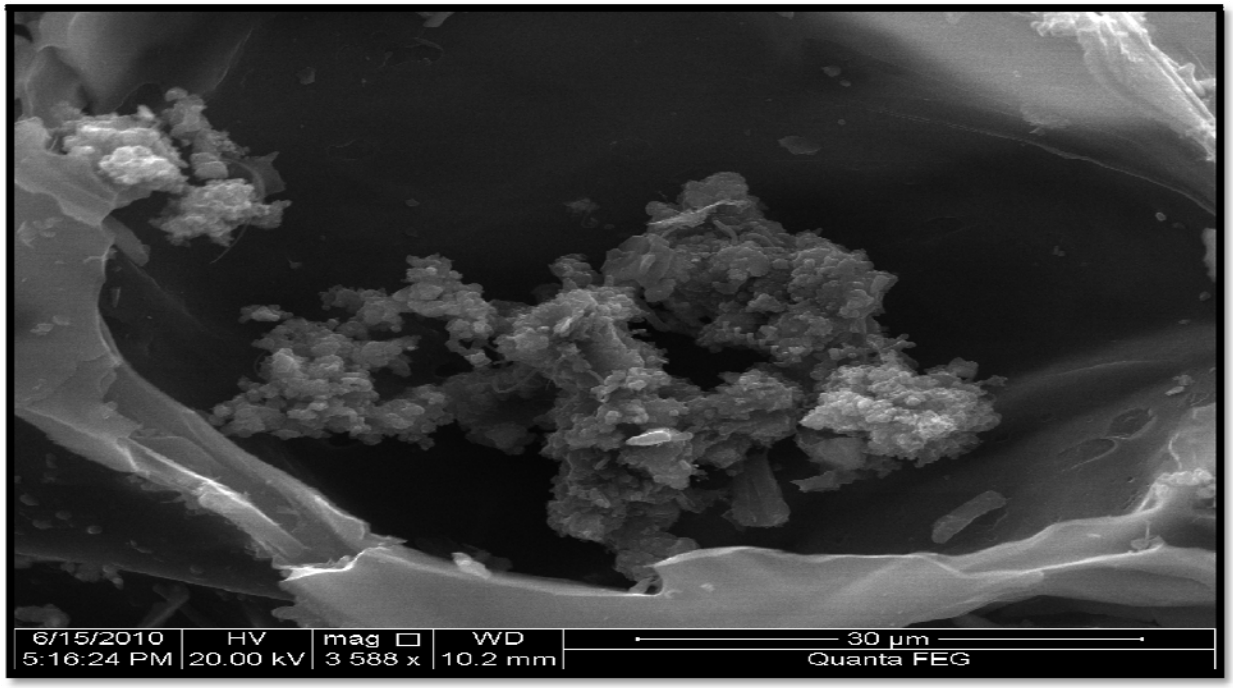

Figure 5.26: SEM Picture of used char retrieved after longevity study with biochar (6 days run at 800°C, inlet toluene concentration ppmv, mass of catalyst 3.8 g, space time 0.09 kg_{cat} h m^{-3}).

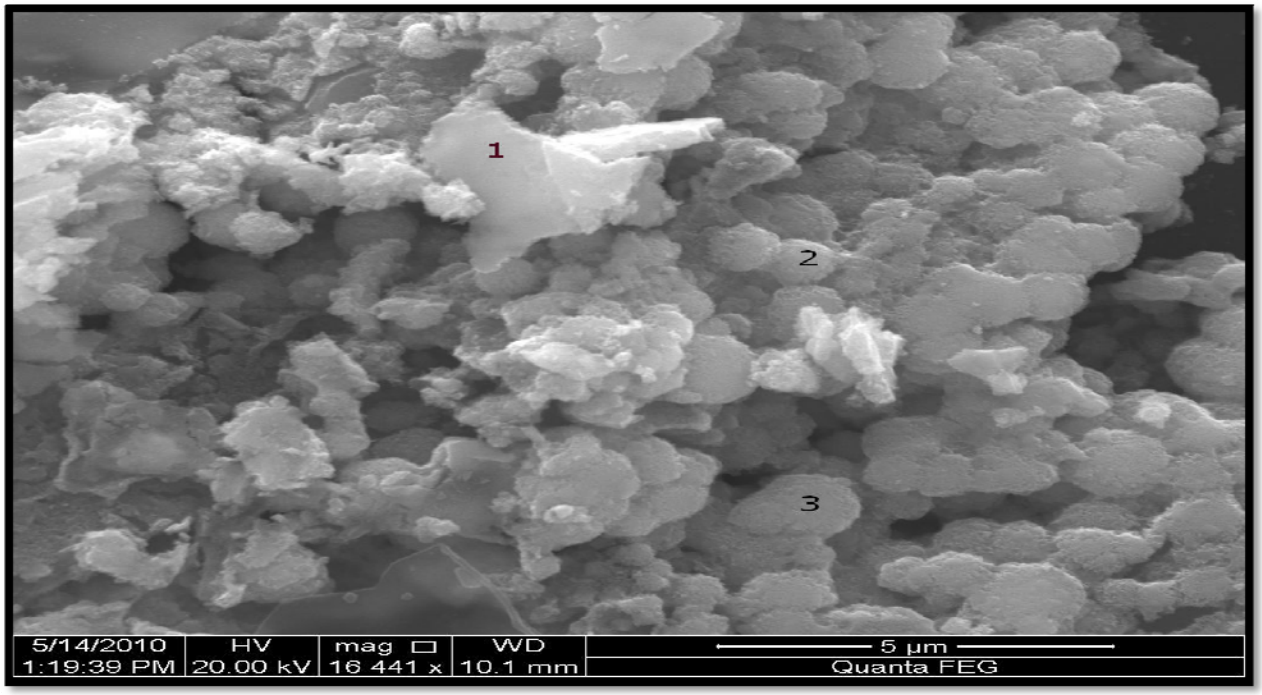

Figure 5.27: SEM picture for Fresh 9.89% iron loaded biochar

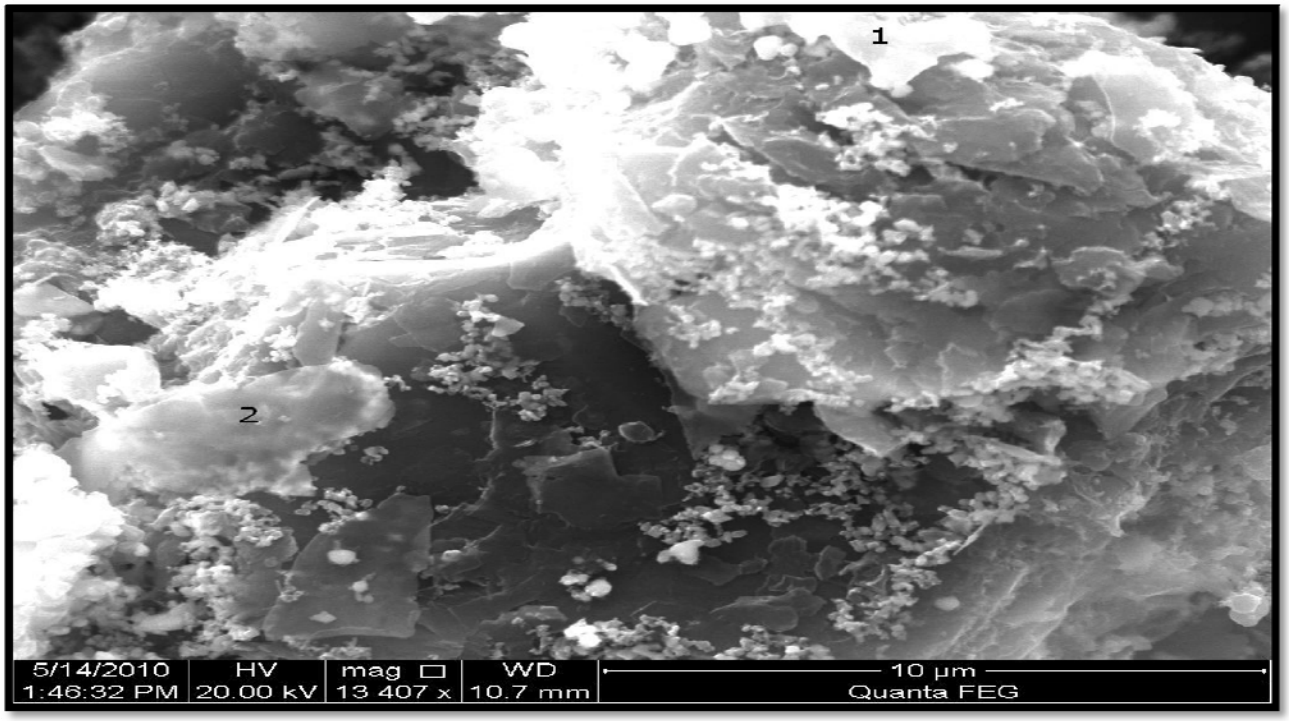

Figure 5.28: SEM picture for Used 9.89% iron loaded biochar (2500 ppm toluene concentration, temperature exposed: 600-900°C)

Table 5.6: Elemental composition of the positions shown in SEM pictures.

Catalyst	Position	Carbon %	Oxygen %	Iron %
Fresh 9.89% iron loaded char	1	32.59	18.94	48.46
	2	38.97	19.55	41.48
	3	17.04	19.39	63.56
Used 9.89% iron loaded char	1	46.01	03.36	50.63
	2	84.10	02.63	13.27

CHAPTER 6

SUMMARY AND FUTURE RECOMMENDATIONS

Syngas, a useful gas produced from gasification, has a lot of applications including direct combustion, power generation by gas engines and turbines, production of liquid fuels, and H_2 production. This gas contains higher aromatic compounds collectively called tars, which when present in unacceptable levels, pose a big problem towards the further applications of syngas. Major problems occur due to its condensation in downstream processes and blocking gas coolers, filters and engine suction channels. Present cleaning solutions include wet scrubbing, which converts the waste from gaseous to liquid form that is difficult to dispose of. Another method is thermal cracking, which requires a very high temperature (1000-1200°C) to completely crack tars leading to high energy consumption. A suitable method for cracking tars is catalytic cracking, which can perform tar removal at lower temperatures than thermal cracking (600-900°C)). The catalysts presently used are costly or if inexpensive, have a problem with sintering, attrition or coke formation. Therefore, an inexpensive alternative technology is needed to eliminate these tars.

This research investigated char generated from biomass as a low cost catalyst, produced from pyrolysis of pine bark at 950°C, to decompose toluene as model tar compound. A temperature range of 600-900ºC was used to investigate the catalytic properties of char. Kinetic parameters were calculated considering the packed bed reactor

as differential reactor in range of 550-700ºC. Toluene decomposition was also observed using char loaded with iron in three different concentrations (9.89%, 13% and 18.7%). Activation energy was calculated for 18.7% iron loaded char (500-900°C).The major conclusions obtained from this research can be summarized as follows.

1. Catalytic cracking with biochar gave toluene conversions higher than thermal cracking (over temperature range of 600-900°C with inlet toluene concentration of ~2500ppmv) which demonstrated the catalytic property of biochar. In addition to higher fractional conversions of toluene in the presence of the biochar catalyst (~96% at 900°C), two unknown peaks were observed. One of these peaks was analyzed to be benzene.
2. The char has a highly porous structure and a high surface area which is suggested by increase in toluene fractional conversion with increase in inlet toluene concentration till 4600 ppmv. This is reasoned by the capacity of char to stay unsaturated till such a high concentration of toluene.
3. Metallic Iron can be held responsible for the catalytic activity of char. This conclusion is supported by increase in toluene fraction conversion (from ~46 to 95%) at 800°C by impregnation of iron on the char. Benzene was completely decomposed at this temperature for iron loaded chars.
4. Benzene is the intermediate compound in the pathway of toluene breakdown as no benzene was observed after 700°C in case of iron loaded char.
5. Decomposition of toluene with char and iron loaded was found to follow a first order rate law but with iron loaded char the R^2 value was lower than that for char

(indicating a non-linear fit), which indicates a change in the overall mechanism in the presence of iron.

6. Both char and iron loaded char catalysts are comparable to other commercially available catalysts. The activation energy of toluene decomposition with biochar was found to be 90.33 kJ/mol which is of the range of 80.24 kJ/mol for Ni/Mayenite and 196 kJ/mol for Ni/Olivine and much less than the activation energy for thermal cracking of toluene (365kJ/mol). Iron loaded char further reduced the activation energy to 49.18kJ/mol which demonstrates the iron as the active specie in char.
7. Benzene is a carcinogenic compound of tar and is an environmental hazard. Iron loaded char was able to decompose this intermediate compound above 700°C completely.
8. Char was observed to work for continuously 6 days without a significant reduction in toluene conversion which indicates that char is a long term catalyst. Char does not need to be regenerated, since steam gasification apparently helps in maintaining and enhancing the micro pores on char and thus the catalytic activity of char is maintained.
9. Iron loaded char at 18.7% was found to be the best catalyst for tar breakdown at 800°C for an inlet concentration of ~2000 ppmv because of maximum toluene reforming, minimum CO_2 and CH_4 formation with zero benzene selectivity.
10. The iron loaded char is apparently reduced during toluene decomposition which is shown by the reduction in oxygen percentage on the surface of used 9.89% iron loaded catalyst as compared to the fresh 9.89% iron loaded catalyst.

11. The deactivation in the iron loaded catalyst occurs due to the agglomeration of iron at certain places on the surface of the catalyst, which can be seen by the SEM-EDS analysis on the iron loaded char.

Future Recommendations

As we have seen in this study and previous related work, char has shown to be a good catalyst for tar reforming; this work can be extended in a lot of ways to make char a better catalyst. Currently, the mechanism of tar breakdown on char is not clear. Understanding the mechanism would help improve the characteristics of char as a catalyst. The work presented here shows the effect of char as catalyst on toluene, but looking at industrial scale, there is a need to address a solution for complete tar removal. The decomposition behavior of each compound of tar may be different as compared to when worked as model compound. This should be approached by using direct syngas slit from the gasifier to the downstream reactor. In case of working with single model compound, the industrial scale reactor should be designed according to the rate limiting compound.

Different types of chars (i.e., using different biomass types) can be synthesized to determine the effect of char origin on its activity. Iron loaded on char showed a greater activity and increased rate of reactions for toluene breakdown, but further research is required to understand the cause of tar breakdown over iron loaded char surface. Further characterization of the catalyst by Mossbauer technology and Temperature programmed reaction (TPR) could contribute an understanding of the catalytic mechanism in the presence of iron and thus potentially improve the catalytic activity of char.

Coke formation can be a hindrance to the catalytic activity of char in decomposition of aromatics. This problem should be studied and as stated in this thesis, since aromatics breakdown into coke, a different pathway of aromatic breakdown should be initiated.

Another extension of this work would be to determine the effect of other metals present in char (Al, K, Ca, Mg, and Cu) for their involvement in catalytic activity of char. The mineral composition of char is given in Appendix E.

REFERENCES

Abu El-Rub, Z., Bramer, E., and Brem, G., 2008. Experimental comparison of biomass chars with other catalysts for tar reduction. *Fuel* 87:2243-2252.

Agata Lamacz, Andrzej Krztoń, Andrea Musi and Patrick Da Costa, 2009. Reforming of model gasification tar compounds. *Catalysis Letters* 128: 40-48.

Alden, H., Espenas, B., and Rensfelt, E., 1988. Conversion of tar in pyrolysis gas from wood using a fixed dolomite bed. *Resource of Thermochemical Biomass Conversion* :987-1001.

Amacz, A., Krzto , A., Musi, A., and Costa, P., 2009. Reforming of Model Gasification Tar Compounds. *Catalysis Letters* 128:40-48.

Aznar, M., Delgado, J., Corella, J., and Lahoz, J., 1989. Steam Gasification of Biomass in Fluidized Bed with a Secondary Catalytic Bed.-II. Tar Cracking with Dolomite in the Secondary Reactor. *Pyrolysis and Gasification*.

Aznar, P., Delgado, J., Corella, J., Lahoz, J., and Aragues, J. 1992. Fuel and Useful Gas by Steam Gasification of Biomass in Fluidized Bed with Downstream methane and Tar Steam Reforming: New Results In *Biomass for Energy Industry and Environment, 6th EC Conference; Grassi, G., Collina, A., Zibetta, H., Eds.;* Elsevier Applied Science: London, 1992;. 707-713.

Baker, E., Brown, M., Elliott, D., and Mudge, L., 1988. Characterization and treatment of tars and biomass gasifiers.

Bayarsaikhan Bazardorj, Nozomu Sonoyama, Sou Hosokai, Taihei Shimada, Jun-ichiro Hayashi, Chun-Zhu Li and Tadatoshi Chiba, 2006. Inhibition of steam gasification of char by volatiles in a fluidized bed under continuous feeding of a brown coal. *Fuel* 85: 340-349

Boerrigter, H., Van Paasen, S., Bergman, P., Könemann, J., Emmen, R., and Wijnands, A., 2005. OLGA tar removal technology. *Energy research Centre of the Netherlands, ECN-C--05-009*.

Boroson, M., Howard, J., Longwell, J., and Peters, W., 1989. Product yields and kinetics from the vapor phase cracking of wood pyrolysis tars. *AIChE Journal* 35:120-128.

Brage, C., Yu, Q., Chen, G., and Sjöström, K., 2000. Tar evolution profiles obtained from gasification of biomass and coal. *Biomass and Bioenergy* 18:87-91.

Brandt, P., Larsen, E., and Henriksen, U., 2000. High tar reduction in a two-stage gasifier. *Energy Fuels* 14:816-819.

Bridgwater, A., 1994. Catalysis in thermal biomass conversion. *Applied Catalysis. A, General* 116:5-47.

Bruinsma, O. and Moulijn, J., 1988. The pyrolytic formation of polycyclic aromatic hydrocarbons from benzene, toluene, ethylbenzene, styrene, phenylacetylene and n-decane in relation to fossil fuels utilization. *Fuel Processing Technology* 18:213-236.

Bruinsma, O., Tromp, P., De Sauvage Nolting, H., and Moulijn, J., 1988. Gas phase pyrolysis of coal-related aromatic compounds in a coiled tube flow reactor 2. Heterocyclic compounds, their benzo and dibenzo derivatives. *Fuel* 67:334-340.

Caballero, M., Aznar, M., Gil, J., Martin, J., Frances, E., and Corella, J., 1997. Commercial Steam Reforming Catalysts To Improve Biomass Gasification with Steam Oxygen Mixtures. 1. Hot Gas Upgrading by the Catalytic Reactor. *Industrial and Engineering Chemical Research* 36:5227-5239.

Caputo, A., Palumbo, M., Pelagagge, P., and Scacchia, F., 2005. Economics of biomass energy utilization in combustion and gasification plants: effects of logistic variables. *Biomass and Bioenergy* 28:35-51.

Chembukulam, S., Dandge, A., Rao, N., Seshagiri, K., and Vaidyeswaran, R., 1981. Smokeless fuel from carbonized sawdust. *Industrial and Eng*ineering *Chemistry Product Research and Development* 20: 714–719.

Cheng, H., Yue, B., Wang, X., Lu, X., and Ding, W., 2009. Hydrogen production from simulated hot coke oven gas by catalytic reforming over Ni/Mg (Al) O catalysts. *Journal of Natural Gas Chemistry* 18:225-231.

Coll, R., Salvado, J., Farriol, X., and Montane, D., 2001. Steam reforming model compounds of biomass gasification tars: conversion at different operating conditions and tendency towards coke formation. *Fuel Processing Technology* 74:19-31.

Corella J., J.H., J. Gonzalez-Saiz, F.J. Alday and J.L. Rodriguez-Trujillo, 1988. Fluidized bed steam gasification of biomass with dolomite and with a commercial FCC catalyst. In: Kuester, A. V. B. a. J. L. (ed.), *Research in Thermochemical Biomass Conversion*, page 754.

Corella, J., Toledo, J., and Padilla, R., 2004. Olivine or dolomite as in-bed additive in biomass gasification with air in a fluidized bed: Which is better? *Energy & Fuels* 18:713-720.

Corma, A., Huber, G., Sauvanaud, L., and O'connor, P., 2007. Processing biomass-derived oxygenates in the oil refinery: catalytic cracking (FCC) reaction pathways and role of catalyst. *Journal of Catalysis* 247:307-327.

Courson, C., Udron, L., Wierczy Ski, D., Petit, C., and Kiennemann, A., 2002. Hydrogen production from biomass gasification on nickel catalysts tests for dry reforming of methane. *Catalysis Today* 76:75-86.

Dayton, D., 2002. A review of the literature on catalytic biomass tar destruction. *US DOE NREL Report Golden, CO*:510-32815.

Deglise, X., Magne, P., Donnot, A. and Reningovolo, J. 1985. "Wood Tars Cracking in Gasifiers: Kinetics Data," paper 13-12 in *Symposium on Forest Products Research International— Achievements and Future*, CSIR Conference Centre, Pretonn, Republic of South Africa, April.

Delgado, J., Aznar, M., and Corella, J., 1996. Calcined dolomite, magnesite, and calcite for cleaning hot gas from a fluidized bed biomass gasifier with steam: life and usefulness. *Industrial and Engineering Chemical Research* 35:3637-3643.

Demirbas A., 2001. Biomass resource facilities and biomass conversion processing for fuels and chemicals. *Energy Conservation and Management* 42:1357-1378.

Depner, H. and Jess, A., 1999. Kinetics of nickel-catalyzed purification of tarry fuel gases from gasification and pyrolysis of solid fuels. *Fuel* 78:1369-1377.

Devi, L., Ptasinski, K., and Janssen, F., 2003. A review of the primary measures for tar elimination in biomass gasification processes. *Biomass and Bioenergy* 24:125-140.

Devi, L., Craje, M., Thüne, P., Ptasinski, K., and Janssen, F., 2005a. Olivine as tar removal catalyst for biomass gasifiers: Catalyst characterization. *Applied Catalysis A, General* 294:68-79.

Devi, L., Ptasinski, K., and Janssen, F., 2005b. Pretreated olivine as tar removal catalyst for biomass gasifiers: investigation using naphthalene as model biomass tar. *Fuel Processing Technology* 86:707-730.

Devi, L., Ptasinski, K., Janssen, F., Van Paasen, S., Bergman, P., and Kiel, J., 2005c. Catalytic decomposition of biomass tars: use of dolomite and untreated olivine. *Renewable energy* 30:565-587.

Dinkelbach, L., Meijden, C., Brenneisen, L., Strating, S., Geleijn, M., and Wubbe, R., 2005. GASREIP: GASREIniging en Prime mover design: fase A: realisatie en beproeving van een basisconfiguratie ten behoeve van biomassa warmte-kracht koppeling. http://www.ecn.nl/docs/library/report/2000/c00084.pdf

Donnot, A., Reningovolo, J., Magne, P., and Deglise, X., 1985. Flash pyrolysis of tar from the pyrolysis of pine bark. *Journal of Analytical and Applied Pyrolysis* 8:401.

Dou, B., Gao, J., Sha, X., and Baek, S., 2003. Catalytic cracking of tar component from high-temperature fuel gas. *Applied Thermal Engineering* 23:2229-2239.

Dou, B.L., Pan, W.G., Ren, J.X., Chen, B.B., Hwang, J.H., and Yu, T.U., 2008. Removal of tar component over cracking catalysts from high temperature fuel gas. *Energy Conversion and Management* 49:2247-2253.

Ekstrom, C., Lindman, N., and Petterson, R., 1985.Catalytic conversion of tars, carbon black and methane from pyrolysis/gasification of biomass. In: R.P. Overend, T.A. Milne

and L.K. Mudge, Editors, *Fundamentals of thermochemical biomass conversion*, Elsevier Applied Science, London, pp. 601–618.

El-Rub, A. and Kamel, Z., 1990. Biomass char as an in-situ catalyst for tar removal in gasification systems. *Fuel* 69:1219-1225.

El-Rub, Z.A., Brem, G., and Bramer, E.A., 2004. Review of Catalysts for Tar Elimination in Biomass Gasification processes. *Industrial and Engineering Chemical Research* 43:6911-6919.

Elliott, D. 1988. Relation of reaction time and temperature to chemical composition of pyrolysis oils. *Pyrolysis oils from Biomass,* Chapter 6, pg 55-66.

Faaij, A., 2006. Bio-energy in Europe: changing technology choices. *Energy Policy* 34:322-342.

Foust, T., Aden, A., Dutta, A., and Phillips, S., 2009. An economic and environmental comparison of a biochemical and a thermochemical lignocellulosic ethanol conversion processes. *Cellulose* 16:547-565.

Fukase, S. and Suzuka, T., 1993. Residual Oil Cracking with Generation of Hydrogen: Deactivation of Iron Oxide Catalyst in the Steam-Iron Reaction. *Applied Catalysis. A, General* 100:1-17.

Garg M., J.P., D. Radlein and D.S. Scott, 1987. Catalytic hydrogasification of wood. In: Grassi, G. (ed.), *Biomass for Energy and Industry.*

Gil, J., Caballero, M., Martin, J., Aznar, M., and Corella, J., 1999. Biomass gasification with air in a fluidized bed: effect of the in-bed use of dolomite under different operation conditions. *Industrial and Engineering Chemical Research* 38:4226-4235.

Griffiths DML, Mainhood JSR, 1967. Cracking of tar vapor and aromatic compounds on activated carbon. *Fuel* 46:167–76.

Hagen, J., 2006. *Industrial catalysis: a practical approach*. Wiley-Vch.

Han, J. and Kim, H., 2008. The reduction and control technology of tar during biomass gasification/pyrolysis: an overview. *Renewable and Sustainable Energy Reviews* 12:397-416.

Hanaoka, T., Yoshida, T., Fujimoto, S., Kamei, K., Harada, M., Suzuki, Y., Hatano, H., Yokoyama, S., and Minowa, T., 2005. Hydrogen production from woody biomass by steam gasification using a CO_2 sorbent. *Biomass and Bioenergy* 28:63-68.

Hatano, T. and Suzuki, Y., 2003. High tar reduction with porous particles for low temperature biomass gasification: Effects of porous particles on tar and gas yields during sawdust pyrolysis. *Journal of Chemical Engineering of Japan* 36:12.

Hayashi Ji, Iwatsuki M, Morishita K, Tsutsumi A, Li CZ, Chiba T, 2002. Roles of inherent metallic species in secondary reactions of tar and char during rapid pyrolysis of brown coals in a drop-tube reactor. *Fuel* 81:1977–87.

Hepola, J., Mccarty, J., Krishnan, G., and Wong, V., 1999. Elucidation of behavior of sulfur on nickel-based hot gas cleaning catalysts. *Applied Catalysis B, Environmental* 20:191-203.

Hosokai S., Hayashi Ji, Shimada T, Kobayashi Y, Kuramoto K, Li CZ, Chiba T., 2005. Spontaneous generation of tar decomposition promoter in a biomass steam reformer. *Chemical Engineering Research and Design* 83:1093–102.

Hosokai Sou, Kazuhiro Kumabe, Mikio Ohshita, Koyo Norinaga, Chun-Zhu Li, Jun-ichiro Hayashi, 2008. Mechanism of decomposition of aromatics over charcoal and necessary condition for maintaining its activity. *Fuel* 87: 2914–2922

Houben, M., 2004. Analysis of tar removal in a partial oxidation burner. http://www.mate.tue.nl/mate/pdfs/4414.pdf.

Hosoya T., Kawamoto H. and Saka S., 2008. Pyrolysis gasification reactivities of primary tar and char fractions from cellulose and lignin as studied with a closed ampoule reactor. *Journal of Analytical and Applied Pyrolysis* 83: 71-77.

Jenssen, P., Larsen, E., and Jørgensen, K. Tar reduction by partial oxidation In *Biomass for Energy and Environment: Proceedings of the 9th European Bioenergy Conference,* June 1996. Edited by P. Chartier et al. Copenhagen, Denmark: Pergamon, 1371–1375.

Jess, A., 1996. Mechanisms and kinetics of thermal reactions of aromatic hydrocarbons from pyrolysis of solid fuels. *Fuel* 75:1441-1448.

Kastner, J.R. and Das, K.C. 2002. Wet Scrubber Analysis of Volatile Organic Compound Removal in the Rendering Industry. *Journal of Air and Waste Management Association* 52:459-469.

Kinoshita, C., Wang, Y., and Zhou, J., 1994. Tar formation under different biomass gasification conditions. *Journal of analytical and applied pyrolysis* 29:169-181.

Kinoshita, C., Wang, Y., and Zhou, J., 1995. Effect of reformer conditions on catalytic reforming of biomass-gasification tars. *Industrial & engineering chemistry research* 34:2949-2954.

Knoef, H. and Ahrenfeldt, J., 2005. Handbook of Biomass Gasification. BTG Biomass Technology Group.

http://www.btgworld.com/uploads/documents/Paper%20Handbook%20Biomass%20Gasification.pdf

Kuhn, J., Zhao, Z., Felix, L., Slimane, R., Choi, C., and Ozkan, U., 2008. Olivine catalysts for methane-and tar-steam reforming. *Applied Catalysis B, Environmental* 81:14-26.

Lapidus, A., Krylova, A., Paushkin, Y., Rathouský, J., Zukal, A., and Stárek, J., 1994. Synthesis of liquid fuels from products of biomass gasification. *Fuel* 73:583-590.

Lee, W. and Kim, S., 1995. Catalytic activity of alkali and transition metal salt mixtures for steam-char gasification. *Fuel* 74:1387-1393.

Levenspiel O., 1975. Chemical Reaction Engineering. New York, John Wiley and Sons.

Li, C., Hirabayashi, D., and Suzuki, K., 2009. Development of new nickel based catalyst for biomass tar steam reforming producing H_2-rich syngas. *Fuel Processing Technology* 90:790-796.

Li, C. and Nelson, P., 1996. Fate of aromatic ring systems during thermal cracking of tars in a fluidized-bed reactor. *Energy Fuels* 10:1083-1090.

Lin, J., 2007. Combination of a biomass fired updraft gasifier and a stirling engine for power production. *Journal of Energy Resources Technology* 129:66.

Matsuhara T., Hosokai S., Norinaga K., Matsuoka K., Li C. and Hayashi J., 2010. In-situ reformimg of tar from the rapid pyrolysis of a brown coal over char. *Energy and Fuels* 24: 76-83.

Matsuoka, K., Shimbori, T., Kuramoto, K., Hatano, H., and Suzuki, Y., 2006. Steam reforming of woody biomass in a fluidized bed of iron oxide-impregnated porous alumina. *Energy and Fuels* 20:2727-2731.

Mckee, D., 1983. Mechanisms of the alkali metal catalysed gasification of carbon. *Fuel* 62:170-175.

Md. Azhar Uddin, Hiroshi Tsuda, Shengji Wu and Eiji Sasaoka, 2006. Catalytic decomposition of biomass tars with iron oxide catalysts. *Fuel* 87: 451–459

Milne, T., Evans, R., and Abatzaglou, N. 1998. Biomass Gasifier"Tars": Their Nature, Formation, and Conversion. *NREL/TP-570-25357*, National Renewable Energy Laboratory, Golden, CO (US).

Milne, T., Evans, R., and Abatzoglou, N. 1997. Biomass Gasifier" Tars": Their Nature, Formation, Destruction, and Tolerance Limits in Energy Conversion Devices.

Nacken, M., Ma, L., Heidenreich, S., and Baron, G.V., 2009. Performance of a catalytically activated ceramic hot gas filter for catalytic tar removal from biomass gasification gas. *Applied Catalysis B-Environmental* 88:292-298.

Narvaez, I., Orio, A., Aznar, M., and Corella, J., 1996. Biomass gasification with air in an atmospheric bubbling fluidized bed. Effect of six operational variables on the quality of the produced raw gas. *Industrial Engineering Chemical Research* 35:2110-2120.

Neeft, J., Knoef, H., and Ojani, P., 1998. Behaviour of tar in biomass gasification systems. Tar related problems and their solutions. *Energy from Waste and Biomass, Enschede/Petten, BTG/ECN, Novem-EWAB* 9919:74.

Nordgreen Thomas, Truls Liliedahl and Krister Sjöström, 2005. Metallic iron as a tar breakdown catalyst related to atmospheric, fluidised bed gasification of biomass. *Fuel* 85: 689-694.

Orio, A., Corella, J., and Narvaez, I., 1997. Performance of different dolomites on hot raw gas cleaning from biomass gasification with air. *Industrial Engineering Chemical Research* 36:3800-3808.

Radovic, L., Walker, P., and Jenkins, R., 1984. Catalytic coal gasification: use of calcium versus potassium. *Fuel* 63:1028-1030.

Radwan, A., Kyotani, T., and Tomita, A., 2000. Characterization of coke deposited from cracking of benzene over USY zeolite catalyst. *Applied Catalysis A, General* 192:43-50.

Rapagna, S., Jand, N., Kiennemann, A., and Foscolo, P., 2000. Steam-gasification of biomass in a fluidised-bed of olivine particles. *Biomass and bioenergy* 19:187-197.

Raskin, N., Palonen, J., and Nieminen, J., 2001. Power boiler fuel augmentation with a biomass fired atmospheric circulating fluid-bed gasifier. *Biomass and bioenergy* 20:471-481.

Seshadri, K. and Shamsi, A., 1998. Effects of Temperature, Pressure, and Carrier Gas on the Cracking of Coal Tar over a Char Dolomite Mixture and Calcined Dolomite in a Fixed-Bed Reactor. *Industrial Engineering Chemical Research* 37:3830-3837.

Shilling, N. and Jones, R., 2003. The Response of Gas Turbines to a CO_2 Constrained Environment Paper Presented at the *Gasification Technology Conference*, October 2003, San Francisco, CA, USA.

Simell, P., Leppälahti, J., and Bredenberg, J., 1992. Catalytic purification of tarry fuel gas with carbonate rocks and ferrous materials. *Fuel* 71:211-218.

Simell, P., Hakala, N., Haario, H., and Krause, A., 1997. Catalytic decomposition of gasification gas tar with benzene as the model compound. *Industrial Engineering Chemical Research* 36:42-51.

Simell, P., Hirvensalo, E., Smolander, V., and Krause, A., 1999. Steam reforming of gasification gas tar over dolomite with benzene as a model compound. *Industrial Engineering Chemical Research* 38:1250-1257.

Singh, S., Walawender, W., Fan, L., and Geyer, W., 1986. Steam gasification of cottonwood (branches) in a fluidized bed. *Wood and Fiber Science* 18:327–344.

Sridhar, G., Paul, P., and Mukunda, H., 2001. Biomass derived producer gas as a reciprocating engine fuel—an experimental analysis. *Biomass and Bioenergy* 21:61-72.

Srinakruang Jumluck**,** Kazuhiro Sato, Tharapong Vitidsant and Kaoru Fujimoto 2005. A highly efficient catalyst for tar gasification with steam. *Catalysis Commumnications* 6: 437-440.

Stiles, H. and Kandiyoti, R., 1989. Secondary reactions of flash pyrolysis tars measured in a fluidized bed pyrolysis reactor with some novel design features. *Fuel* 68:275-282.

Sutton, D., Kelleher, B., and Ross, J., 2001. Review of literature on catalysts for biomass gasification. *Fuel Processing Technology* 73:155-173.

Suzuki, T., Ohme, H., and Watanabe, Y., 1992. Alkali metal catalyzed CO_2 gasification of carbon. *Energy & Fuels* 6:343-351.

Swierczynski, D., Courson, C., and Kiennemann, A., 2008. Study of steam reforming of toluene used as model compound of tar produced by biomass gasification. *Chemical Engineering & Processing: Process Intensification* 47:508-513.

Taralas, G., Vassilatos, V., Delgado, J., and Sjostrom, K., 1991. Thermal and catalytic cracking of n-heptane in presence of CaO, MgO and calcined dolomites. *Canadian Journal of Chemical Engineering* 69:1413-1419.

Taralas, G., 1996. Catalytic steam cracking of n-heptane with special reference to the effect of calcined dolomite. *Industrial Engineering Chemical Research* 35:2121-2126.

Taralas, G., Kontominas, M., and Kakatsios, X., 2003. Modeling the thermal destruction of toluene (C7H8) as tar-related species for fuel gas cleanup. *Energy and Fuels* 17:329-337.

Tesner, P. and Shurupov, S., 1997. Soot formation during pyrolysis of naphthalene, anthracene and pyrene. *Combustion Science and Technology* 126:139-152.

Tijmensen, M., Faaij, A., Hamelinck, C., and Van Hardeveld, M., 2002. Exploration of the possibilities for production of Fischer Tropsch liquids and power via biomass gasification. *Biomass and Bioenergy* 23:129-152.

Vassilatos, V.B.C.; Taralas, G.; Sjöström, K. , 1992. The Effects of Temperature and Additives on Product Composition in Thermal Cracking of Biomass, p. 762–765, *Biomass for Energy, Industry and Environment*, 6th E.C. Conference. London: Elsevier.

Walton, S., He, X., Zigler, B., and Wooldridge, M., 2007. An experimental investigation of the ignition properties of hydrogen and carbon monoxide mixtures for syngas turbine applications. *Proceedings of the Combustion Institute* 31:3147-3154.

Watanabe, M., Inomata, H., and Arai, K., 2002. Catalytic hydrogen generation from biomass (glucose and cellulose) with ZrO2 in supercritical water. *Biomass and bioenergy* 22:405-410.

Wornat, M., Sarofim, A., and Longwell, J., 1987. Changes in the degree of substitution of polycyclic aromatic compounds from pyrolysis of a high-volatile bituminous coal. *Energy & Fuels* 1:431-437.

Xu, W. and Tomita, A., 1989. Effect of metal oxides on the secondary reactions of volatiles from coal. *Fuel* 68:673-676.

Yamaguchi, T., Yamasaki, K., Yoshida, O., Kanai, Y., Ueno, A., and Kotera, Y., 1986. Deactivation and regeneration of catalyst for steam gasification of wood to methanol synthesis gas. *Industrial & Engineering Chemistry Product Research and Development* 25:239-243.

Yang, W. Handbook of fluidization and fluid-particle systems, 2003. Siemens Westinghouse Power Corporation Pittsburgh, Pennsylvania, U.S.A. Taylor & Francis Group LLC

Yeboah, Y., Longwell, J., Howard, J., and Peters, W., 1980. Effect of calcined dolomite on the fluidized bed pyrolysis of coal. *Industrial & Engineering Chemistry Process Design and Development* 19:646-653.

Yu J., Tian F. McKenzie L.J. and Li C., 2007. Char supported nano iron catalyst for water gas-shift reaction Hydrogen production from coal/biomass gasification. *Process safety and environmental protection* 84(B2): 125-130.

Zanzi, R., Sjöström, K., and Björnbom, E., 2002. Rapid pyrolysis of agricultural residues at high temperature. *Biomass and bioenergy* 23:357-366.

Zhang, T. and Amiridis, M., 1998. Hydrogen production via the direct cracking of methane over silica-supported nickel catalysts. *Applied Catalysis A, General* 167:161-172.

Zhang, X., 2003. The mechanism of tar cracking by catalyst and the gasification of biomass. . Zhejiang University (China).

Zhang, R., Brown, R., Suby, A., and Cummer, K., 2004. Catalytic destruction of tar in biomass derived producer gas. *Energy Conversion and Management* 45:995-1014.

Zhang Yuwen, Cheng Hongwei, Lu Xionggang, Ding Weizhong, and Zhou Guozhi, 2009. Influence of rare earth promoters on the performance of Ni/Mg(Al)O catalysts for hydrogenation and steam reforming of toluene. *Rare Metals* 28:582-589

Zhao, H., Draelants, D., and Baron, G., 2000. Performance of a nickel-activated candle filter for naphthalene cracking in synthetic biomass gasification gas. *Industrial Engineering Chemical Research* 39:3195-3201.

APPENDIX A

LITERATURE REVIEW FOR DECOMPOSITION OF MODEL COMPOUNDS OF BIOMASS TARS

Tar model compound	Catalyst	Operating Conditions					Observations	Reference
		Tar concentration	Additional cpd	Carrier Gas	Flow rate ml/min	Temp.		
Benzene	Dolomite	50-400 ppm	CO_2	Nitrogen	0.06-0.18m^3/h	600-900	A very low conversion	pekka a. simell
Toluene	Ni/CeZrO2	1000 ppm	Steam	Argon	250	900	High conversion of toluene to CO and CO_2 at lower temperatures.	Agata Lamacz (2008)
Toluene	Ni/dolomite	1.4% wt by mol	Steam	He+H2	50	770	99.3% conversion obtained. Even at low temperatures, catalyst inhibited carbon formation	Jumluck Srinakruang (2004)
Toluene	ZC	3000ppm	H_2	He	100 sccm		24% conversion obtained. Tungsten was effective catalyst at above 750^oC.	Pansare (2008)
n-heptane	MgO, Cao, Dolomite, NiMo/alumina	2.9-4.7kPa				700-900	From 700- 900^oC, 7.21-51.4% conversion with MgO; 6.44-61.7% with CaO, 13.5-61.3% with dolomite and 20.1-40.1% with NiMo/alumina. Coke formation with Ni.	taralas (1998)

Tar model compound	Catalyst	Operating Conditions					Observations	Reference
		Tar concentration	Additional cpd	Carrier Gas	Flow rate ml/min	Temp.		
90%Toluene/ 10% Naphthalene	H_2S/ZrO_2	15 g/m^3	Syngas simulation		2dm^3/min	600-900	85% toluene 70% naphthalene conversion was obtained	hanne (2009)
Naphthalene	Co/MgO	1g/hr	Steam	Nitrogen	20	900	12% Co/MgO gave the maximum conversion of 23%	Takeshi Furusawa (2004)-a
Naphthalene	Ni/MgO	1g/hr	Steam	Nitrogen	20	900	The conversion was less than 23%	Takeshi Furusawa(2004)-b
Naphthalene	Char	90 g/nm^3	Steam			900	High conversion of 99.60% obtained for naphthalene	
Phenol	Char	8-13g/nm^3	Steam			700, 900	The conversion of phenol increased from 6.3% to 98% by temperature increase from 700 to 900°C.	Z. abu el rub (2008)
Naphthalene	Olivine	3.2-9.3g/m^3	Syngas simulation/steam		1000	900	Untreated olivine did not gaive more than 25% conversion but heating pre treatment gave 81% conversions.	L. Devi (2005)
	Dolomite					900		
	Pretreated olivine					900		
Naphthalene, Benzene	Ni/MgO	0.1-1.4% benzene and 0.05-1% naphthalene	CH_4, H_2, N_2, NH_3, H_2S	Nitrogen	150l/hr	1150-1400	A complete conversion for naphthalene was obtained at around 750°C but benzene showed a maximum conversion of 30%	Depner and Jess (1999)

APPENDIX B

STANDARD CURVE GENERATION

B1. Toluene and Benzene

A standard curve for toluene (gas phase) in the range of 50-5000 ppmv was prepared from liquid standards. A known volume of toluene (liquid phase) was mixed with a known volume of nitrogen and the final mixture thus obtained was assumed to be in gaseous phase owing to the low concentration of toluene in the liquid phase. The mixture was analyzed using the GC/FID. The respective peak area of toluene was measured. The same procedure was repeated for different concentrations of toluene in the range of 50-5000 ppmv. Finally the standard curve (figure A.1.1) was obtained by plotting the concentration of toluene against the corresponding peak area. The standard curve obtained was used for the further analysis of the inlet and outlet concentrations of toluene in the catalytic decomposition experiments and periodically confirmed throughout the course of study.

Same procedure was followed for benzene (gas phase) in the range of 50-2500 ppmv. The standard curve for benzene is shown in figure B.2. The standard curve obtained was used for the further analysis of the concentrations of benzene in the exit gas of the catalytic decomposition experiments and periodically confirmed throughout the course of study.

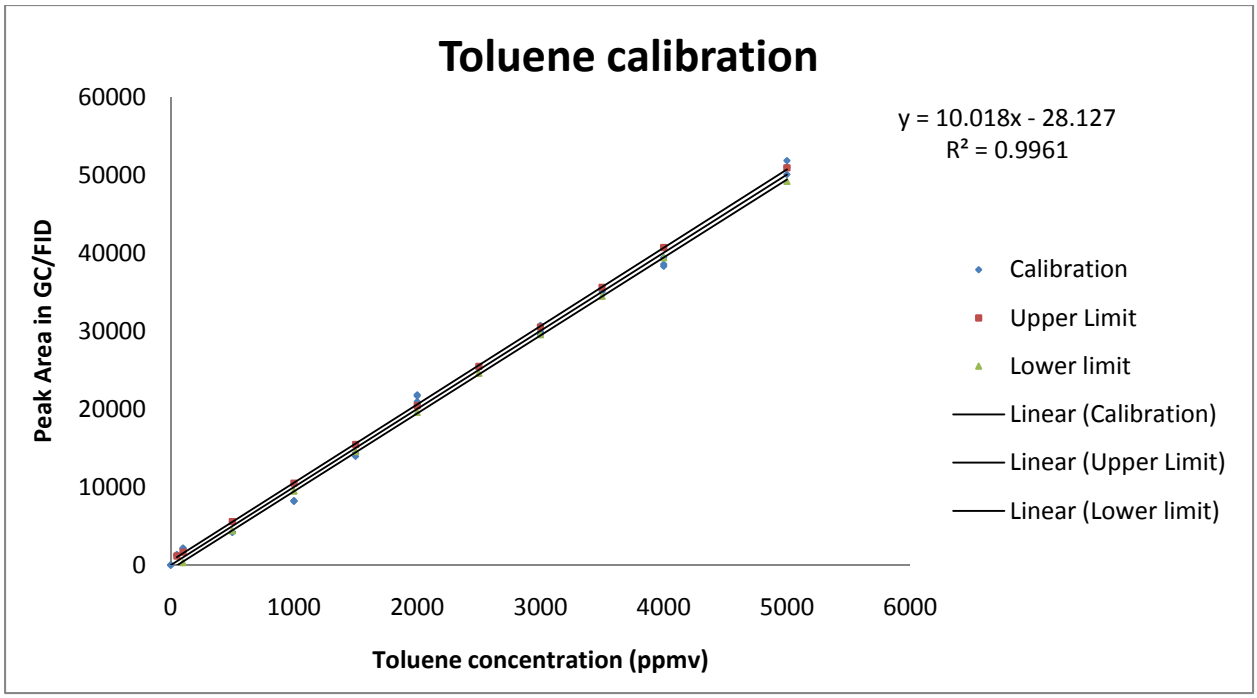

Figure B.1(a). Standard Curve for toluene

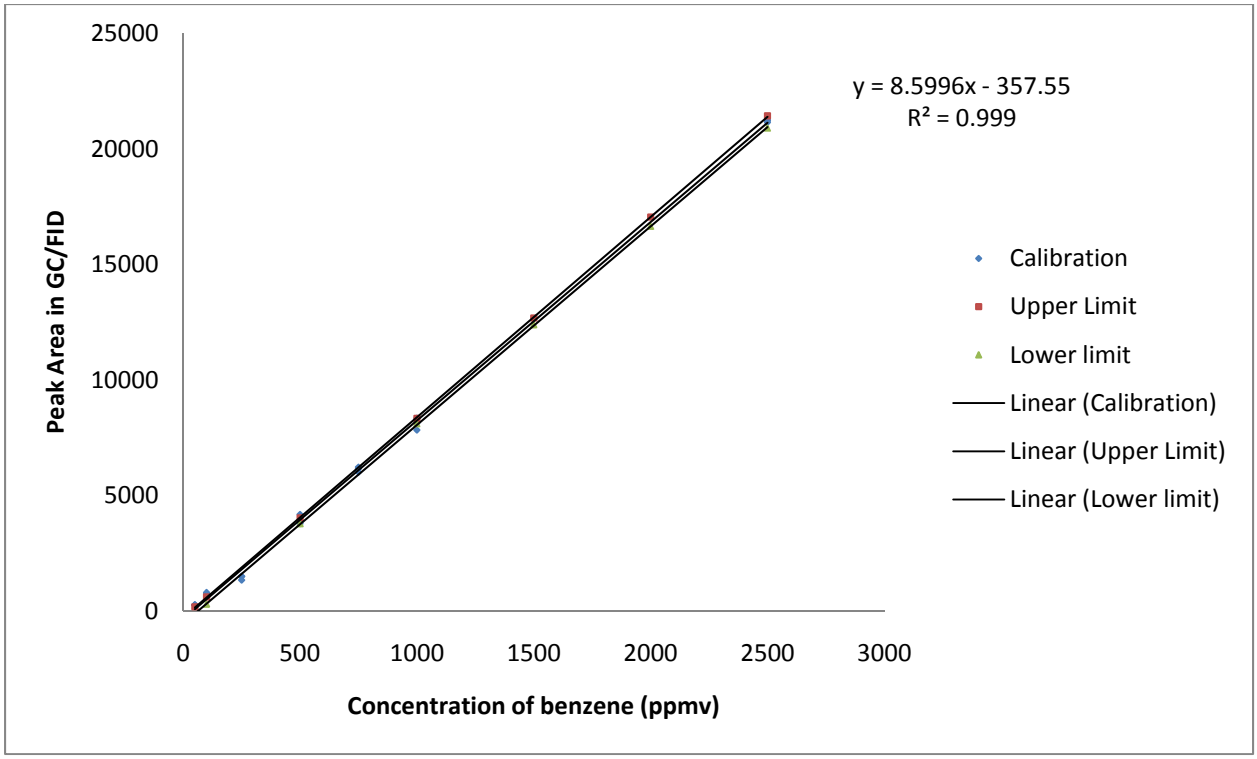

Figure B.1(b): Standard Curve for benzene

B2. CO_2 and CH_4

Standard curve for CO_2 and CH_4 was made by adding known percentages of respective gases in rest of nitrogen. The mix of gases was analyzed using GC-TCD. 30µl of sample was injected to find the area under curve. A linear trend was observed and linear equation was calculated. The standard curve for CO_2 is shown in figure B.3 and that of CH_4 is shown in figure B.4.

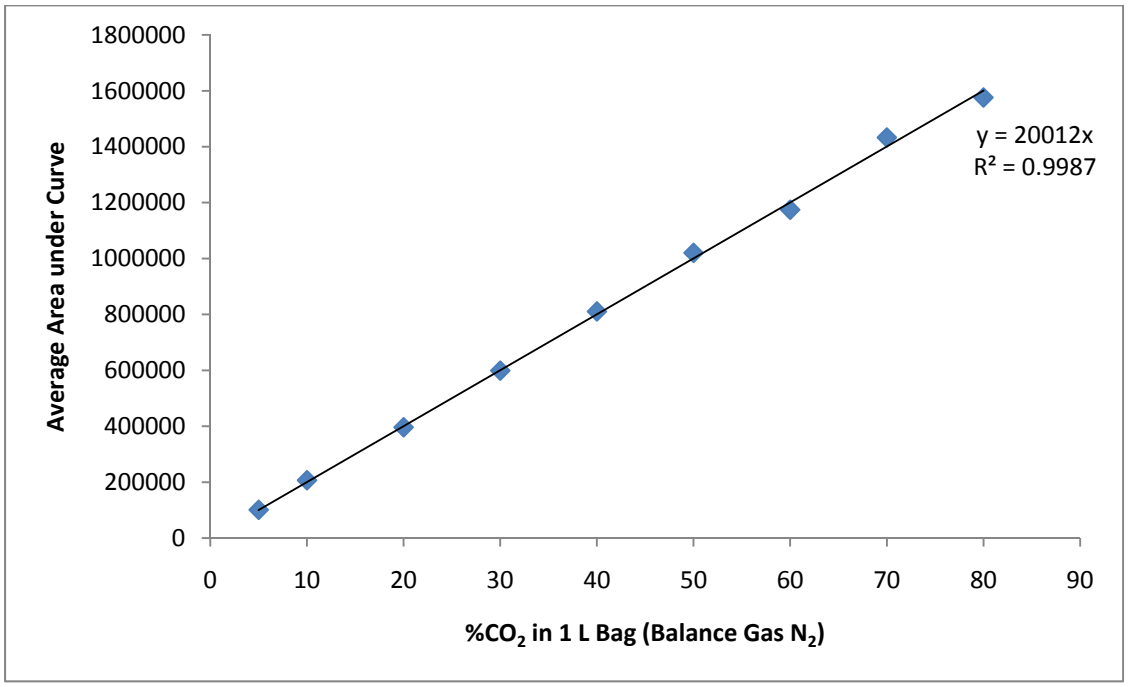

Figure B.2 (a): Standard Curve for CO_2

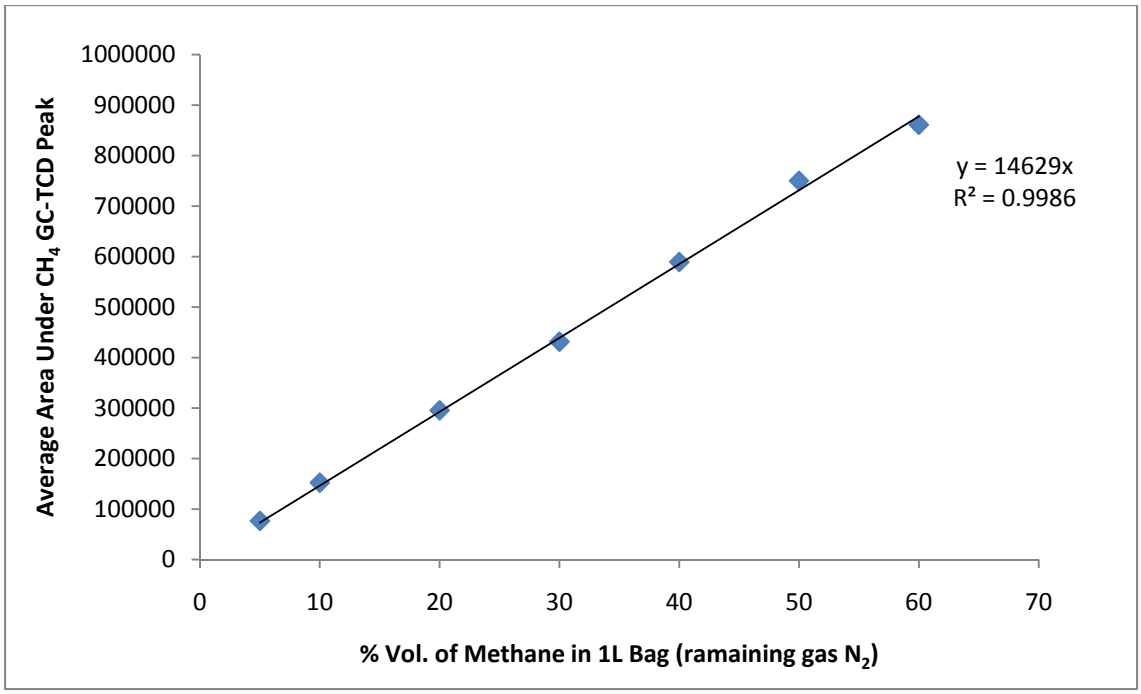

Figure B.2 (b): Standard Curve for CH_4

APPENDIX C

SAS OUTPUTS

C.1: SAS output for difference in thermal cracking with quartz beads and empty bed

The SAS System

The GLM Procedure

Dependent Variable: Conv

Source	DF	Sum of Squares	Mean Square	F Value	Pr > F
Model	4	3.31732457	0.82933114	2815.08	<.0001
Error	59	0.01738159	0.00029460		
Corrected Total	63	3.33470615			

R-Square	Coeff Var	Root MSE	Conv Mean
0.994788	7.255353	0.017164	0.236570

Source	DF	Type I SS	Mean Square	F Value	Pr > F
TEMP	3	3.24285462	1.08095154	3669.18	<.0001
TRT	1	0.07446995	0.07446995	252.78	<.0001

Source	DF	Type III SS	Mean Square	F Value	Pr > F
TEMP	3	3.24285462	1.08095154	3669.18	<.0001
TRT	1	0.07446995	0.07446995	252.78	<.0001

****

C.2: SAS Output for difference in 3 loadings in terms of toluene fractional conversion

```
*******************************************************************************

                                The SAS System

                              The GLM Procedure

Dependent Variable: Conversion

                                      Sum of
 Source                     DF        Squares    Mean Square   F Value   Pr > F

 Model                      11    15.69769468     1.42706315   34364.7   <.0001

 Error                     180     0.00747486     0.00004153

 Corrected Total           191    15.70516954


           R-Square     Coeff Var      Root MSE    Conversion Mean

           0.999524      0.945318      0.006444           0.681691


 Source                     DF      Type I SS    Mean Square   F Value   Pr > F

 Temp                        3    14.68640009     4.89546670    117886   <.0001
 Loading                     2     0.48304143     0.24152072   5815.99   <.0001
 Temp*Loading                6     0.52825316     0.08804219   2120.12   <.0001


 Source                     DF    Type III SS    Mean Square   F Value   Pr > F

 Temp                        3    14.68640009     4.89546670    117886   <.0001
 Loading                     2     0.48304143     0.24152072   5815.99   <.0001
 Temp*Loading                6     0.52825316     0.08804219   2120.12   <.0001

*******************************************************************************

                                The SAS System

                              The GLM Procedure

                Duncan's Multiple Range Test for Conversion

   NOTE: This test controls the Type I comparisonwise error rate, not the
                         experimentwise error rate.


                      Alpha                          0.05
                      Error Degrees of Freedom        180
                      Error Mean Square          0.000042


            Number of Means           2           3           4
```

Critical Range	.002596	.002732	.002823

Means with the same letter are not significantly different.

Duncan Grouping	Mean	N	Temp
A	0.961579	48	900
B	0.952190	48	800
C	0.445202	48	700
D	0.367792	48	600

****

The SAS System

The GLM Procedure

Duncan's Multiple Range Test for Conversion

NOTE: This test controls the Type I comparisonwise error rate, not the experimentwise error rate.

Alpha	0.05
Error Degrees of Freedom	180
Error Mean Square	0.000042

Number of Means	2	3
Critical Range	.002248	.002366

Means with the same letter are not significantly different.

Duncan Grouping	Mean	N	Loading
A	0.734995	64	loading3
B	0.695569	64	loading2
C	0.614508	64	loading1

****

C.3: SAS Output for difference in 3 loadings in terms of Benzene formation

```
********************************************************************************

                                The SAS System

                              The GLM Procedure

Dependent Variable: Benzene

                                     Sum of
 Source                      DF       Squares    Mean Square   F Value   Pr > F

 Model                        7    0.32042543     0.04577506    318.13   <.0001

 Error                      120    0.01726646     0.00014389

 Corrected Total            127    0.33769190


              R-Square     Coeff Var      Root MSE    Benzene Mean

              0.948869      10.40264      0.011995        0.115310


 Source                      DF      Type I SS    Mean Square   F Value   Pr > F

 Temp                         3    0.22022671     0.07340890    510.18   <.0001
 Loading                      2    0.06718282     0.03359141    233.46   <.0001
 Temp*Loading                 2    0.03301591     0.01650796    114.73   <.0001


 Source                      DF    Type III SS    Mean Square   F Value   Pr > F

 Temp                         3    0.21660839     0.07220280    501.80   <.0001
 Loading                      2    0.06718282     0.03359141    233.46   <.0001
 Temp*Loading                 2    0.03301591     0.01650796    114.73   <.0001
********************************************************************************

                                The SAS System

                              The GLM Procedure

                  Duncan's Multiple Range Test for Benzene

   NOTE: This test controls the Type I comparisonwise error rate, not the
                         experimentwise error rate.


                    Alpha                          0.05
                    Error Degrees of Freedom        120
                    Error Mean Square          0.000144
                    Harmonic Mean of Cell Sizes       24

                      NOTE: Cell sizes are not equal.
```

Number of Means	2	3	4
Critical Range	.006856	.007216	.007455

Means with the same letter are not significantly different.

Duncan Grouping	Mean	N	Temp
A	0.142110	48	600
B	0.134104	48	700
C	0.071363	16	900
D	0.022475	16	800

****

The SAS System

The GLM Procedure

Duncan's Multiple Range Test for Benzene

NOTE: This test controls the Type I comparisonwise error rate, not the experimentwise error rate.

Alpha	0.05
Error Degrees of Freedom	120
Error Mean Square	0.000144
Harmonic Mean of Cell Sizes	38.4

NOTE: Cell sizes are not equal.

Number of Means	2	3
Critical Range	.005420	.005704

Means with the same letter are not significantly different.

Duncan Grouping	Mean	N	Loading
A	0.156031	32	loading2
B	0.102252	64	loading1
B			
B	0.100706	32	loading3

****

C.4: SAS Output for difference in 3 loadings in terms of CO_2 formation

```
********************************************************************************

                                The SAS System

                              The GLM Procedure

Dependent Variable: CO2

                                     Sum of
 Source                      DF       Squares    Mean Square   F Value   Pr > F

 Model                       11    11.44158919     1.04014447   2523.32   <.0001

 Error                      180     0.07419836     0.00041221

 Corrected Total            191    11.51578755


              R-Square     Coeff Var      Root MSE      CO2 Mean

              0.993557      8.409247      0.020303      0.241437


 Source                      DF      Type I SS    Mean Square   F Value   Pr > F

 Temp                         3     8.32032316     2.77344105   6728.17   <.0001
 Loading                      2     1.26822727     0.63411364   1538.32   <.0001
 Temp*Loading                 6     1.85303876     0.30883979    749.22   <.0001


 Source                      DF    Type III SS    Mean Square   F Value   Pr > F

 Temp                         3     8.32032316     2.77344105   6728.17   <.0001
 Loading                      2     1.26822727     0.63411364   1538.32   <.0001
 Temp*Loading                 6     1.85303876     0.30883979    749.22   <.0001

********************************************************************************

                                The SAS System

                              The GLM Procedure

                    Duncan's Multiple Range Test for CO2

   NOTE: This test controls the Type I comparisonwise error rate, not the
                         experimentwise error rate.


                      Alpha                          0.05
                      Error Degrees of Freedom        180
                      Error Mean Square          0.000412


            Number of Means           2           3           4
            Critical Range       .008178     .008608     .008895
```

Means with the same letter are not significantly different.

Duncan Grouping	Mean	N	Temp
A	0.493202	48	700
B	0.400854	48	600
C	0.037446	48	800
C			
C	0.034246	48	900

****

The SAS System

The GLM Procedure

Duncan's Multiple Range Test for CO2

NOTE: This test controls the Type I comparisonwise error rate, not the experimentwise error rate.

Alpha	0.05
Error Degrees of Freedom	180
Error Mean Square	0.000412

Number of Means	2	3
Critical Range	.007082	.007455

Means with the same letter are not significantly different.

Duncan Grouping	Mean	N	Loading
A	0.348347	64	loading2
B	0.224530	64	loading1
C	0.151434	64	loading3

****

C.5: SAS Output for difference in 3 loadings in terms of CH_4 formation

```
*******************************************************************************

                                The SAS System

                              The GLM Procedure

Dependent Variable: CH4

                                     Sum of
 Source                      DF       Squares    Mean Square   F Value   Pr > F

 Model                        5    0.03523868     0.00704774    102.31   <.0001

 Error                       90    0.00619983     0.00006889

 Corrected Total             95    0.04143851


               R-Square     Coeff Var      Root MSE      CH4 Mean

               0.850385      8.761826      0.008300      0.094727


 Source                      DF      Type I SS    Mean Square   F Value   Pr > F

 Temp                         1    0.03248704     0.03248704    471.60   <.0001
 Loading                      2    0.00099179     0.00049590      7.20   0.0013
 Temp*Loading                 2    0.00175984     0.00087992     12.77   <.0001


 Source                      DF    Type III SS    Mean Square   F Value   Pr > F

 Temp                         1    0.03248704     0.03248704    471.60   <.0001
 Loading                      2    0.00099179     0.00049590      7.20   0.0013
 Temp*Loading                 2    0.00175984     0.00087992     12.77   <.0001
*******************************************************************************

                                The SAS System

                              The GLM Procedure

                    Duncan's Multiple Range Test for CH4

   NOTE: This test controls the Type I comparisonwise error rate, not the
                         experimentwise error rate.


                      Alpha                          0.05
                      Error Degrees of Freedom         90
                      Error Mean Square          0.000069


                         Number of Means              2
                         Critical Range         .003366
```

Means with the same letter are not significantly different.

Duncan Grouping	Mean	N	Temp
A	0.113123	48	900
B	0.076331	48	800

****

The SAS System

The GLM Procedure

Duncan's Multiple Range Test for CH4

NOTE: This test controls the Type I comparisonwise error rate, not the experimentwise error rate.

Alpha	0.05
Error Degrees of Freedom	90
Error Mean Square	0.000069

Number of Means	2	3
Critical Range	.004122	.004338

Means with the same letter are not significantly different.

Duncan Grouping	Mean	N	Loading
A	0.098506	32	loading2
A			
A	0.095025	32	loading3
B	0.090650	32	loading1

****

C.6: SAS Output for difference in toluene conversion for char and fly ash

The GLM Procedure

Dependent Variable: Conv Toluene Fractional conversion

Source	DF	Sum of Squares	Mean Square	F Value
Model	4	5.59558125	1.39889531	2466.49
Error	59	0.03346250	0.00056716	
Corrected Total	63	5.62904375		

Source	Pr > F
Model	<.0001
Error	
Corrected Total	

R-Square	Coeff Var	Root MSE	Conv Mean
0.994055	5.494481	0.023815	0.433438

Source	DF	Type I SS	Mean Square	F Value
Cat	1	0.01322500	0.01322500	23.32
Temp	3	5.58235625	1.86078542	3280.88

Source	Pr > F
Cat	<.0001
Temp	<.0001

Source	DF	Type III SS	Mean Square	F Value
Cat	1	0.01322500	0.01322500	23.32
Temp	3	5.58235625	1.86078542	3280.88

Source	Pr > F
Cat	<.0001
Temp	<.0001

APPENDIX D

RATE OF REACTION CALCULATION

The overall reaction rate was calculated from the measured fractional conversion, mass of the ash, volumetric gas flow rate, inlet mole fraction, pressure, and temperature using the following equation.

$$-r = Q\left(\frac{P}{RT}\right) y \left(\frac{X}{W}\right) MW$$

where,

- r = reaction rate mole g^{-1} min^{-1}

Q = total gas flow rate (Nitrogen + toluene), L min^{-1}

y = mole fraction of toluene in the inlet

X = fractional conversion of toluene = $(C_{in} - C_{out})/ C_{out}$

C_{in} = toluene concentration at the inlet of the packed-bed reactor

C_{out} = toluene concentration at the outlet of the packed-bed reactor system

W = mass of the catalyst (g)

MW = Molecular weight of toluene (g/mol)

P = pressure, atm

R = ideal gas constant, L-atm mol^{-1} K^{-1}

T = Temperature, K

The sample calculations for an inlet toluene concentration of 2500 ppmv, steam concentration of 6250 ppm (=2.5 * steam concentration) and total gas flow rate of 0.7 L min-1, catalyst weight of 3.8 g and toluene fractional conversion of 0.10.

Inlet toluene moles calculation

Using the ideal gas law,

$$PV = n_{toluene}RT$$

Where,

P = 1 atm

V = volume of toluene in a gas mixture of 0.7 L (on a minute basis)

= ((2500* 0.7)/10^6) L

R = 0.08206 L-atm mol^{-1} K^{-1}

T = 873 K (reaction temperature)

$n_{toluene}$ = PV/RT = ((2500* 0.7)/10^6) * (1/ (0.08206*873)) = 2.464 E-05 moles

Toluene mole fraction in total inlet gas mixture

The inlet gas mixture contains toluene, water and nitrogen. In order to calculate the mole fraction of toluene in the gas mixture, the number of moles of each gas present in the mixture was first calculated.

$n_{steam} = PV_{steam}/RT$

where,

V_{steam} = (6250*0.7)/ (10^6) = 0.004375

n_{steam} = (0.004375)/ (0.08206*873) = 6.16 E-05 moles

$n_{nitrogen} = PV_{nitrogen} / RT = 1* 0.7/(0.08206*873) = 0.0099$ moles

$Y_{toluene} = n_{toluene} / (n_{toluene} + n_{steam} + n_{nitrogen})$

$= 2.464$ E-05/(2.464 E-05 + 6.16 E-05 + 0.0099)

$= 0.0025$

Calculation of reaction rate

$$-r = Q\left(\frac{P}{RT}\right) y \left(\frac{X}{W}\right) MW$$

$$= 0.7 * \left(\frac{1}{.08203*873}\right) * .0025 * \left(\frac{0.10}{3.8}\right) * 92.18$$

$= 5.92$E -05 mol g^{-1} min^{-1}

$= 9.88$E -07 mol g^{-1} sec^{-1}

APPENDIX E

MINERAL COMPOSITION OF CATALYSTS

Element symbol	Char	9.89% Iron Loaded char	13% Iron Loaded char	18.9% Iron Loaded char
Al	1455	140	186	742
B	14.98	9.36	11.7	29.1
Ca	3279	29.2	36.4	59.7
Cd	<0.45	947	863	1019
Cr	3.83	19.7	23.2	35.1
Cu	161.6	88.5	69.8	94.7
Fe	261.2	98911	129768	186535
K	2002	12.6	16.5	28.4
Mg	726.1	184	174	290
Mn	89.6	117	162	211
Mo	0.58	<0.73	<0.64	<0.9
Na	269.6	2.44	74.2	<1.8
Ni	3.28	<8.71	<7.73	<10.8
P	492.0	1231	1167	1205
Pb	<2.40	17.8	15.3	100
S	139.1	114	133	115
Si	185.0	48.1	64.2	110
Zn	37.38	80.9	44.5	45

APPENDIX F

CARBON BALANCE CALCULATIONS

The carbon balance was performed by using the following equation

$$\%\ error = \frac{(Carbon\ in\ the\ inlet - Carbon\ in\ the\ exit)}{Carbon\ in\ the\ inlet} * 100$$

The sample calculations for an inlet toluene concentration of 2500 ppmv at 800°C with the exit gas composition of 1500 ppmv toluene, 150 ppmv of benzene, 2500 ppmv of CO_2 and 2500 ppmv of CH_4 and a total flow rate of 0.7 l/min are shown below.

Toluene inlet = 2500 ppmv

Toluene exit = 1500 ppmv

Toluene used = 2500-1500 = 1000 ppmv

Moles of toluene used = $\frac{\frac{1000}{1000000}*0.7}{0.0821*(800+273)} = 7.95 * 10^{-6}$

Moles of carbon used = 7* Moles of toluene used = $5.56 * 10^{-5}$

Moles of benzene in the exit = $\frac{\frac{150}{1000000}*0.7}{0.0821*(800+273)} = 1.19 * 10^{-6}$

Moles of carbon from benzene in the exit = 6* Moles of benzene = $7.15 * 10^{-5}$

Moles of CO_2 in the exit = $\frac{\frac{2500}{1000000}*0.7}{0.0821*(800+273)} = 1.99 * 10^{-5}$

Moles of carbon in the exit from CO_2 = $1.99 * 10^{-5}$

Moles of CH_4 in the exit = $\frac{\frac{2500}{1000000}*0.7}{0.0821*(800+273)} = 1.99 * 10^{-5}$

Moles of carbon in the exit from CO_2 = $1.99 * 10^{-5}$

Total carbon in the exit = $(7.15 + 1.99 + 1.99) * 10^{-5} = 4.69 * 10^{-5}$

$\% \, error = \frac{(5.56*10^{-5} - 4.69*10^{-5} -)}{5.56*10^{-5}} * 100 = 15.71\%$